AN ABSTRACT OF THE THESIS OF

Jesse Attias for the degree of Master of Science in Water Resources Science
presented on September 04, 2025.

Title: Linking Snowpack Dynamics and Summer Streamflow in Transient and Seasonal Snow Zones of the Western Cascades

Abstract approved: _____

Catalina Segura

Despite extensive research on snow in the western United States, the effects of climate and snowpack on streamflow are poorly understood in forested mountain watersheds of the Pacific Northwest, USA. This study assessed relationships among air temperature, precipitation, snow, and streamflow over the period 1998 to 2020 from nine watersheds (8.5 to 580 ha) dominated by conifer forest, spanning transient (410 to 800 m) and seasonal (800 to 1630 m) snow zones in the H.J. Andrews Experimental Forest, Oregon. Data were summarized by season—fall (Oct–Dec), winter (Jan–Mar), spring (Apr–Jun), and summer (Jul–Sep) – and analyzed using linear regression and all-subsets regression. Daily snowmelt losses and streamflow were analyzed using cross-correlation.

Air temperature was strongly related to snow and streamflow. Snow fraction (the fraction of precipitation falling as snow) was negatively related to air temperature during the snow season. Runoff ratios (unit-area streamflow divided by precipitation) were negatively related to air temperature in winter and spring in the transient snow zone and in spring in the seasonal snow zone. Summer streamflow (on July 1 and during minimum summer streamflow) also was negatively related to spring air temperature and positively related to spring precipitation in both transient and seasonal snow zones. Controlling for air temperature, winter runoff ratios

declined over the study period in transient snow zone watersheds, including watersheds with maturing forest plantations.

Relationships of streamflow to measures of snowpack differed by watershed elevation. Runoff ratios were positively related to snow fraction in winter and spring in the transient snow zone, in spring in the seasonal snow zone, and in summer in the highest elevation watershed (757 to 1620 m). Snow disappearance date and snow fraction also explained the timing of minimum summer streamflow in most study watersheds. Several snow variables were highly correlated with one another. Daily snowmelt was significantly positively cross-correlated with streamflow for 120 days at watersheds in the transient snow zone and for 150 days at watersheds in the seasonal snow zone.

These findings indicate that precipitation falling as snow contributes to streamflow during both winter and spring in the transient snow zone but only in spring in the seasonal snow zone. Findings also imply that in these conifer-forest dominated watersheds, when air temperature is higher, more precipitation falls as rain, and evapotranspiration is greater, which in turn decreases streamflow. These effects vary with elevation, occurring during winter and spring in watersheds below 800 m, and in spring and summer in watersheds above 800 m. Also, based on daily data, the positive effect of snowmelt on streamflow persists for five months in the seasonal snow zone compared to four months in the transient snow zone. Long-term declines in runoff ratios in winter, after removing the effects of air temperature, also imply that winter evapotranspiration has increased over the 23-year study period, perhaps as a result of forest growth.

These findings highlight the combined influence of vegetation, snow regime, air temperature and precipitation on the sensitivity of streamflow to snowpacks. These findings underscore the need for water resource planning to account for forest age,

forest management, and snow regime effects on streamflow, particularly where rising temperatures may increase evapotranspiration and lessen snowmelt contributions to streamflow.

Linking Snowpack Dynamics and Summer Streamflow in Transient and Seasonal Snow Zones of the Western Cascades

by

Jesse Attias

A THESIS

submitted to

Oregon State University

in partial fulfillment of
the requirements for the
degree of

Master of Science

Presented September 04, 2025
Commencement June 2026

Master of Science thesis of Jesse Attias presented on September 04, 2025

APPROVED:

Major Professor, representing Water Resources Science

Director of the Water Resources Graduate Program

Dean of Graduate Education

I understand that my thesis will become part of the permanent collection of Oregon State University libraries. My signature below authorizes release of my thesis to any reader upon request.

Jesse Attias, Author

ACKNOWLEDGEMENTS

This study was made possible due to decades of work by staff and researchers at the H.J. Andrews Experimental Forest (one of 27 sites within the Long Term Ecological Research Network). Here's to many more years of continuous, high-resolution data, offering a window into the past, insight into the present, and a prediction of what has yet to come. Long-term monitoring is critical in achieving these three goals. You can only read tea leaves if the tea has steeped long enough.

A sincere thank you to Dr. Catalina Segura for sharing her expertise, exhibiting patience, helping me gain fluency in hydrologic and statistical jargon I lacked, cracking jokes, and hosting dinners for students whose home-cooked meals are too far away to appreciate. Thank you to Dr. Julia Jones for her warmth, the wellspring of knowledge she so readily shares, and for her impressive transcription of my gibberish to concise ideas and sentences. You are old growth—steadfast and invaluable! I did not enter the program thinking I would study snow. Thank you, Dr. Mark Raleigh, for making snow endlessly intriguing (there is a reason I took three of your courses) and for being someone I always look forward to running into on campus.

To my family, thank you for pretending to understand what I study and the meaning behind it. Your continual love and support is everything. To my friends, you rock. You're the other half of everything. To the inhabitants of 1524, sharing a living space means sharing time, and it has been awfully nice sharing time with you. To the inhabitants of 380, thanks for swiveling your chairs toward me to shoot the breeze, lend coding and statistical insights, and occasionally commiserate. To the Cuban salsa crowd, thanks for showing me that with passion and effort, I can go from being bad to being mediocre at something. Perhaps that's the moral of this experience.

The USGS hasn't yet mapped or named you, but thank you to the creek I grew up on and the forest it ran through. You sent me on a wending path toward animals, water, and curiosity, and I would have it no other way.

CONTRIBUTION OF AUTHORS

Jesse Attias: Conceptualization, Methodology, Formal analysis, Investigation, Writing – Original Draft, Writing – Review & Editing, Visualization.

Catalina Segura: Conceptualization, Funding Acquisition, Methodology, Resources, Writing – Review & Editing, Visualization, and Supervision.

Julia Jones: Conceptualization, Funding Acquisition, Methodology, Resources, Writing – Review & Editing, Visualization, and Supervision.

TABLE OF CONTENTS

TABLE OF CONTENTS (Continued)

Page

LIST OF FIGURES

Figure Page

LIST OF FIGURES (Continued)

Figure Page

LIST OF FIGURES (Continued)

Figure Page

LIST OF FIGURES (Continued)

Figure Page

LIST OF FIGURES (Continued)

Figure Page

LIST OF TABLES

LIST OF APPENDICES

LIST OF APPENDIX TABLES

1. Introduction

In mountainous areas of the western United States, seasonal snowpacks act as reservoirs of water, releasing meltwater downstream in spring and summer, when precipitation is low, and societal and ecological water demand is often greatest (Barnett et al. 2005, Mote et al. 2005). Most runoff available to municipalities, agriculture, and aquatic ecosystems in the western United States originates as snowpack meltwater (Barnett et al. 2005; Li et al. 2017, Safeeq et al. 2013). Globally, however, ~2 billion people may experience nearly a 70% decrease in snow supply within the 21st century (Mankin et al. 2015). The substantial reduction of snowpack in the western United States that has taken place in the past century (Mote et al. 2005, Mote et al. 2018), is linked to anthropogenic climate change (Adam et al., 2009; Pierce et al., 2008), and snowpack loss is likely to accelerate in the future (Stewart et al. 2004).

Warm, isothermic, maritime snowpacks in the Pacific Northwest of the United States are particularly susceptible to reductions in snowfall and earlier spring melt (Knowles et al., 2006). Changes in snowpack dynamics can alter the timing and magnitude of streamflow. Indeed, reduced snowpacks in western North America have been linked to earlier streamflow timing (Stewart et al. 2004) and more pronounced and persistent water stress (Musselman et al. 2021).

Multiple processes associated with a changing climate may reduce streamflow, either directly or through effects on snow. These processes include (1) a reduction in the fraction of precipitation falling as snow rather than rain (Huntington et al. 2004, Jefferson 2011; Knowles et al., 2006, McCabe et al., 2018); (2) earlier snowmelt occurrence; (3) increased evapotranspiration; and (4) reduced precipitation.

A warming climate reduces the fraction of precipitation that occurs as snow, which has been linked to reduced annual streamflow throughout the contiguous United States (Berghuijs et al. 2014). Increased spring air temperature leads to earlier but slower spring melt rates (Musselman et al. 2017, Trujillo and Molotch, 2014). This seemingly counter-intuitive response of slower melt rate associated with increased spring air temperature is attributed to lower available melt energy — lower sun angles, shorter day lengths, cooler air temperature (weaker

sensible/latent fluxes), higher snow albedo, and possible freezing temperature at nights (Musselman et al., 2017, Trujillo and Molotch, 2014).

Increasing air temperature in spring also could increase evapotranspiration (ET) in vegetated environments, potentially reducing spring and summer streamflow (Barnett et al., 2005, Berghuijs et al., 2017, Leach et al., 2024). In a warmer climate, independent of changes in snowpack, elevated air temperature increases the atmosphere's capacity to hold moisture, raising the vapor pressure deficit, intensifying evaporative demand and evapotranspiration (Bosson et al. 2012), and reducing streamflow.

Climate change is also associated with reduced precipitation in some regions of the US (Jones and Driscoll 2022; Hudson et al., 2022), with corresponding reductions in streamflow (Campbell et al., 2022). Slower snowmelt rates are associated with weaker meltwater pulses, which can limit deep percolation below the root zone, increase soil moisture retention, and increase evapotranspiration (ET) (Barnhart et al. 2016), further reducing streamflow. In other words, increased air temperature can reduce streamflow both directly through increased ET and indirectly through a slower snowmelt rate, which also increases ET.

Climatic shifts vary seasonally. On the western slope of Oregon's Cascade Range, minimum and maximum air temperatures have increased most rapidly in late spring and summer over the past half century, both in openings and under the canopy of old-growth forest (Jones et al. 2025). These seasonal trends may play a key role in determining the fate of snowmelt. Recent work suggests that the degree of synchrony between snowmelt timing and the onset of the growing season can significantly affect the snowpack–streamflow relationship, when increased vegetation cover over time increases ET in spring, reducing water partitioning to streamflow later in the water year (Newcomb et al. 2024). Thus, summer streamflow depends not only on snowpack magnitude and timing, but also on air temperature, relative humidity, vapor pressure deficit, and ET.

Despite growing evidence of snowpack decline, uncertainty remains around how meltwater timing and watershed characteristics influence summer streamflow, especially in watersheds with varying subsurface storage. Reduced snowpack has been associated with lower groundwater recharge (Godsey et al. 2013) and faster transit times in the western United

States (Segura 2021). Groundwater recharge and transit times mediate the amount and timing of groundwater discharge to streams, whether through fast-draining shallow subsurface soils or slow-draining deeper groundwater (Tague et al. 2007). Declining snowpack and associated reductions in groundwater recharge rates and accelerated transit times may alter summer streamflow in headwater streams that depend on groundwater inputs in the summer (Ortega et al., 2025).

Despite decades of research on snowmelt-driven streamflow, streamflow response to a changing climate remains uncertain. Gordon et al. (2022) propose that streamflow response to climate change effects on snow depends on three mechanisms: snow season mass and energy exchanges, the intensity of snow season liquid water inputs, and the synchrony of energy and water availability. Their analysis used the CAMELS dataset (Addor et al., 2017), and it indicated that the latter two mechanisms are most likely to affect streamflow in the Pacific Northwest. However, the CAMELS dataset consists of a subset of the USGS GAGES-II dataset, a set of reference watersheds which range in size from roughly 1 to 25 800 km^2 with a median size of about 335 km^2 (Newman et al. 2015), and are likely not representative of small, mountainous systems.

The mechanisms for streamflow response to climate-induced changes in snowpack proposed by Gordon et al. (2022) have not been tested using empirical records from small headwater streams in the transient snow zone compared to the seasonal snow zone. The transient snow zone occurs at lower elevation, where mixed rain–snow conditions create an intermittent, temperature-sensitive snowpack. Shifts from snow to rain-dominated winter precipitation regimes are expected to greatly reduce snowpacks in the transient snow zone, which occupies much of the area of the Cascade and Olympic mountain ranges in the Pacific Northwest (Nolin and Daly, 2006). Such changes are expected to produce different snowpack responses in the transient snow zone compared to the seasonal snow zone (Jefferson, 2011). The transient snow zone also tends to have less snow water equivalent than the seasonal snow zone. Maximum SWE is strong predictor of summer low flow volume in arid watersheds within California, Oregon, Nevada, and Washington (Boisramé et al. (2024), but this relationship is weaker in wetter Pacific Northwest watersheds. Given the likelihood of future air temperature

increases and correspondingly elevated ET in the transient snow zone, it is valuable to understand how these potential climate changes will influence connectivity between winter snowpacks and summer streamflow.

This study examined how snowpack dynamics influence summer streamflow using long-term climatological and hydrologic records from headwater watersheds in the H.J. Andrews Experimental Forest in the western Cascades Range of Oregon. This study aims to understand the mechanisms governing snow response to climate variation and their subsequent effects on streamflow. The study watersheds (8.5 to 580 ha) span the transient and seasonal snow zones and include detailed information on disturbance history, land management, geology, and hydrology.

Specifically, the study questions are:

1. How have air temperature, precipitation, snow regime, and streamflow changed in steep forested headwater watersheds in the western Cascades over the period 1998–2020?

2. How are air temperature and precipitation related to seasonal and interannual variation in snow and streamflow across an elevation gradient spanning transient to seasonal snow zones?

These analyses further our understanding of snowmelt's contribution to watershed-scale streamflow and how climate variability influences snow and water-resource management. By integrating climate, snow, and streamflow records with a well-documented vegetation history and contextualization of local ecological processes, this study provides an unprecedented view of snow–streamflow linkages across low- to mid-elevation, forested watersheds.

2. Study Area

This study was conducted in the H.J. Andrews Experimental Forest (Andrews Forest), a 64 km^2 fifth-order mountain watershed located in the western Cascades of Oregon, 44º12' N, 122º7' W (Figure 1). Analyses used climate data from five meteorological stations, PRIMET (Primary Meteorological Station), H15MET (High 15 Meteorological Station), CENMET (Central Meteorological Station), VANMET (Vanilla Leaf Meteorological Station), and UPLMET (Upper

Lookout Meteorological Station) (Table 1) and streamflow data from nine study watersheds (8.5 to 580 ha) (Table 2). Meteorological stations and study watersheds are distributed across a broad elevation gradient (410 –1630 m) with varying forest structure, aspect, slope, and underlying lithology (Table 2). Although meteorological and stream gauging stations are not co-located, their spatial proximity allows for meaningful interpretations (Figure 1).

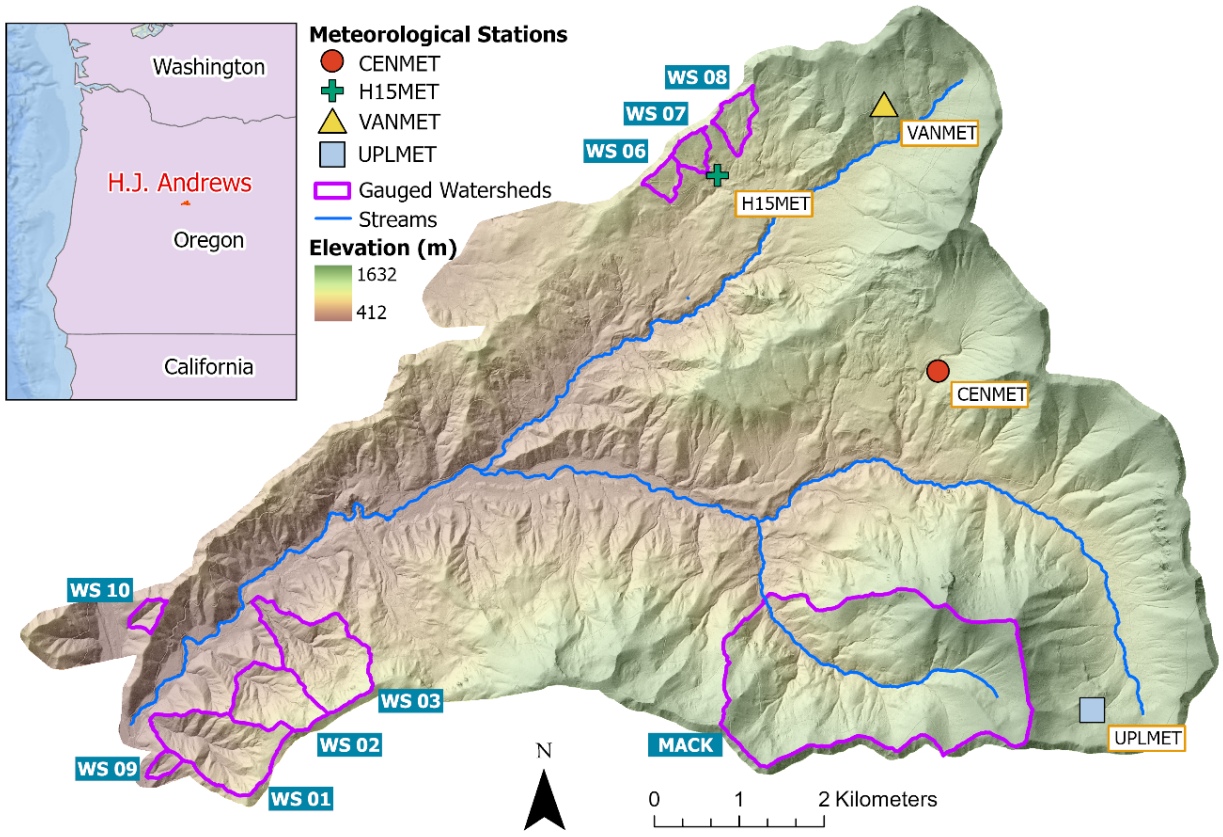

Figure 1. Location of the H. J. Andrews Experimental Forest, showing meteorological stations, study watersheds, elevation gradient, and higher order (3rd -5th order) streams.

2.1 Climate

The climate at the Andrews Forest is maritime, characterized by high precipitation and mild temperature throughout the year. Snow persistence zone designations are indicative of prevailing precipitation regime. Orographic lifting leads to more precipitation on average in

higher elevation watersheds than in lower ones. During the study period, extending between water years 1998 and 2020, mean annual precipitation was 2115 mm and mean annual air temperature was 8°C (at 1028 m.a.s.l) at CENMET, but temperature and precipitation vary depending on elevation and aspect. Approximately 80% of precipitation occurs between October and April, with little precipitation falling between June and September (Swanson and Jones, 2002).

2.2 Vegetation

Vegetation in study watersheds is dominated by Douglas-fir (*Pseudotsuga menziesii*), western hemlock (*Tsuga heterophylla*), and western redcedar (*Thuja plicata*). Seventy-five percent of the area of the Andrews Forest is mature and old-growth forest originated after fire in the 1500s and mid-1800s. About 25% of the forest area, including five of the study watersheds, was clearcut from the early 1950s to the early 1980s and replanted with Douglas-fir plantations (Goodman et al., 2022). As of 2025, plantations in WS01, WS03, WS06, WS07, and WS10 are 50 to 60 years old.

2.3 Geology and Geomorphology

Geology within the Andrews Forest is volcanic in origin and consists of three primary formations. WS01, WS02, WS03, WS09, and WS10 are underlain by late Oligocene and Miocene friable, altered volcanoclastic ash flows and mudflows (the Little Butte Formation) in areas below 760 m. The upper elevations of WS01, WS02, and WS03, all of WS06, WS07, and WS08, and parts of Mack Creek are underlain by welded and nonwelded ash flows and basaltic and andesitic lava flows (the Sardine Formation between 760-1200 m). Areas above 1200 m (Mack Creek) are underlain by basaltic and andesitic lava flows (the Pliocascade Formation (Swanson and James, 1975).

Table 1. Characteristics of meteorological stations in the H.J. Andrews Experimental Forest, Oregon. Daily precipitation, snow water equivalent, and air temperature data were obtained from 5 meteorological stations (Daly and McKee, 2019). Data span a period of 23 water years (1998-2020).

Meteorological Station	Elevation (m)	Aspect (degrees)
CS2MET	482	19
PRIMET	436	8
H15MET	900	215
CENMET	1028	224
VANMET	1268	183
VARMET	1315	
UPLMET	1284	72

2.4 Snow Zones

Watersheds were categorized based on their position within zones defined by snow persistence: the transient snow zone and the seasonal snow zone (Christner and Harr 1982; Berris and Harr 1987; Jones and Perkins 2010). In the transient snow zone, precipitation may fall as either rain or snow, and snow accumulates and melts multiple times each winter (Berris and Harr, 1987). In the seasonal snow zone, most winter precipitation falls as snow, and snowpacks typically persist throughout the winter and melt in the spring.

Two watersheds (WS09 and WS10) are fully within the transient snow zone (400–800 m); three watersheds (WS01, WS02, and WS03) span both transient and seasonal snow zones; and four watersheds (WS06, WS07, WS08, and Mack Creek) are situated entirely within the seasonal snow zone (>800 m), following the classification of Jones and Perkins (2010). Watersheds with mean elevations below 800 m (WS01, WS02, WS03, WS09, and WS10) are representative of the transient snow zone. In contrast, watersheds with mean elevations above 800 m (WS06, WS07, WS08, and Mack Creek) are considered representative of the seasonal snow zone (Table 2).

While this zonation is based on mean elevation, watersheds that span both snow zones can also be characterized by the percentage of their area within the seasonal snow zone. Of the watersheds with elevation ranges that encompass both the transient and seasonal snow zones, WS01, WS02, and WS03 are between 31-45% in the seasonal snow zone. Mack Creek is 99% within the seasonal snow zone.

Table 2. Characteristics of study watersheds in the H.J. Andrews Experimental Forest, Oregon. Landscape characteristics were derived from a 2020 LiDAR flight conducted by the U.S. Forest Service (Office for Coastal Management Partners, 2025). Daily streamflow data were obtained from 10 stream gaging stations (Johnson et al., 2019) and daily meteorological data were obtained from four meteorological stations (Daly and McKee, 2019). Data span a period of 23 water years (1998-2020). Watersheds WS 06, WS07, and WS08 used H15MET for precipitation data in analyses, but VANMET for all other climate data in analyses. Mack Creek used the mean between CENMET and UPLMET for all analyses, referred to as CENUPL.

Watershed	Elevation Range (m) (mean)	Mean Slope (degrees)	Mean Aspect (degrees)	Gaged Area (ha)	Percent in Seasonal Zone	Corresponding Meteorological Stations
01	439 – 1013 (713)	33 (10)	210	95.9	31	CENMET
02	548 – 1078 (796)	32 (10)	237	60.3	44	CENMET
03	484 – 1075 (773)	31 (11)	219	101.1	45	CENMET
06	873 – 1025 (957)	17 (7)	166	13	100	H15MET, VANMET
07	919 – 1097 (1013)	19 (7)	162	15.4	100	H15MET, VANMET
08	957 – 1178 (1048)	18 (8)	174	21.4	100	H15MET, VANMET
09	424 – 715 (567)	35 (6)	237	8.5	0	CENMET
10	459 – 688 (593)	33 (9)	233	10.2	0	CENMET
Mack Creek	757-1620 (1195)	28 (10)	195	580	99	CENMET, UPLMET

3. Methods

3.1 Overview

This analysis relates climate data (precipitation, SWE, and air temperature from four meteorological stations) to streamflow records from nine small watersheds for the period of 1998 to 2020. Temporal trends in precipitation, temperature, SWE, and streamflow were fitted to determine stationarity. Multiple linear regression, cross correlation, and simple linear regression analyses were used to assess the influence of climate, snow, and evapotranspiration on summer streamflow.

3.2 Matching Climate and Streamflow Data

For analysis, climate data were matched to each watershed based on the nearest meteorological station. For most analyses, climate data (precipitation, SWE, and temperature) from CENMET were related to streamflow in WS01, WS02, WS03, WS03, WS09, and WS10; data from VANMET were related to streamflow in WS06, WS07, and WS08; and an average of data from CENMET and UPLMET, referred to CENUPL, was related to streamflow in Mack Creek, to best approximate climatic conditions in a watershed with a particularly broad elevational gradient. Because of large amounts of missing and erroneous precipitation data at VANMET, precipitation data from H15MET were substituted for VANMET data for all years.

Although CENMET is located at a higher elevation than WS01, WS02, WS03, WS09, and WS10, likely resulting in systematic overestimation of precipitation and SWE at these lower-elevation watersheds, it was used for most analyses to provide consistency. However, precipitation data at PRIMET were used for the calculation of runoff ratios at lower elevation watersheds, WS01, WS02, WS03, WS09, and WS10, to provide more accurate estimates of watershed-specific precipitation inputs. Because of this standardized matching process, most analyses of climate data refer to watersheds, not to meteorological stations.

3.3 Data

This study used climate data on air temperature (Daly and McKee, 2019), precipitation, and snow from five meteorological stations (Table 1) for the period January 1, 1997 to

September 30, 2020, Precipitation and air temperature data have been collected at PRIMET since 1972 and at CENMET, VANMET, and UPLMET since 1994. Data on snow water equivalent (SWE) have been collected at CENMET, VANMET, and UPLMET since 1997 (Table 1). All climate data were expressed on a mean daily basis. Linear interpolation and linear relations were used to fill missing data (Appendix A). Mean daily streamflow data (Johnson et al. 2019) were converted to unit-area streamflow daily values. Streamflow data for the period of record were complete and did not require interpolation.

3.4 Variables Used in Analyses

Analyses were based on a set of variables representing temperature, precipitation, snowpack, and streamflow. Variables were calculated from daily data for each water year (October 1 – September 30) and each season: fall (October 1–December 31), winter (January 1–March 31), spring (April 1–June 30), and summer (July 1–September 30).

Climate variables, including air temperature and precipitation, were summarized for each water year and for multiple seasons to assess their influence on snow–streamflow relationships. Mean daily air temperature was calculated for each water year and each season at each meteorological station (Table 1, Table 3). Temperature is a primary driver of evapotranspiration, together with water availability, solar radiation, vapor pressure deficit, and wind, making it relevant for understanding vegetation effects on snow–streamflow relationships. Total precipitation was calculated for each water year and for the winter and spring seasons.

Snow variables were quantified to characterize the amount, timing, and rate of snow accumulation and melt across the study watersheds. Five snow variables were used in analyses: snow fraction, maximum SWE, the date of maximum SWE, the snow disappearance date, and snow melt rate, (Figure 2, Table 3). Snow variables were calculated from snow water equivalent measured at snow pillows at CENMET, VANMET, and UPLMET. Snow fraction is the proportion of total annual precipitation falling as snow. For this analysis, snow fraction was calculated as maximum SWE in a year divided by total annual precipitation, expressed as a percentage**.** Maximum SWE was the SWE value on the day with the highest daily SWE value in the snow

season (Figure 2). In snow-dominated watersheds, which rarely experience significant midseason melt, this value is often a reliable indicator of total seasonal accumulation.

Snow timing metrics were calculated to capture key snow accumulation and ablation dynamics. Three variables were used in analyses to represent the timing of snow: the date of maximum SWE, the snow disappearance date, and the melt rate (Figure 2, Table 3). All timing variables were recorded as water year day but are referred to as "date" hereafter. The melt rate was calculated as maximum SWE divided by the time between the date of maximum SWE and the snow disappearance date (mm/day).

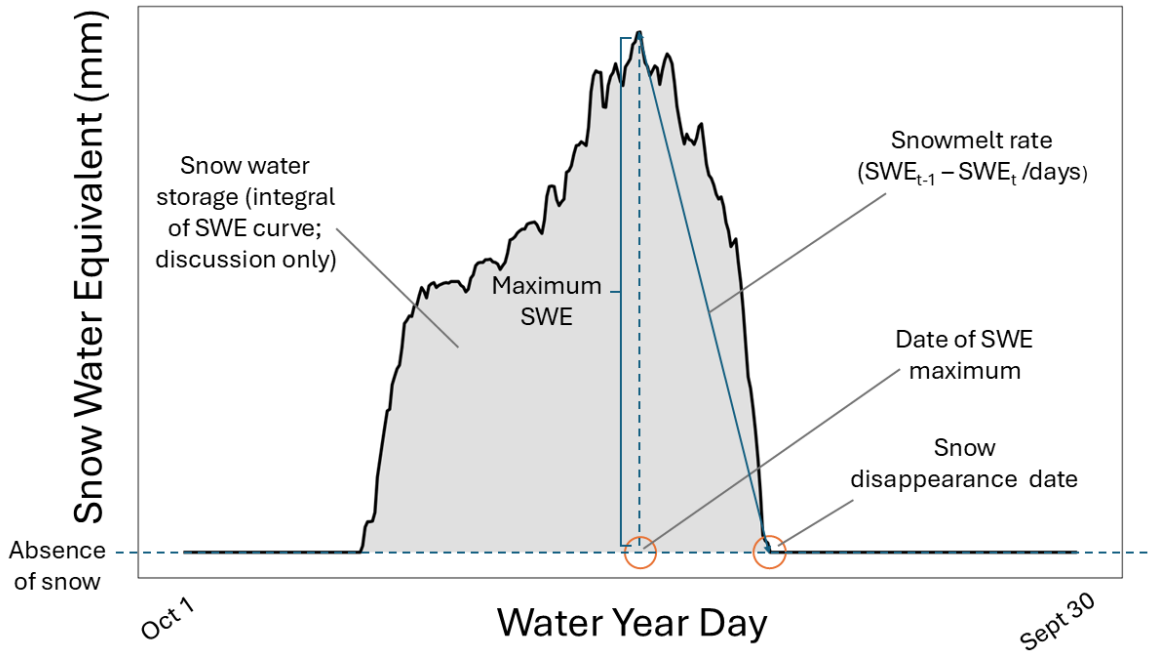

Figure 2. Snow water equivalent (SWE) variables determined from the snow accumulation and snowmelt curve and used in analysis or mentioned in the discussion.

Runoff ratios were calculated to evaluate the proportion of precipitation converted to streamflow across seasons and water years. Runoff ratios were calculated as total unit-area streamflow (mm) divided by total annual precipitation (mm) at each watershed for each water year and for fall, winter, and spring (Table 3). Runoff ratios typically range from 0 to 1. In Oregon and other dry climates, summer streamflow often exceeds summer precipitation, producing runoff ratios greatly exceeding 1. To obtain runoff ratios less than 1, the runoff ratio for the summer season was calculated as summer total streamflow divided by spring precipitation. The runoff ratio is a measure of losses of precipitation to evapotranspiration and water storage in snow and soil. At times, especially for higher elevation watersheds, runoff ratios exceeded 1. This was possibly due to meteorological and stream gauge station spatial mismatch, precipitation gauge undercatch, soil water storage and release, and/or snow water storage and melt (section 5.4).

Five variables were calculated for summer streamflow for each watershed: July 1 streamflow, mean summer streamflow, minimum streamflow, date of minimum flow, and the summer hydrograph recession rate (Figure 3, Table 3). Unit area streamflow on July 1 (mm) represents streamflow magnitude at the start of the low-flow season. Mean summer streamflow is the average daily flow for the summer season, from July 1 to September 30. Minimum summer streamflow was determined as the minimum value of the 7-day running mean of daily unit area streamflow from July 1 to September 30. The date of minimum flow was determined as the start date of the minimum 7-day mean summer flow period and was recorded in water year day format. Streamflow recession rate was calculated as the difference between July 1 streamflow and August 31 streamflow, divided by the number of days between these dates (61 days with complete data), such that positive values indicate a decline in flow over July–August (Table 3).

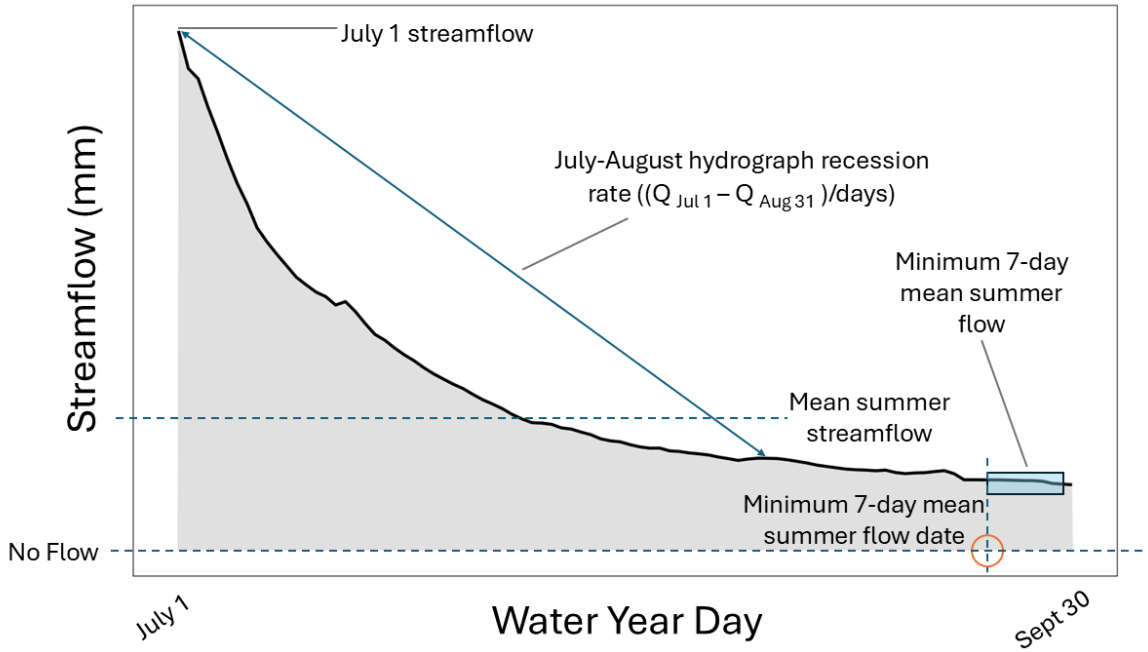

Figure 3. Summer streamflow variables determined from the summer (July 1 - September 30) hydrograph and used in analysis.

Table 3. Summary of snow and streamflow variables used in analyses of climate, snow, and streamflow relationships in the H.J. Andrews Experimental Forest, Oregon (1998–2020). For each variable, derivation from raw daily records, the analyses in which it was used, and the temporal scale at which it was computed are included in the table.

	Calculation Method	Relevant Analyses
Snow Variables		
Snow fraction	Total annual precipitation that falls as snow from the beginning of the water year until summer (10-01 to 06-01), as a percentage	Bivariate correlations, linear models
Maximum SWE	Maximum SWE calculated across a water year (WY), in mm	Bivariate correlations, linear models
Maximum SWE date	Date of the SWE maximum for a WY, in water year day	Bivariate correlations, linear models
Snow disappearance date	First date on which SWE=0 in spring and remains 0 for the remainder of the WY, in water year day	Bivariate correlations, linear models
Snowmelt rate	Maximum SWE divided by the time between the maximum SWE date and snow disappearance date (mm/day).	Bivariate correlations, linear models
Streamflow Variables		
July 1 streamflow	Discharge on July 1 for a WY, in unit mm	Bivariate correlations, linear models
Mean summer streamflow	Mean unit discharge calculated between 07/01 and 09/30, in unit mm	Bivariate correlations
Minimum summer low flow	The 7-day running mean of daily unit area streamflow from 07/01 to 09/30, in unit mm	Bivariate correlations, linear models
Minimum summer low flow date	The first date of the minimum summer low flow period, as a water year day	Bivariate correlations, linear models
Summer hydrograph recession rate	The difference between July 1 streamflow and August 31 streamflow, divided by the number of days between these dates, in unit mm	Bivariate correlations

Air Temperature Variables		
Seasonal temperature	Mean daily air temp for the fall (October 1–December 31), winter (January 1–March 31), spring (April 1–June 30), and summer (July 1–September 30), each in °C.	Linear models
Precipitation Variables		
Total annual precipitation	Sum of daily precipitation values for each water year, in mm.	Bivariate correlations
Spring precipitation	Summed daily precipitation values for the spring (April 1–June 30), in mm.	Bivariate correlations, linear models

3.5 Analysis of Interannual Trends

Linear trends over the study period (1998-2020) were estimated for the following variables at each meteorological station (Table 1, Table 3): mean annual temperature, mean daily temperature for each of the four seasons, total annual precipitation, total seasonal precipitation, maximum SWE, and snow fraction (Figures 4 to 7). Linear trends over the study period (1998-2020) were estimated for the following variables at each watershed (Table 2, Table 3): total annual unit streamflow, annual runoff ratio (Figures 8 to 11). Trends were assessed using both linear regression and non-parametric Sen's slope estimates (Sen, 1968). Pearson's r and Kendall's τ indicate the strength of association, and p-values indicate significance. Monotonic trends were assessed using the Mann–Kendall test, and trend magnitude was estimated with Sen's slope (R package trend; Pohlert, 2023). Given the relatively small sample size (N = 23 years), a significance threshold of $p < 0.1$ was used for all trend analyses.

3.6. Bivariate Correlations

Bivariate correlations were calculated for annual values of climate, snow, and streamflow variables (Table 3) for the study period (water years 1998-2020, N=23) for all watersheds (Figure 12). This subset of variables did not include air temperature, which was included in linear modeling (Section 3.7). Climate variables included in bivariate correlations were total annual precipitation and spring precipitation; snow variables were snow fraction, snow disappearance data, date of maximum SWE, maximum SWE, and snowmelt rate; and streamflow variables were July 1 streamflow, mean summer streamflow, minimum summer streamflow, date of minimum streamflow, and summer streamflow recession rate. Climate and snow variables were assigned to watersheds from the nearest meteorological station as described above (section 3.2). The strength and direction of bivariate relationships were assessed using Pearson's correlation coefficient, and their statistical significance was evaluated based on p-values. Results of the bivariate analysis of annual data revealed relationships among precipitation snow variables and streamflow variables, which were used to interpret results of

regression models. Results were displayed in heat map correlation matrices using the corrplot package (Wei and Simko, 2021).

3.7 Linear Models

Linear models were fitted to relate streamflow (response variables) to climate (air temperature, precipitation) and snow over the 23-year study period (1998-2020). First, simple linear models were fitted to relate (1) snow fraction (response variable) to air temperature (Figure 13), (2) runoff ratio (response variable) to air temperature (Figures 14 to 21), and (3) runoff ratio (response variable) to snow fraction (Figures 34 to 41). These models were run for each season (fall, winter, spring and summer) for all watersheds. Residuals from model (2) were related to water year, precipitation, and snow fraction (Figures 22 to 33). Results of this analysis indicated that simple relationships explained some aspects of winter and spring streamflow, but they did not explain summer streamflow. Hence, multiple linear regression models were undertaken to explain summer streamflow response to climate and snow.

Multiple linear regression models were fitted to relate three summer streamflow variables (response variables) to variables representing air temperature, precipitation, and snow over the 23-year study period (water years 1998-2020). The three response variables were: July 1 unit area streamflow, minimum summer flow, and date of minimum summer flow (Figure 3, Table 3). Explanatory variables included: mean winter temperature, mean spring temperature, mean summer temperature, spring precipitation, snow fraction, snowmelt rate, snow disappearance date, the date of maximum SWE, and maximum SWE (Figure 2, Table 3).

All subsets regression (Miller, 2002) was applied to identify the best subset of multiple linear regression models for summer streamflow magnitude and timing at each study watershed (Figures 42-44, Tables 4 to 6 and C.5 in Appendix C). All subsets regression is a model selection approach that evaluates every possible combination of explanatory variables to identify the set that best explains variation in the response variable, based on selection criteria. This method was chosen because it allows a comprehensive comparison of potential explanatory combinations when there are many possible combinations.

A set of competing models was created for each of the three streamflow response variables. To account for the limitations of a relatively small sample size (N = 23 years), models were restricted to a maximum of three explanatory variables. Austin and Steyerberg (2015) advise a minimum of 10 observations per explanatory variable to maintain model stability and avoid overfitting. A total of 3,483 models (129 models for each unique *watershed × dependent-variable* pair) were tested.

Multiple linear regression model selection was conducted using Akaike's Information Criterion (AIC) (Akaike, 1974), retaining only those models within two AIC units of the best-performing model for each streamflow response variable. For each retained model, the coefficients of each explanatory variable and their associated p-values were used to assess the direction and strength of effects. Cross-validated R^2 values provided a measure of overall model performance, while Lindeman–Merenda–Gold (LMG) (Lindeman et al., 1980) regressions were used to estimate the relative importance of each explanatory variable. These statistics were obtained using the DAAG and relaimpo packages, respectively (Grömping, 2006; Maindonald and Braun, 2010).

3.8 Cross-Correlation Analysis

Cross-correlations were calculated between daily snowpack losses and daily unit-area streamflow at each watershed for the study period (1998–2020) (Figures 45 and 46). Snowpack losses were calculated from day-to-day changes in SWE, retaining only negative changes from day t–1 to day t (representing ablation) and setting positive changes (accumulation) to zero. These losses represent days when the snowpack decreased, which may occur through snowmelt and subsequent infiltration—potentially contributing to streamflow—or through sublimation, wind redistribution, or evaporation. Loss values were computed for the entire snow season, not just the spring melt period, to capture mid-season melt events that can influence streamflow at later times. A positive coefficient at a given lag indicates that above-average snowmelt is associated with above-average streamflow at that lag, whereas a negative coefficient indicates that above-average snowmelt is associated with below-average streamflow at that lag. However, coefficients below zero in these results are not interpretable,

as they arise primarily from long consecutive stretches of zero values after the snow season has concluded. The number of lag days when the cross-correlation function declined and crossed the confidence envelope was used to compare the maximum time lags at which snow influenced streamflow for each watershed (Figure 45) or snow zone group (Figure 46). This snow-loss approach focuses on fluxes from the snowpack rather than total snow storage.

4. Results

4.1 Interannual Trends in Climate, Snow, and Streamflow

Long-term trends in air temperature, maximum snow water equivalent (SWE), precipitation, and snow fraction were not significant ($p < 0.1$) at any meteorological station over the 23-year record (water years 1998–2020) (Figures 4-7, Appendix Table B.1). These results suggest that there were no detectable long-term changes in annual meteorological conditions or in seasonal trends of precipitatoin or air temperature (Appendix Table B.3)—either linear or monotonic—over the study period.

There were no significant trends in annual unit area streamflow at any study watershed (Figures 8 and 9, Appendix Table B.2). For unit streamflow, no statistically significant trends were found in any of the nine watersheds under either linear or monotonic trend analysis ($p >$ 0.1 for all tests). This indicates that, despite reductions in runoff ratio in certain watersheds, the total streamflow volume per unit area has remained relatively stable over the study period.

There were no significant trends in annual runoff ratios except at WS07 (Figure 11). At WS07, linear regression analysis yielded a slope of –0.004 (R = –0.465, p = 0.025), while the Mann–Kendall test confirmed a significant monotonic decrease (Kendall's tau = –0.375, p = 0.013; Sen's slope = –0.005) (Appendix Table B.2). This indicates that over the 23-year study period, WS07 has experienced a decline from 0.5 to 0.4 in the proportion of precipitation converted to streamflow. Three additional watersheds—WS03, WS06, and WS10—exhibited marginally significant monotonic declines in runoff ratio, as indicated by the Mann–Kendall test (p = 0.064, 0.064, and 0.057, respectively) (Figures 10 and 11, Appendix Table B.2). Although their linear regression results were not statistically significant ($p > 0.1$), the non-parametric results suggest directional changes over time. WS03 and WS06 both had Kendall's tau values of

–0.281 and Sen's slopes of –0.005 and –0.006, respectively. WS10 had a Kendall's tau of –0.289 and a Sen's slope of –0.004 (Appendix Table B.2). These values suggest modest but consistent monotonic declines in the proportion of precipitation converted to streamflow at these watersheds.

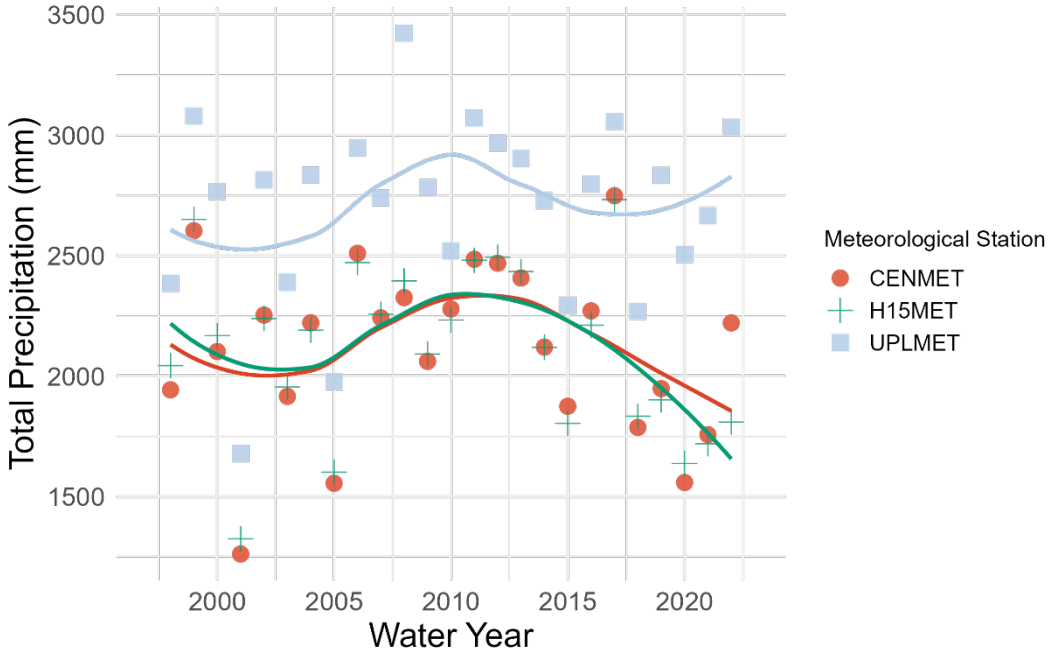

Figure 4. Annual precipitation at meteorological stations within the Andrews Forest, CENMET (1028 m elevation), H15MET (909 m elevation), and UPLMET (1284 m elevation), water years 1998 to 2020. Locally estimated scatterplot smoothing (LOESS) lines are shown for visual reference, using a nonparametric local regression method to highlight trends. Corresponding linear regression, Sen's slope, and Mann–Kendall statistics are provided in Appendix Table B.1.

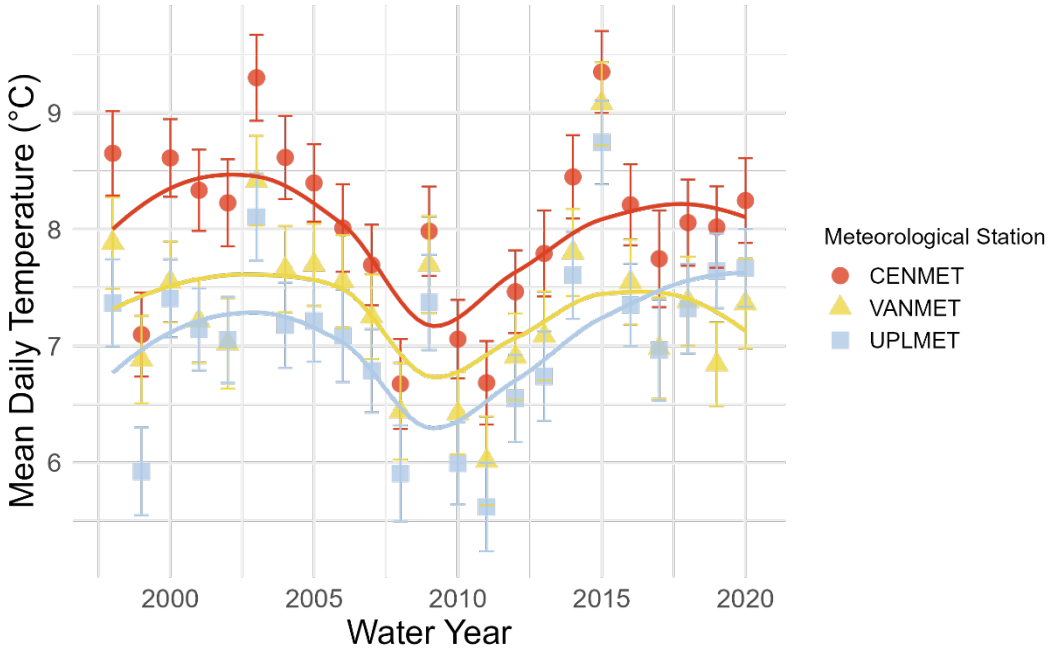

Figure 5. Mean daily temperature at meteorological stations within the Andrews Forest, CENMET (1028 m elevation), VANMET (1268 m elevation), and UPLMET (1284 m elevation), water years 1998 to 2020. Locally estimated scatterplot smoothing (LOESS) lines are shown for visual reference, using a nonparametric local regression method to highlight trends. Mean daily temperature standard error bars are included for each study year. Corresponding linear regression, Sen's slope, and Mann–Kendall statistics are provided in Appendix Table B.1.

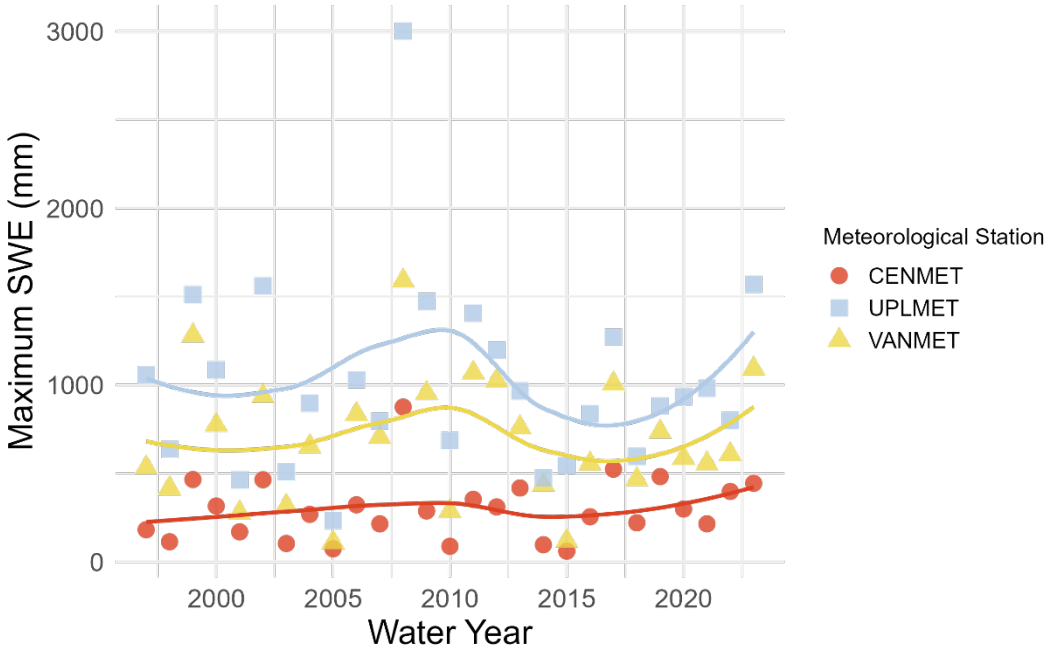

Figure 6. Maximum snow water equivalent (SWE) at meteorological stations within the Andrews Forest, CENMET (1028 m elevation), VANMET (1268 m elevation), and UPLMET (1284 m elevation), water years 1998 to 2020. Locally estimated scatterplot smoothing (LOESS) lines are shown for visual reference, using a nonparametric local regression method to highlight trends. Corresponding linear regression, Sen's slope, and Mann–Kendall statistics are provided in Appendix Table B.1.

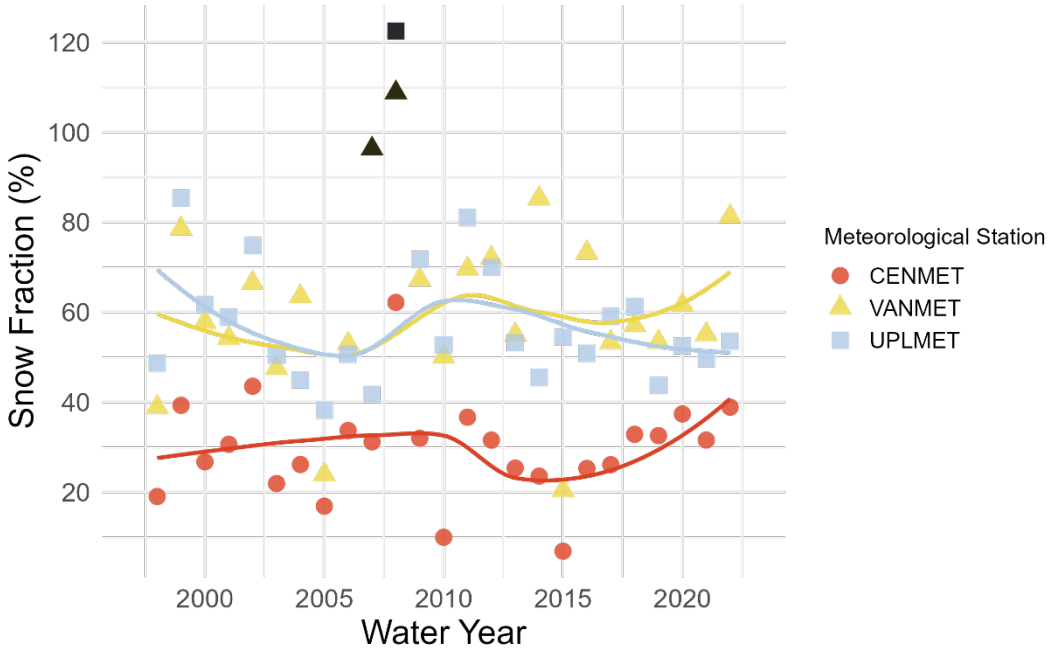

Figure 7. Snow fraction (maximum SWE/total P) at meteorological stations within the Andrews Forest, CENMET (1028 m elevation), VANMET (1268 m elevation), and UPLMET (1284 m elevation), water years1998 to 2020. Locally estimated scatterplot smoothing (LOESS) lines are shown for visual reference, using a nonparametric local regression method to highlight trends. In panel C, black symbols highlight anomalously high snow fraction values: triangles correspond to VANMET and the square to UPLMET. Snow fraction calculations for VANMET use SWE data from VANMET (1268 m) and precipitation data from H15MET (909 m) for all years. This elevational mismatch tends to inflate snow fractions, but the effect is most apparent in 2007 and 2008 due to unusually high snowfall. The high UPLMET value in 2008 likely reflects both a heavy snow year and a heavily interpolated SWE record that winter. Black markers were excluded from the LOESS lines. Corresponding linear regression, Sen's slope, and Mann–Kendall statistics are provided in Appendix Table B.1.

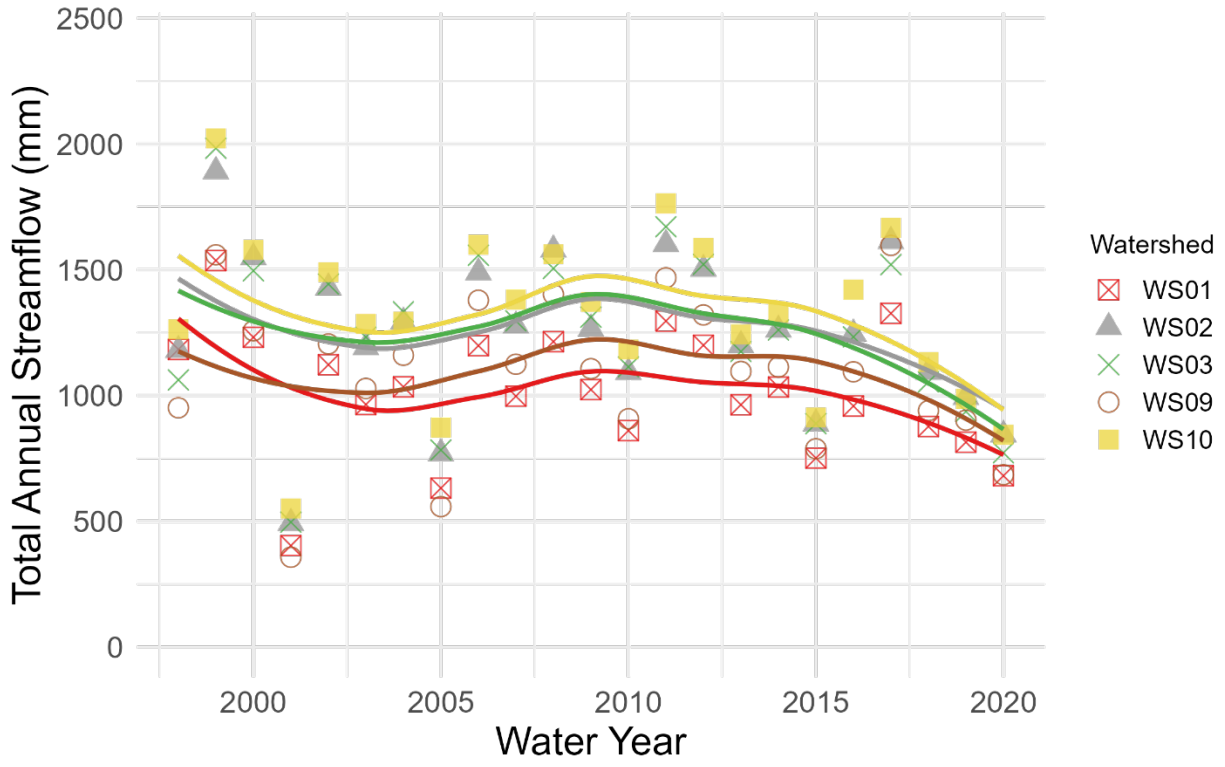

Figure 8. Total annual unit streamflow at 5 stream gaging stations within the transient snow zone in the Andrews Forest water years 1998 to 2020. Locally estimated scatterplot smoothing (LOESS) lines are shown for visual reference, using a nonparametric local regression method to highlight trends. Corresponding linear regression, Sen's slope, and Mann–Kendall statistics are provided in Appendix Table B.2.

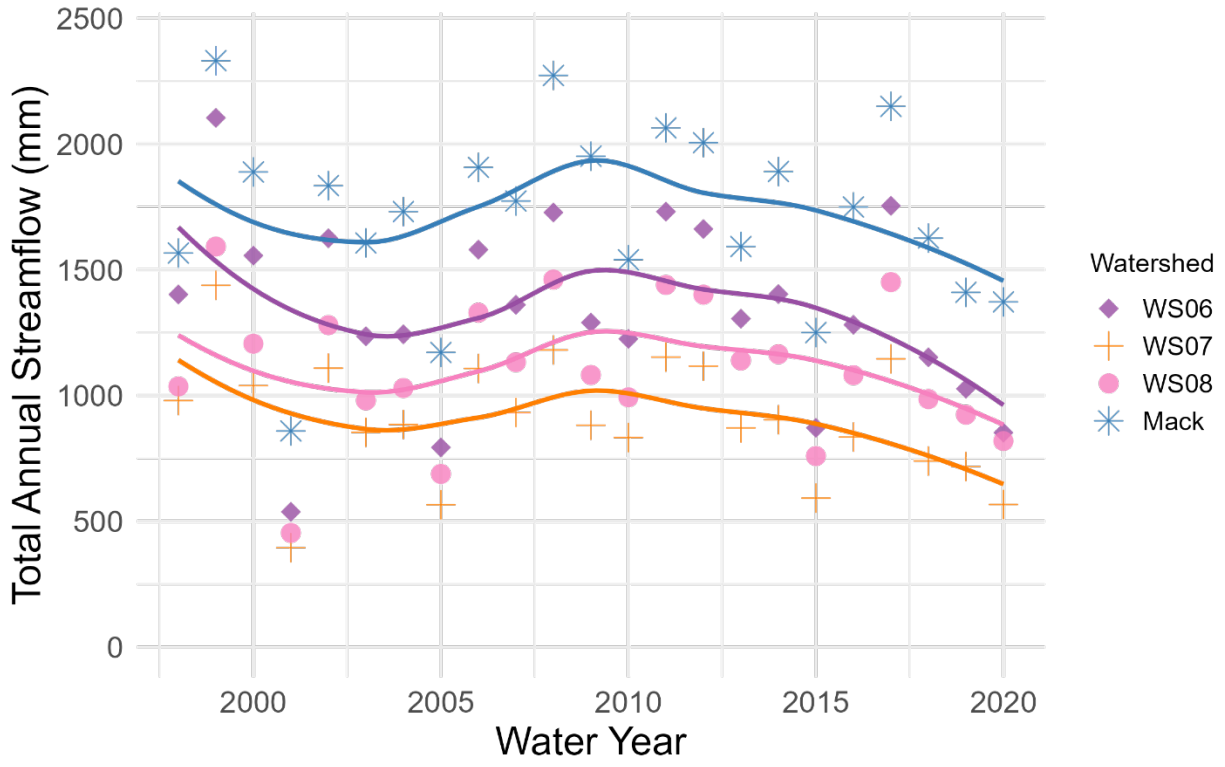

Figure 9. Total annual unit streamflow at 4 stream gaging stations within the seasonal snow zone in the Andrews Forest, water years 1998 to 2020. Locally estimated scatterplot smoothing (LOESS) lines are shown for visual reference, using a nonparametric local regression method to highlight trends. Corresponding linear regression, Sen's slope, and Mann–Kendall statistics are provided in Appendix Table B.2.

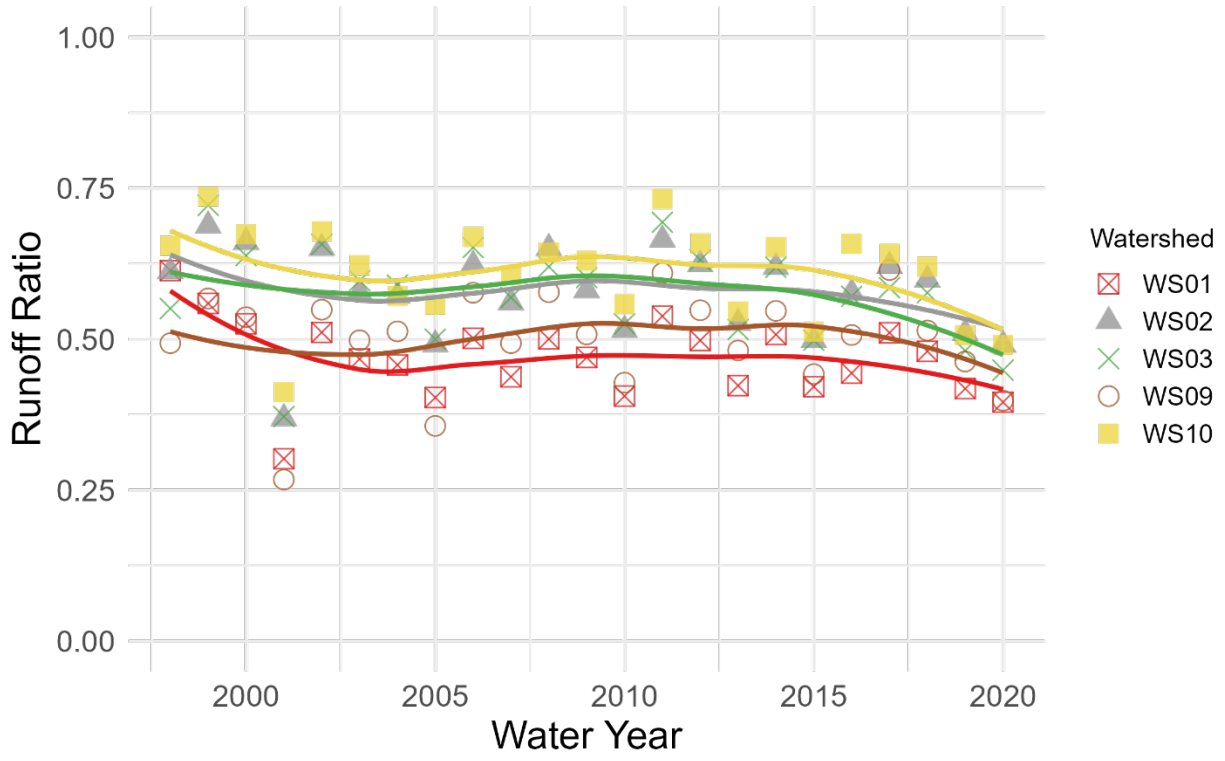

Figure 10. Mean annual runoff ratio at 5 stream gaging stations within the transient snow zone in the Andrews Forest, water years 1998 to 2020. Locally estimated scatterplot smoothing (LOESS) lines are shown for visual reference, using a nonparametric local regression method to highlight trends. Corresponding linear regression, Sen's slope, and Mann–Kendall statistics are provided in Appendix Table B.2.

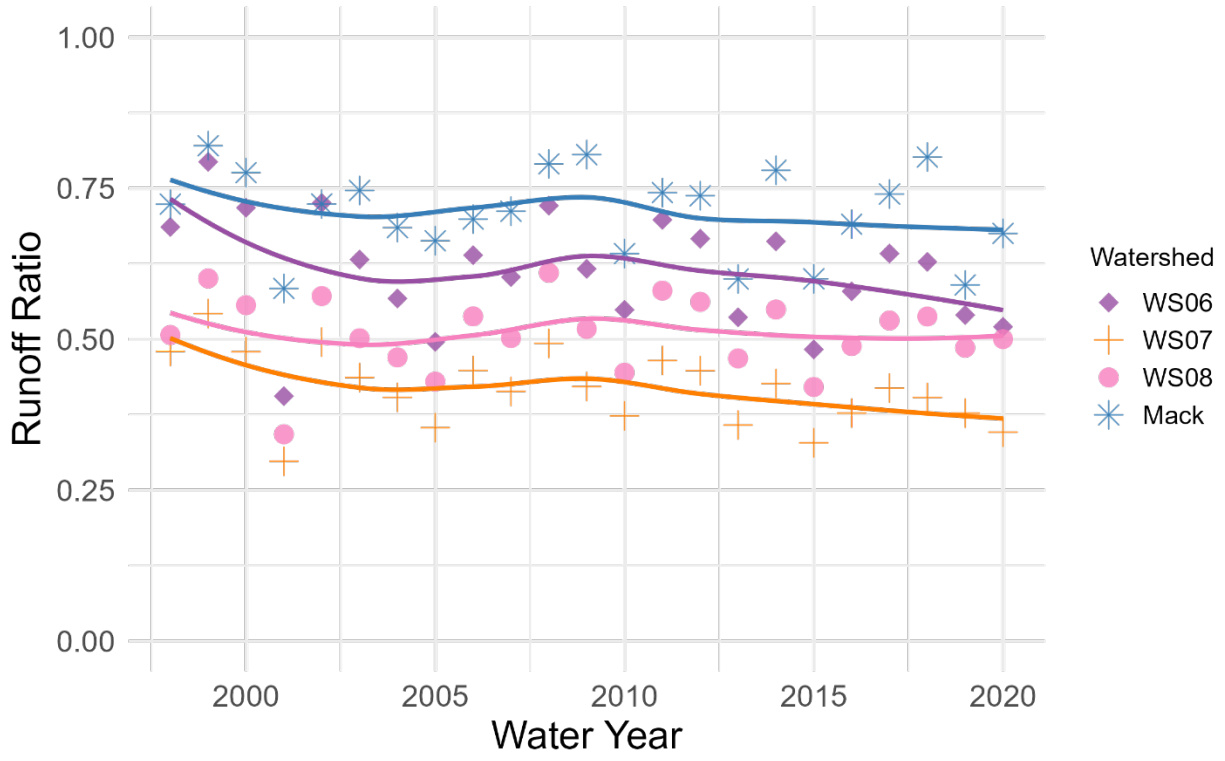

Figure 11. Mean annual runoff ratio at 4 stream gaging stations within the seasonal snow zone in the Andrews Forest, water years 1998 to 2020. Locally estimated scatterplot smoothing (LOESS) lines are shown for visual reference, using a nonparametric local regression method to highlight trends. Corresponding linear regression, Sen's slope, and Mann–Kendall statistics are provided in Appendix Table B.2.

4.2 Bivariate Correlations

Overall, snow variables were strongly correlated among watersheds (data matched from meteorological stations, section 3.2), and streamflow variables were strongly correlated among watersheds (Figure 12). Spring precipitation was correlated with summer streamflow magnitude and recession, but not the timing of minimum summer flow. Snow variables were not correlated with summer streamflow, except for the timing of minimum summer flow, and at Mack Creek, the highest elevation watershed (Figure 12).

Snow variables were strongly and consistently correlated to one another at all watersheds (variables 3 to 7, Figure 12). Snow fraction, snow disappearance date, maximum SWE, melt rate, and snow disappearance date (variables 3 to 7) were all closely interrelated, with high correlation coefficients and low p-values. For example, in nearly every watershed (data matched from meteorological stations, section 3.2), snow fraction was strongly positively correlated with both maximum SWE (typically $r \approx 0.83$ to 0.92) and melt rate ($r \approx 0.78$ to 0.84), with p-values consistently less than 0.001 (Appendix Table C.1). However, the date of maximum SWE (variable 5) was not correlated with maximum SWE or melt rate (variables 6 and 7) at WS06, WS07, WS08 (data from VANMET) or Mack Creek (data from CENUPL) (panels F, G, H, and I in Figure 12).

Summer streamflow variables (July 1 Q, mean streamflow, and minimum streamflow) and to some extent recession rate also were strongly and consistently correlated to one another at all watersheds (variables 8 to 10 and 12, Figure 12). However, the date of minimum summer flow (variable 11) was not related to other summer streamflow variables (variables 8 to 10, 12, Figure 12).

At all watersheds except Mack Creek, spring precipitation and summer streamflow magnitude were strongly correlated (variables 2 and 8, 9, and typically 10, Figure 12). At the lower-elevation, transient snow zone watersheds (WS01, WS02, WS03, WS09, and WS10), spring precipitation was strongly and positively associated with July 1 streamflow, mean summer flow, and summer hydrograph recession rates ($r > 0.75$; Figure 12, Appendix Table C.1). At the high-elevation, seasonal snow zone watersheds (WS06, WS07, WS08, and Mack Creek) spring precipitation was also positively associated with July 1 streamflow, mean summer flow,

and summer hydrograph recession rates, although the correlations were generally weaker and slightly less consistent, as indicated by lighter shades of red for variables 2 vs. 8, 9, and 10, especially for Mack Creek.

Correlations among snow variables and summer streamflow metrics varied by elevation (Figure 12). In the lower-elevation watersheds (in the transient snow zone), snow variables (variables 3 to 7) were weakly correlated with summer flow metrics (variables 8 to 12). In these watersheds, snow variables (variables 3 to 7) were weakly positively correlated with the date of the minimum summer low flow (variable 11), indicating that more snow postponed the date of minimum flow in summer, although these correlations were marginally significant. Correlations of snow variables (variables 3 to 7) with the date of the minimum summer flow (variable 11) were stronger in higher-elevation watersheds (in the seasonal snow zone), particularly WS06, WS08, and Mack Creek, suggesting a greater influence of snowpack on summer low flow timing in the seasonal snow zone compared to the transient snow zone.

Snow variables (variables 3 to 7) were typically not correlated with other measures of summer flow (e.g., July 1 streamflow, mean flow, or minimum flow, or recession, variables 8-10 and 12) at watersheds in the transient snow zone, as indicated by white and pale blue colors in Figure 12, panels A to E. Correlations of snow variables to summer streamflow were weak at most watersheds in the seasonal snow zone including WS06, WS07, and WS08 (panels F to H, Figure 12). At Mack Creek (panel I, Figure 12), however, snow fraction, maximum SWE, and melt rate (variables 3, 6, and 7) were at times strongly positively related to summer flow variables (variables 8 to 12, Figure 12).

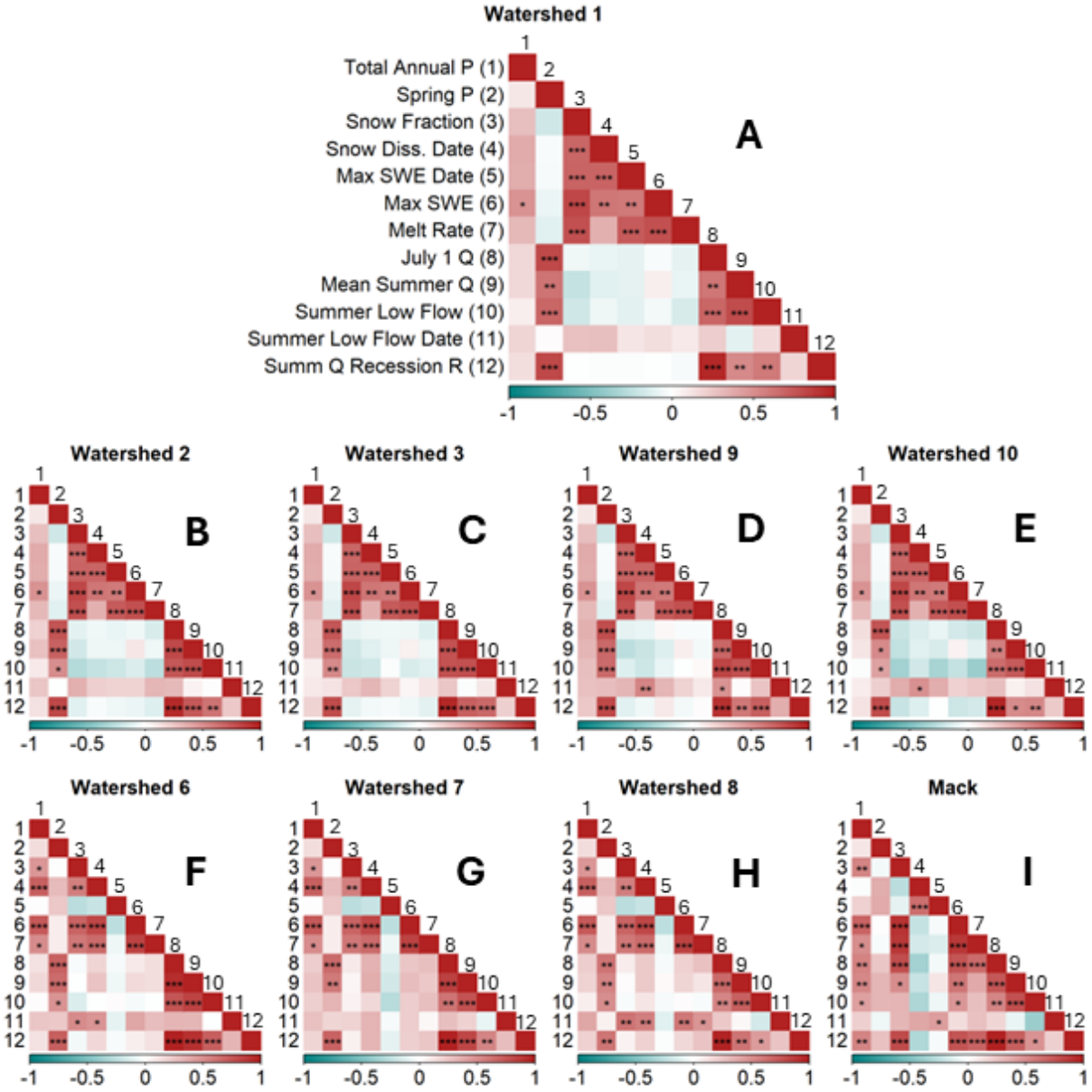

Figure 12. Correlation matrices for all study watersheds, with variables grouped and ordered by precipitation, snow, and summer streamflow metrics. Variables in each watershed include (1) total annual precipitation, (2) total spring precipitation, (3) snow fraction, (4) snow disappearance date, (5) date of maximum SWE, (6) maximum SWE, (7) melt rate, (8) July 1 streamflow, (9) mean summer streamflow, (10) summer low flow, (11) summer low flow date, (12) summer hydrograph recession rate. Panels include (A) WS01, (B) WS02, (C) WS03, (D) WS09, (E) WS10, (F) WS06, (G) WS07, (H) WS08, (I) Mack Creek. Warmer (red) hues indicate positive Pearson's correlation coefficients, while cooler (teal) hues indicate negative values. The color ramp legend at the bottom of each plot denotes Pearson's correlation coefficent strength and direction. Asterisks within matrix cells denote statistical significance ($p < 0.1$ = *, $p < 0.05$ = **, $p < 0.01$ = ***).

4.3 Climate and Snow Effects on Seasonal Streamflow

Seasonal relationships between air temperature and snow fraction, air temperature and runoff ratio, and snow fraction and runoff ratio revealed strong relationships that differed among seasons and among watersheds.

Snow fraction was strongly negatively related to air temperature in the winter ($r = -0.80$, $p < 0.001$ (Figure 13), indicating that in winter, the proportion of snow in precipitation decreased as air temperature increased. Runoff ratio was not related to air temperature in the fall or summer (Figures 14, 15, 20, and 21). In the winter, runoff ratio was significantly negatively related to air temperature at two watersheds (WS09 and WS10, $r = -0.51$ and -0.44, respectively, and $p < 0.05$) and marginally related to air temperature at WS02 ($r = -0.40$, $p = 0.056$) (Figures 16 and 17, Table C.2 in Appendix C). In the spring, runoff ratio was significantly negatively related to air temperature at all watersheds ($r = -0.43$ to -0.51, $p = 0.006$ to 0.042) except Mack Creek, which was marginally significant ($r = 0.36$, $p = 0.095$) (Figures 18 and 19, Table C.2 in Appendix C).

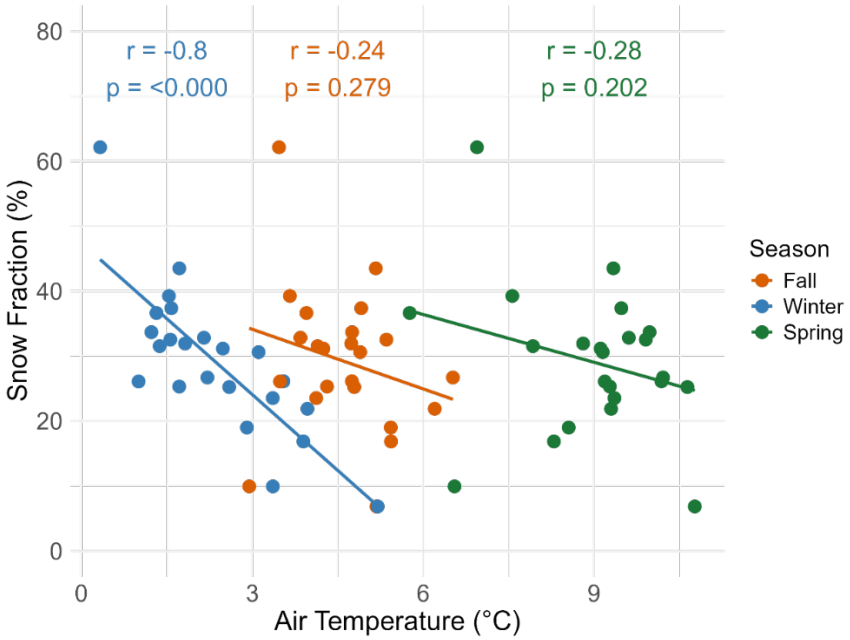

Figure 13. c. Pearson's R correlation coefficient values and p-values are shown for each seasonal linear regression.

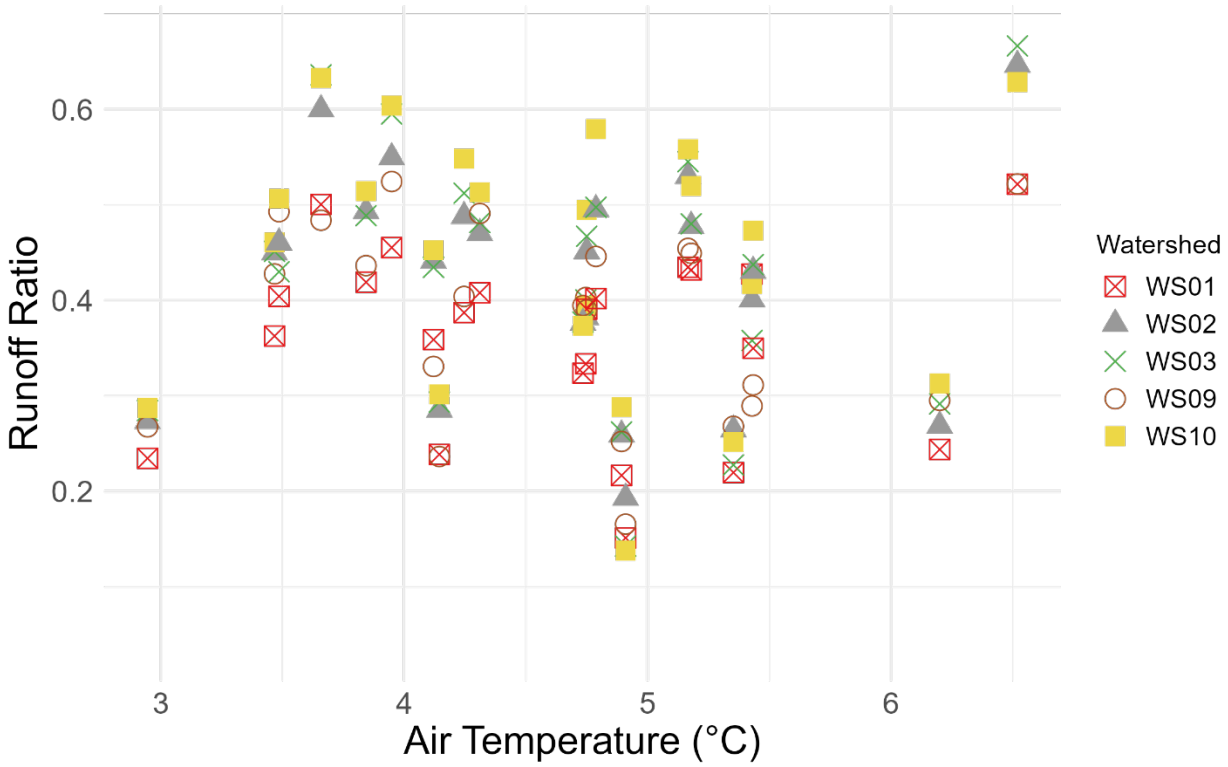

Figure 14. Relationship between runoff ratio and air temperature in fall for five watersheds in the transient snow zone within the Andrews Forest. An absence of regression lines indicates no significant linear relationships ($p > 0.10$ for the regression). Corresponding Pearson correlation coefficients and p-values for each regression are presented in Table C.1 in Appendix C.

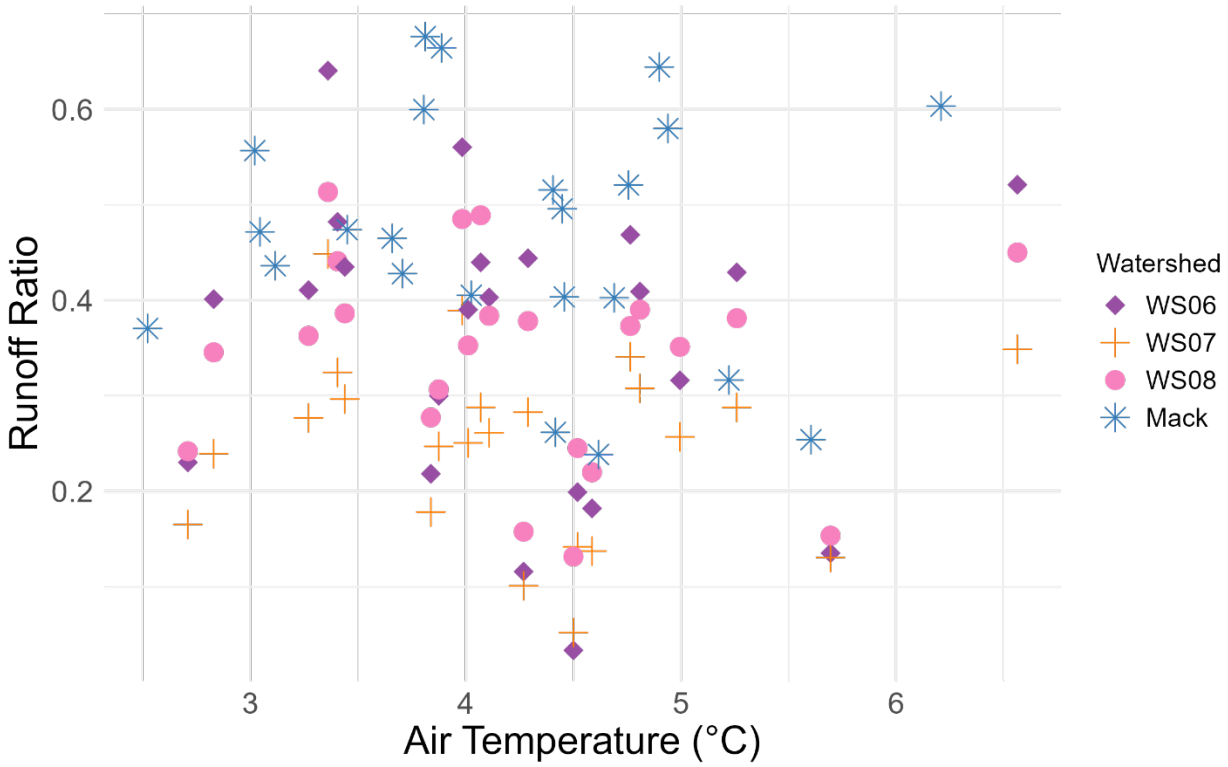

Figure 15. Relationship between runoff ratio and air temperature in fall for four watersheds in the seasonal snow zone within the Andrews Forest. An absence of regression lines indicates no significant linear relationships ($p > 0.10$ for the regression). Corresponding Pearson correlation coefficients and p-values for each regression are presented in Table C.1 in Appendix C.

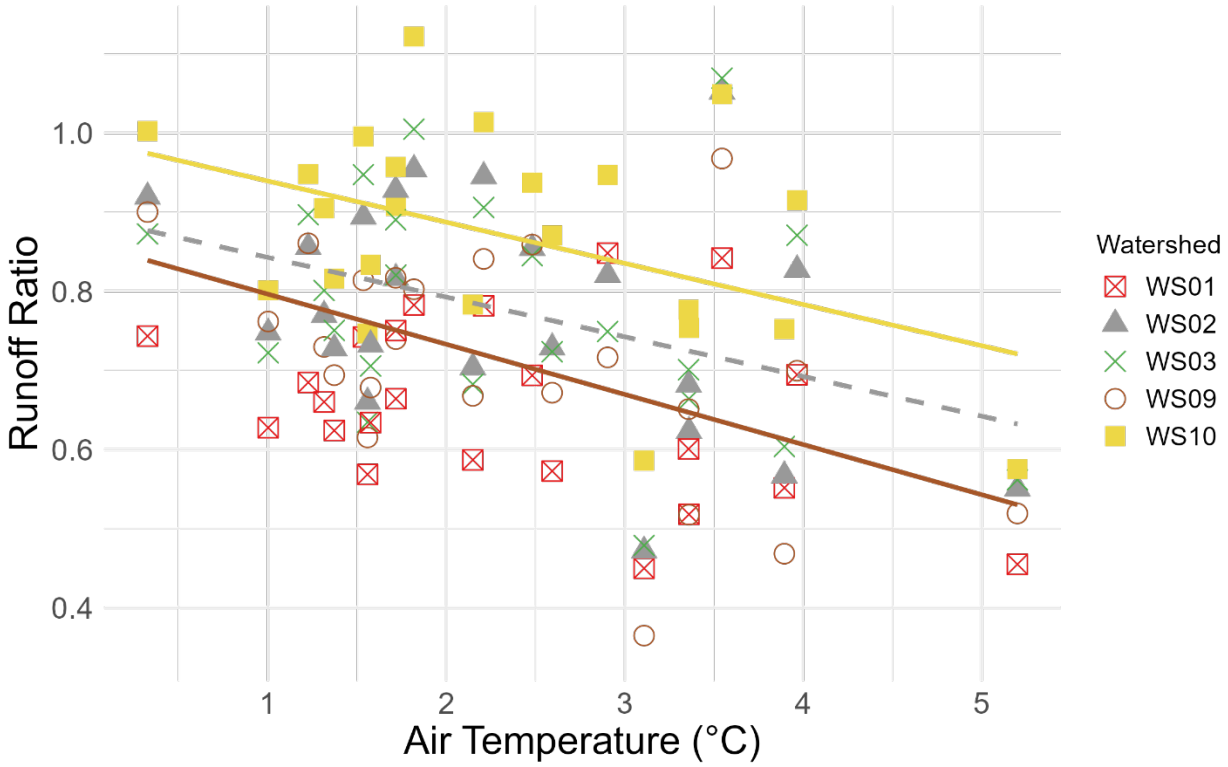

Figure 16. Relationship between runoff ratio and air temperature in winter for five watersheds in the transient snow zone within the Andrews Forest. Solid lines indicate statistically significant regressions ($p < 0.05$ for the regression), and dashed lines indicate marginally significant regressions ($p < 0.1$). Regression lines are omitted for non-significant relationships ($p \geq 0.1$). Corresponding Pearson correlation coefficients and p-values for each regression are presented in Table C.1 in Appendix C.

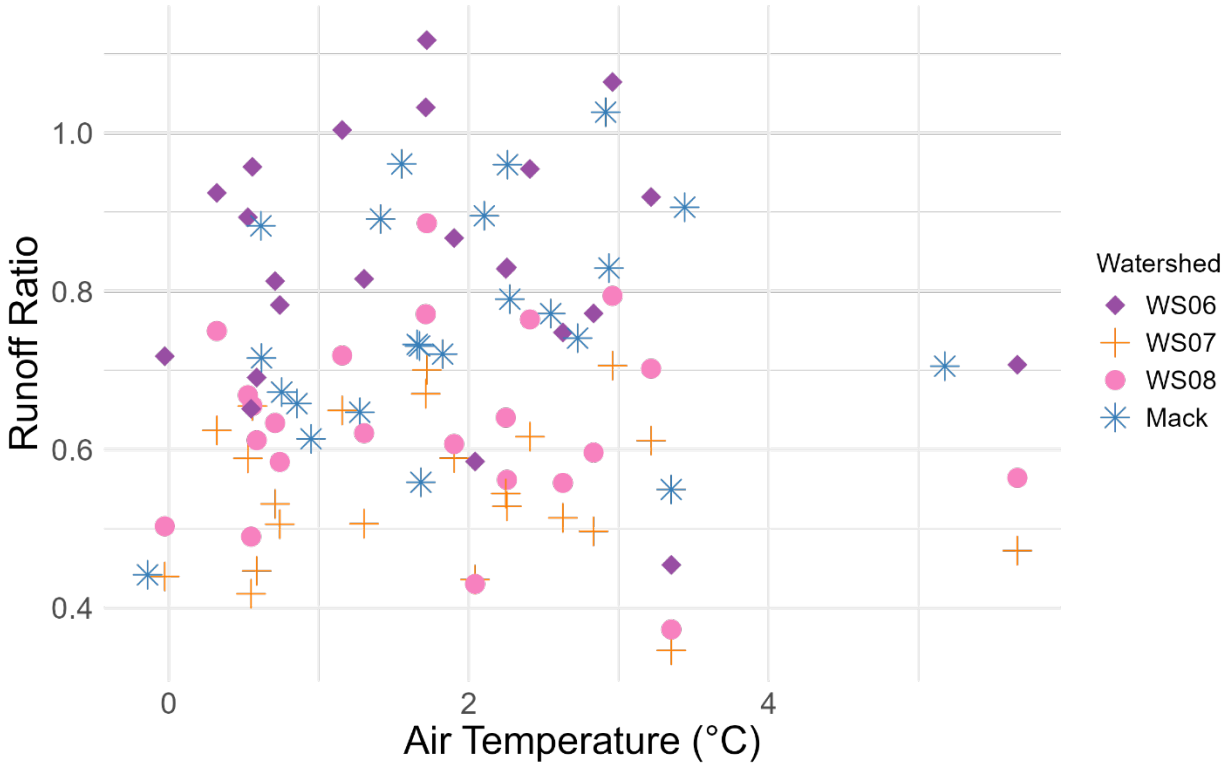

Figure 17. Relationship between runoff ratio and air temperature in winter for four watersheds in the seasonal snow zone within the Andrews Forest. An absence of regression lines indicates no significant linear relationships ($p > 0.10$ for the regression). Corresponding Pearson correlation coefficients and p-values for each regression are presented in Table C.1 in Appendix C.

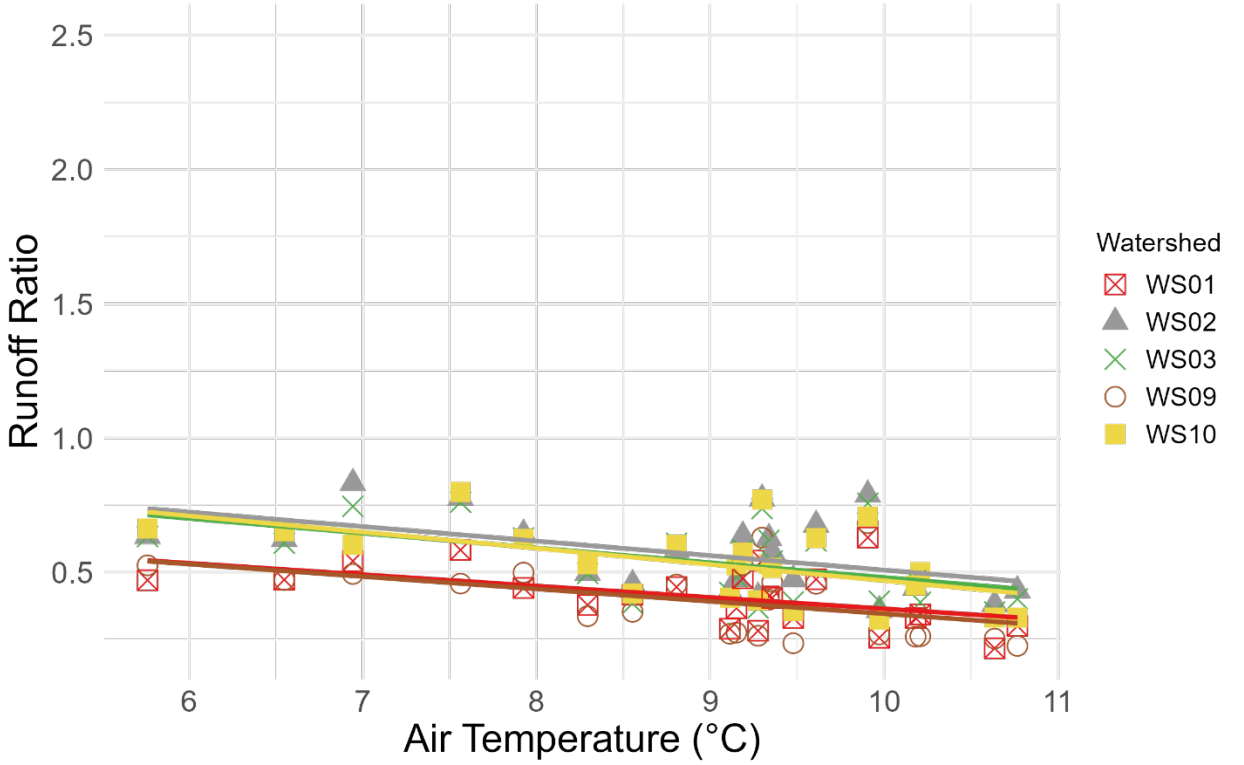

Figure 18. Relationship between runoff ratio and air temperature in spring for five watersheds in the transient snow zone within the Andrews Forest. Solid lines indicate statistically significant regressions ($p < 0.05$ for the regression). Regression lines are omitted for non-significant relationships ($p \geq 0.1$). Corresponding Pearson correlation coefficients and p-values for each regression are presented in Table C.1 in Appendix C.

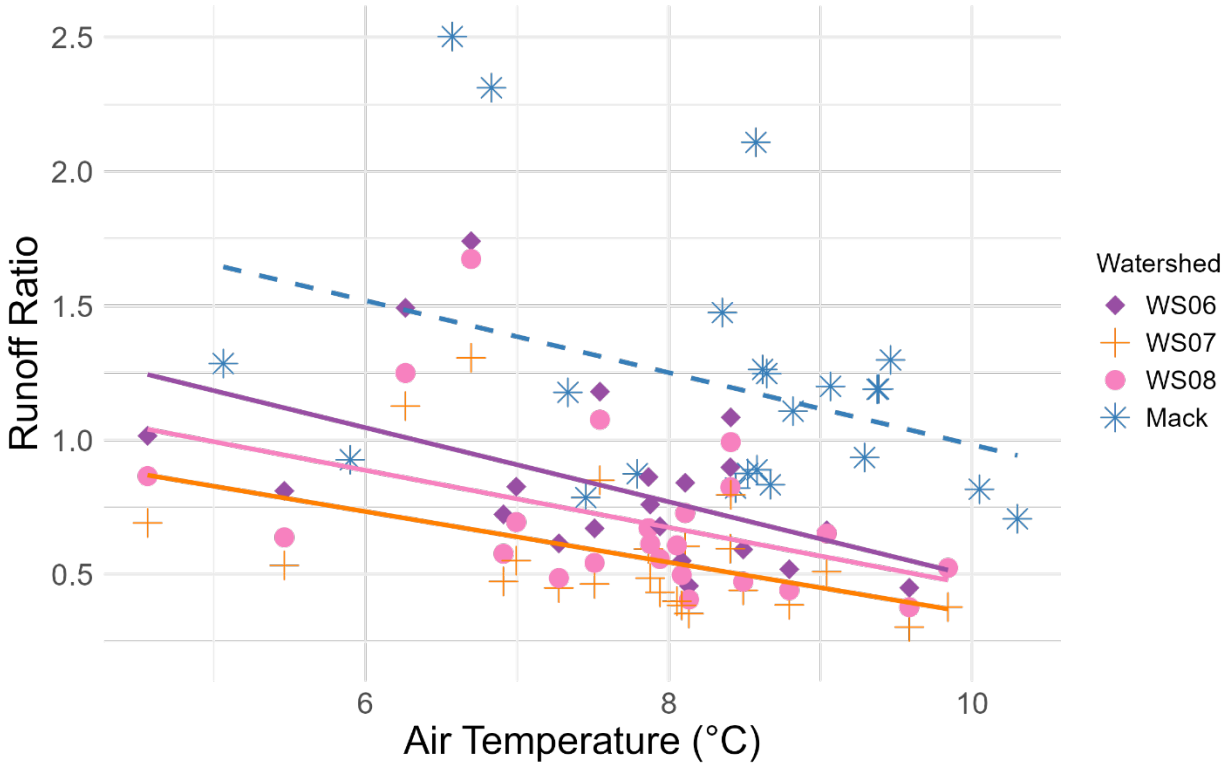

Figure 19. Relationship between runoff ratio and air temperature in spring for four watersheds in the seasonal snow zone within the Andrews Forest. Solid lines indicate statistically significant regressions ($p < 0.05$ for the regression), and dashed lines indicate marginally significant regressions ($p < 0.1$). Corresponding Pearson correlation coefficients and p-values for each regression are presented in Table C.1 in Appendix C.

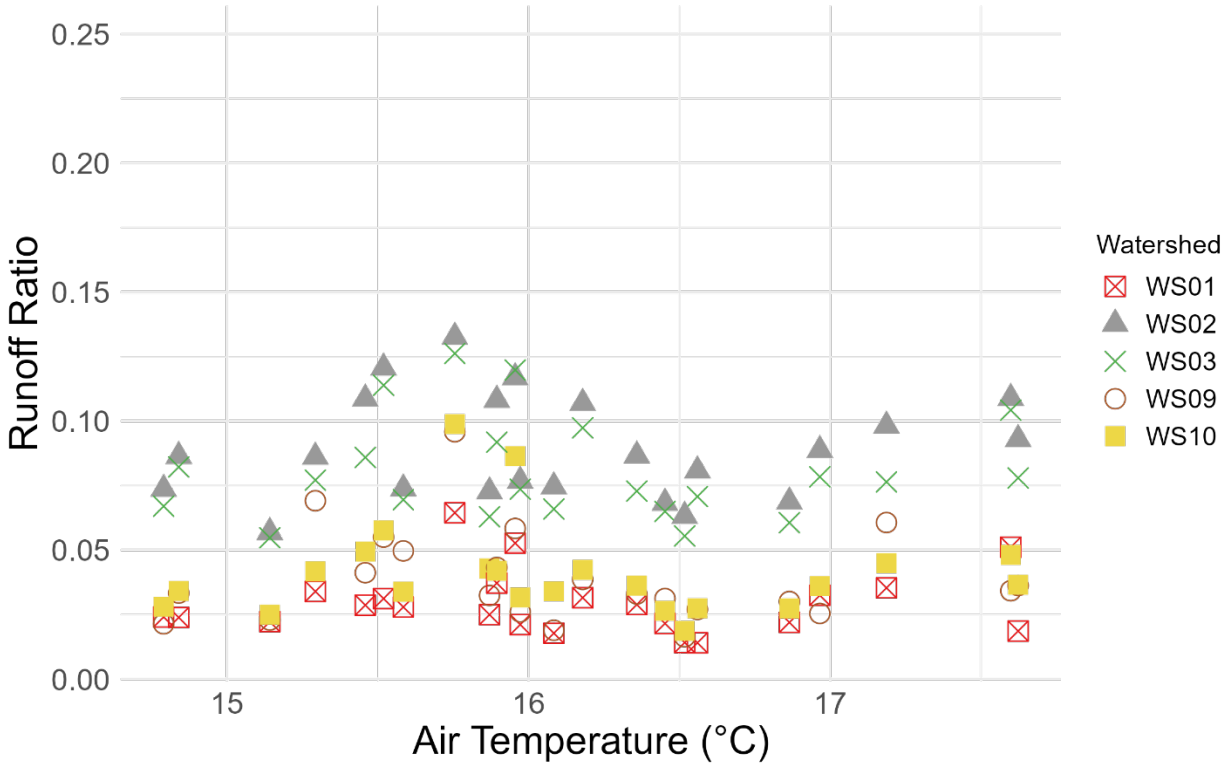

Figure 20. Relationship between runoff ratio and air temperature in summer for five watersheds in the transient snow zone within the Andrews Forest. An absence of regression lines indicates no significant linear relationships ($p > 0.10$ for the regression). Corresponding Pearson correlation coefficients and p-values for each regression are presented in Table C.1 in Appendix C.

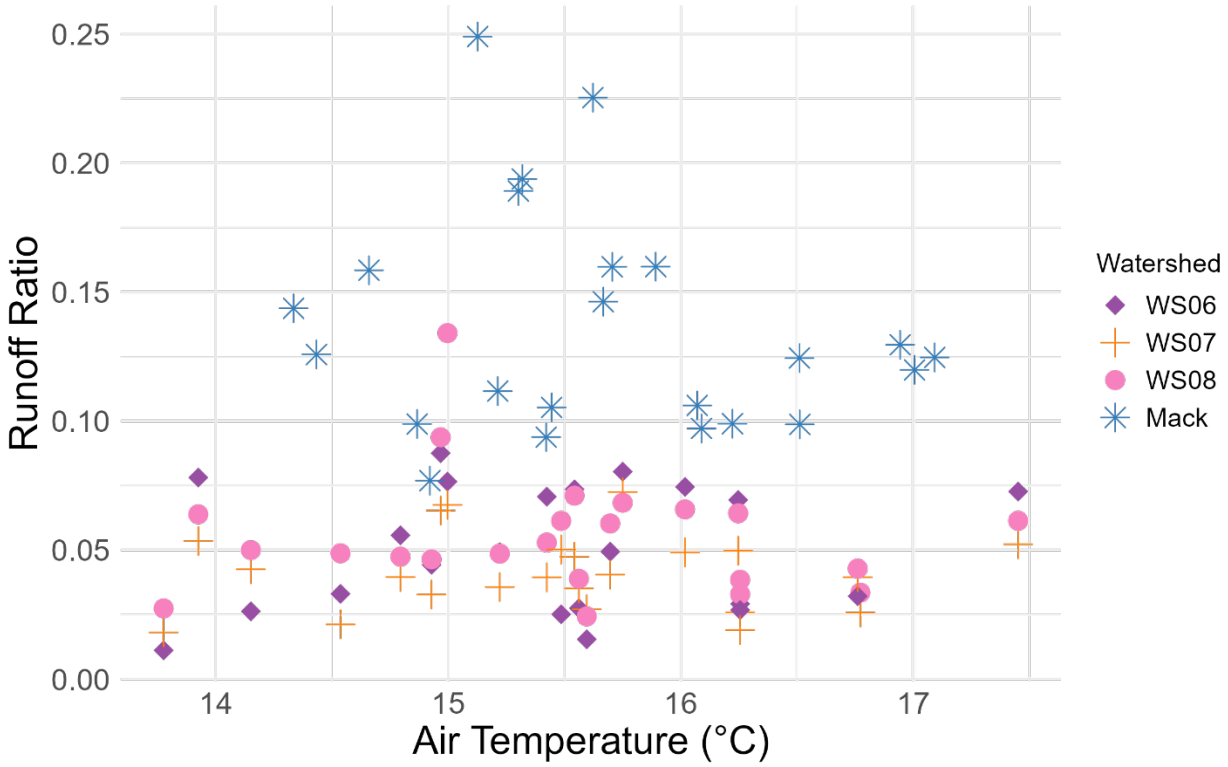

Figure 21. Relationship between runoff ratio and air temperature in summer for four watersheds in the seasonal snow zone within the Andrews Forest. An absence of regression lines indicates no significant linear relationships ($p > 0.10$ for the regression). Summer runoff ratio was calculated as the ratio of summer runoff to spring precipitation (see text, section 3.4). Corresponding Pearson correlation coefficients and p-values for each regression are presented in Table C.1 in Appendix C.

Residuals of the relationship of runoff ratio to air temperature (Figures 22 to 33) were negatively related to water year only in winter at transient snow zone watersheds, WS01, WS02, WS03, and WS10 ($r = –0.41$ to $–0.53$, $p \leq 0.05$) (Figure 22), and not in any other combination of watershed or season, nor in the seasonal snow zone (Figures 23 to 25, Table C.3 in Appendix C). Residuals of the relationship between winter runoff ratio to air temperature shift from positive to negative over the study period, indicating that controlling for air temperature, winter runoff ratio has declined over the study period.

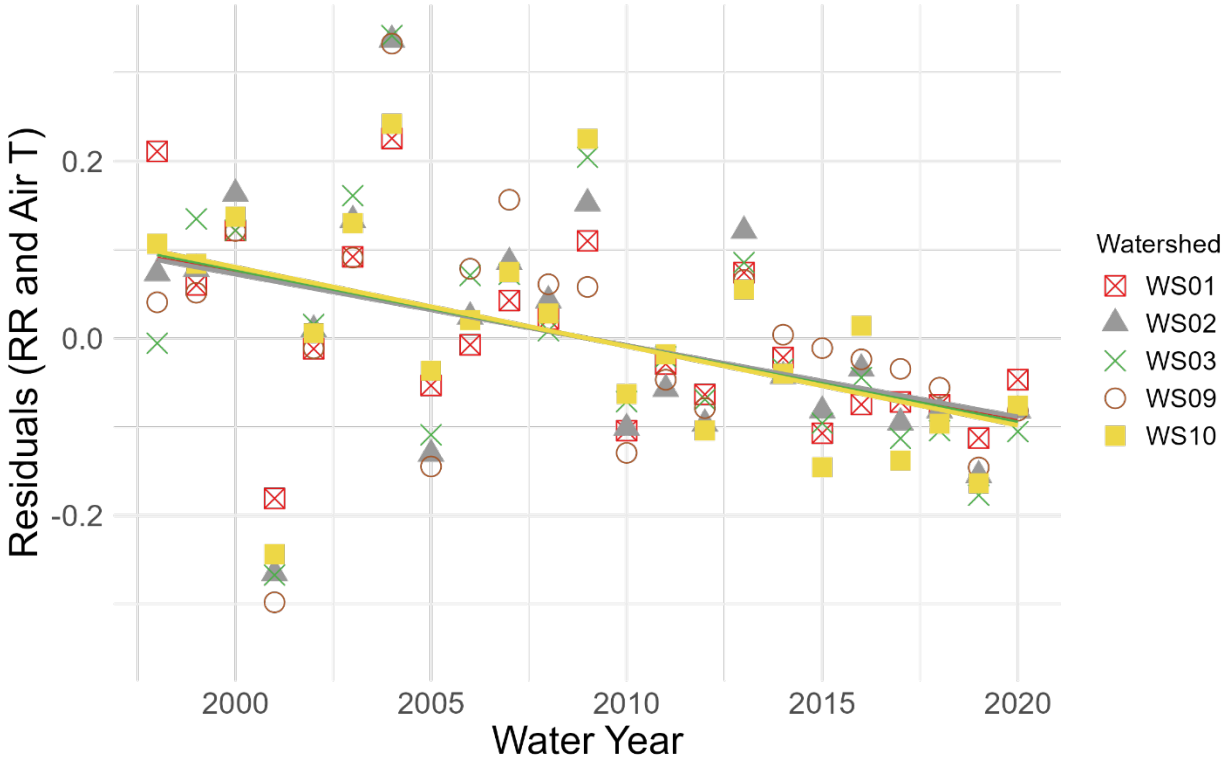

Figure 22. Residuals from linear regressions between winter runoff ratio and air temperature (from Figure 16) for watersheds in the transient snow zone, plotted against water year. Solid lines indicate statistically significant regressions ($p < 0.05$ for the regression), and an absence of regression lines indicates no significant linear relationships ($p > 0.10$). Corresponding Pearson correlation coefficients and p-values for each regression are presented in Table C.3 in Appendix C.

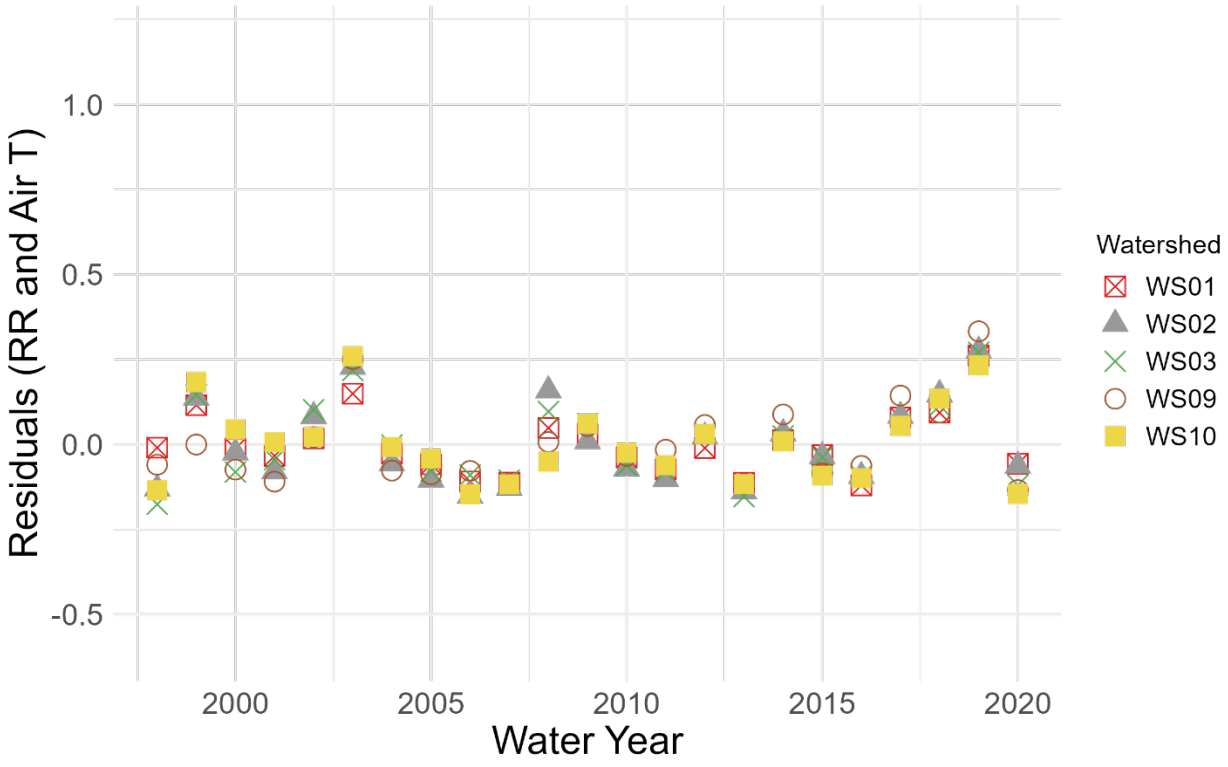

Figure 23. Residuals from linear regressions between spring runoff ratio and air temperature (from Figure 18) for watersheds in the transient snow zone, plotted against water year. Corresponding Pearson correlation coefficients and p-values for each regression are presented in Table B.2 in Appendix B. An absence of regression lines indicates no significant linear relationships ($p > 0.10$ for the regression). Corresponding Pearson correlation coefficients and p-values for each regression are presented in Table C.3 in Appendix C.

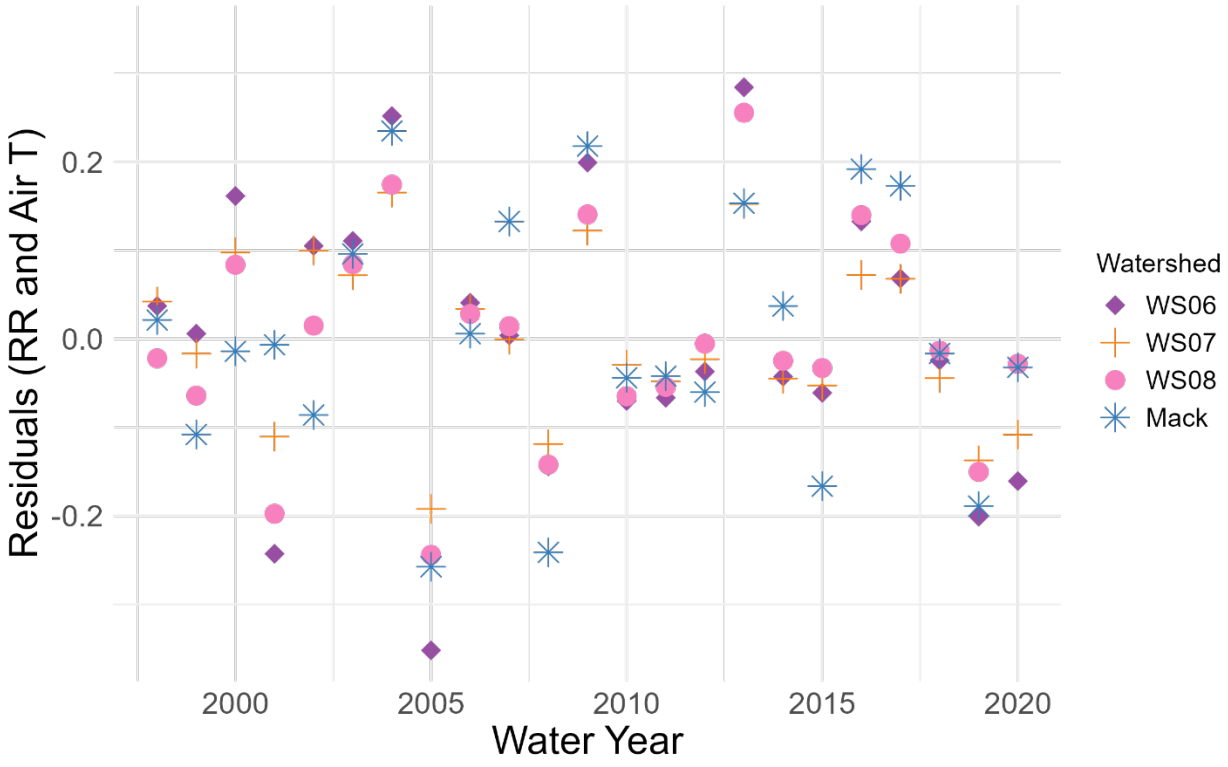

Figure 24. Residuals from linear regressions between winter runoff ratio and air temperature (from Figure 17) for watersheds in the seasonal snow zone, plotted against water year. An absence of regression lines indicates no significant linear relationships ($p > 0.10$ for the regression). Corresponding Pearson correlation coefficients and p-values for each regression are presented in Table C.3 in Appendix C.

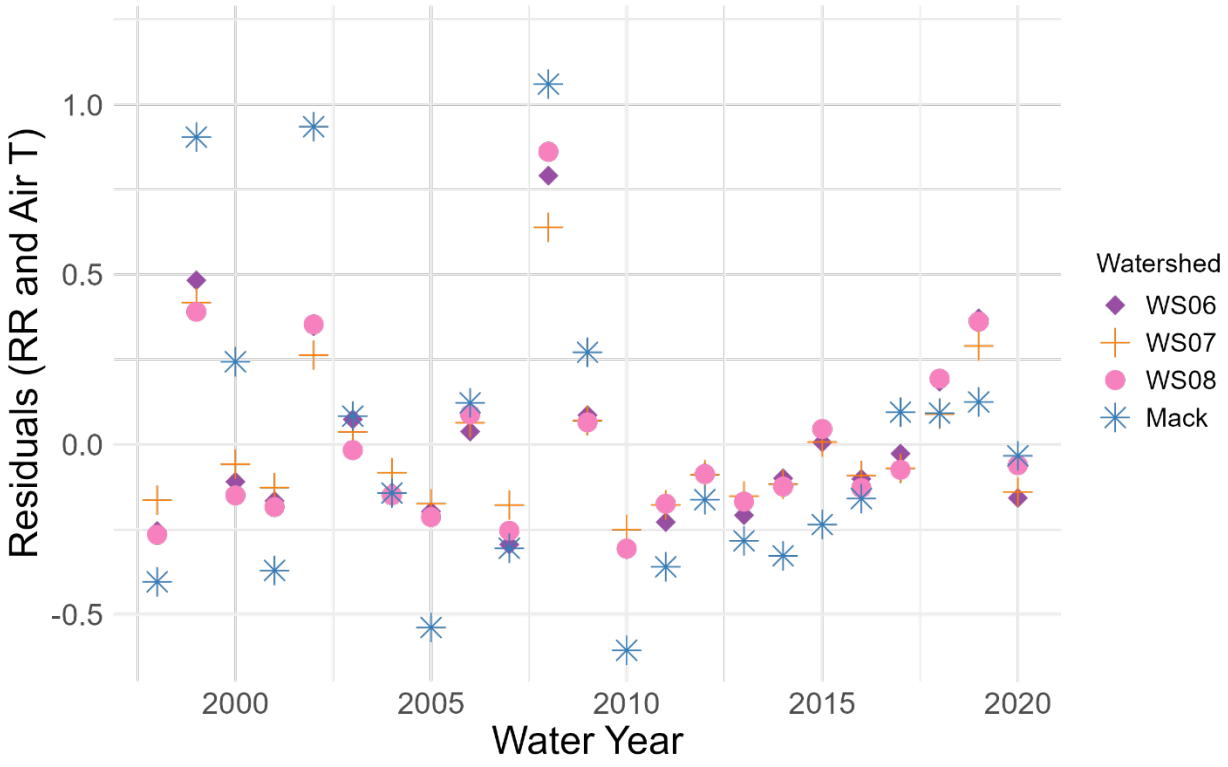

Figure 25. Residuals from linear regressions between spring runoff ratio and air temperature (from Figure 19) for watersheds in the seasonal snow zone, plotted against water year. An absence of regression lines indicates no significant linear relationships ($p > 0.10$ for the regression). Corresponding Pearson correlation coefficients and p-values for each regression are presented in Table C.3 in Appendix C.

Residuals of the relationship between runoff ratio and air temperature were not related in in any combination of watershed or season (Figures 26 to 28, Table C.3 in Appendix C), except for in Mack Creek in the spring. In the Mack Creek in the spring, residuals were negatively and marginally ($p > 0.05$ and <0.1) related to precipitation ($r = –0.38$ to $–0.48$, $p = 0.072$) (Figure 29 Table C.3 in Appendix C). Residuals of the relationship between spring runoff ratio and air temperature shift from positive to negative as precipitation increases at Mack Creek, indicating that controlling for air temperature, spring runoff ratio declines with increases in spring precipitation.

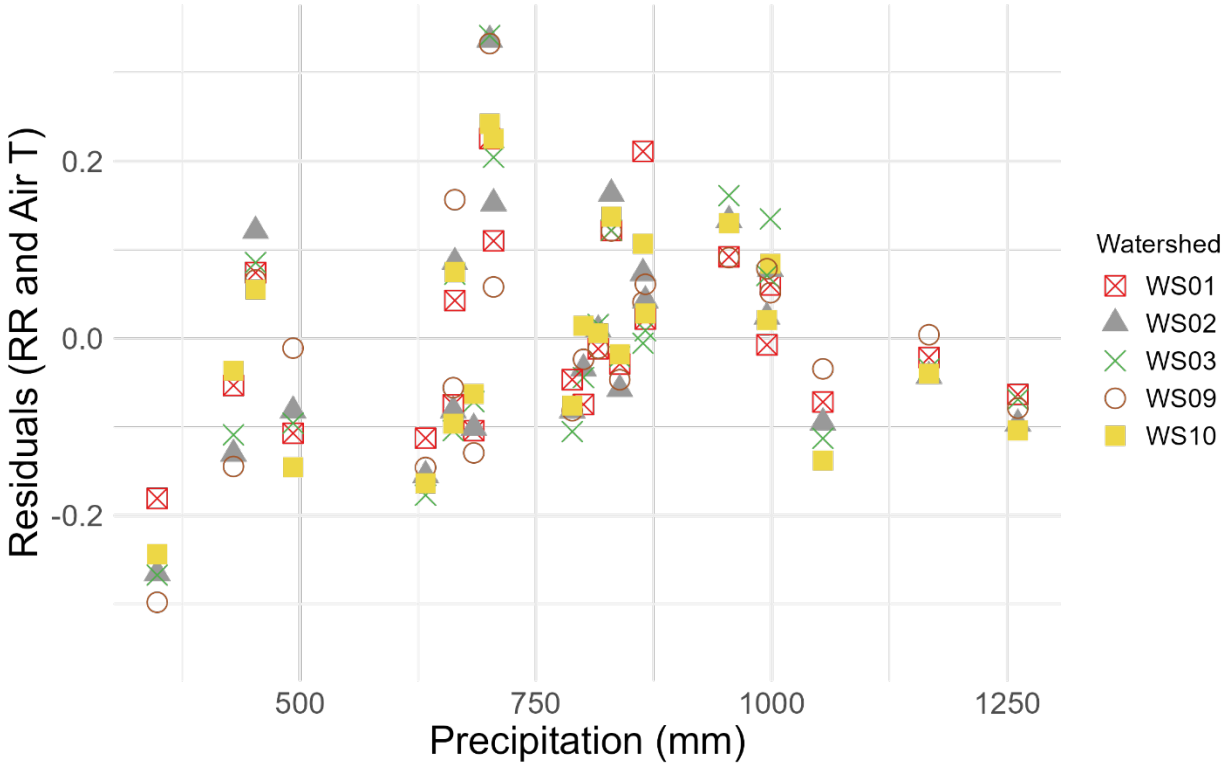

Figure 26. Residuals from linear regressions between winter runoff ratio and air temperature (from Figure 16) for watersheds in the transient snow zone, plotted against precipitation. An absence of regression lines indicates no significant linear relationships ($p > 0.10$ for the regression). Corresponding Pearson correlation coefficients and p-values for each regression are presented in Table C.3 in Appendix C.

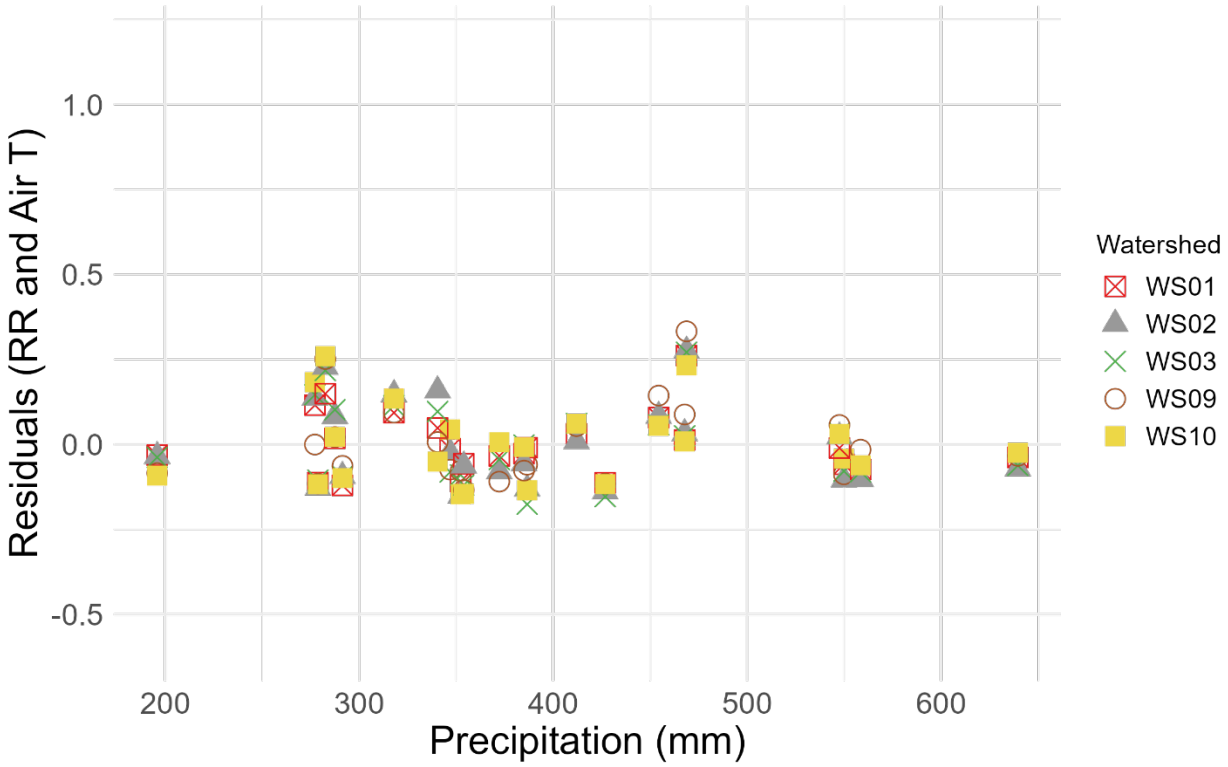

Figure 27. Residuals from linear regressions between spring runoff ratio and air temperature (from Figure 18) for watersheds in the transient snow zone, plotted against precipitation. An absence of regression lines indicates no significant linear relationships ($p > 0.10$ for the regression). Corresponding Pearson correlation coefficients and p-values for each regression are presented in Table C.3 in Appendix C.

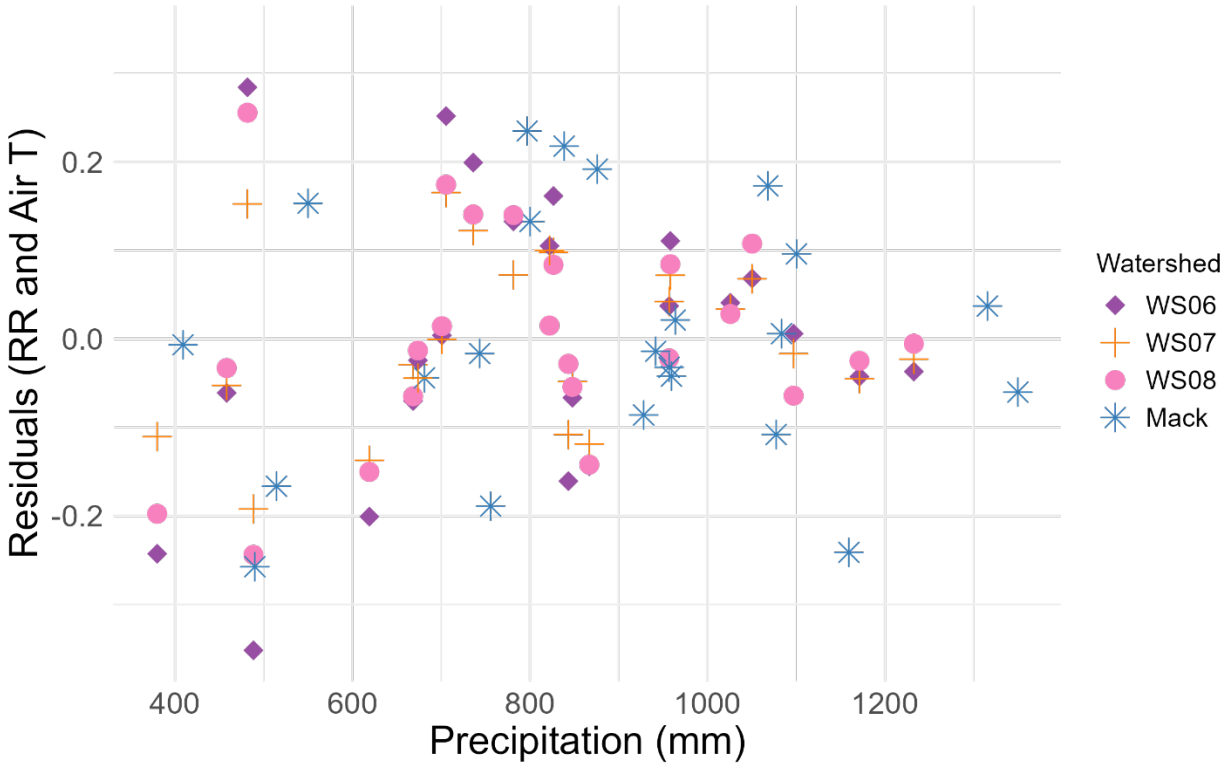

Figure 28. Residuals from linear regressions between winter runoff ratio and air temperature (from Figure 17) for watersheds in the seasonal snow zone, plotted against precipitation. An absence of regression lines indicates no significant linear relationships ($p > 0.10$ for the regression). Corresponding Pearson correlation coefficients and p-values for each regression are presented in Table C.3 in Appendix C.

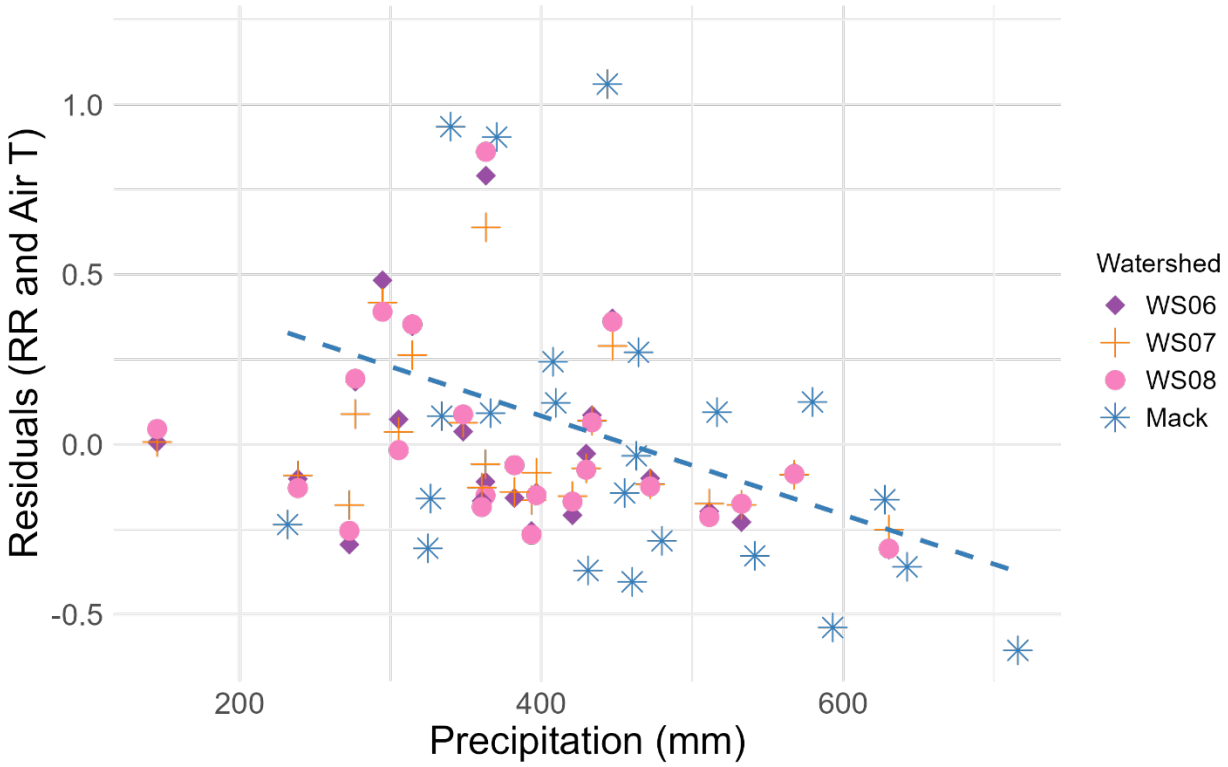

Figure 29. Residuals from linear regressions between spring runoff ratio and air temperature (from Figure 19) for watersheds in the seasonal snow zone, plotted against precipitation. Dashed lines indicate marginally significant regressions ($p < 0.1$ for the regression), and an absence of regression lines indicates no significant linear relationships ($p > 0.10$). Corresponding Pearson correlation coefficients and p-values for each regression are presented in Table C.3 in Appendix C.

Residuals of the relationship between runoff ratio and air temperature were positively related to snow fraction only in spring and only in seasonal snow zone watersheds, WS06, WS07, WS08 ($r = 0.37$ to 0.40, $p = 0.060$ to 0.080), and Mack Creek ($r = 0.77$, $p \leq 0.001$), and not in any other combination of watershed and season (Figures 30 to 33, Table C.3 in Appendix C). Residuals of the relationship of spring runoff ratio to air temperature shift from negative to positive as snow fraction increases in the seasonal snow zone, indicating that controlling for air temperature, spring runoff ratio increases with snow fraction.

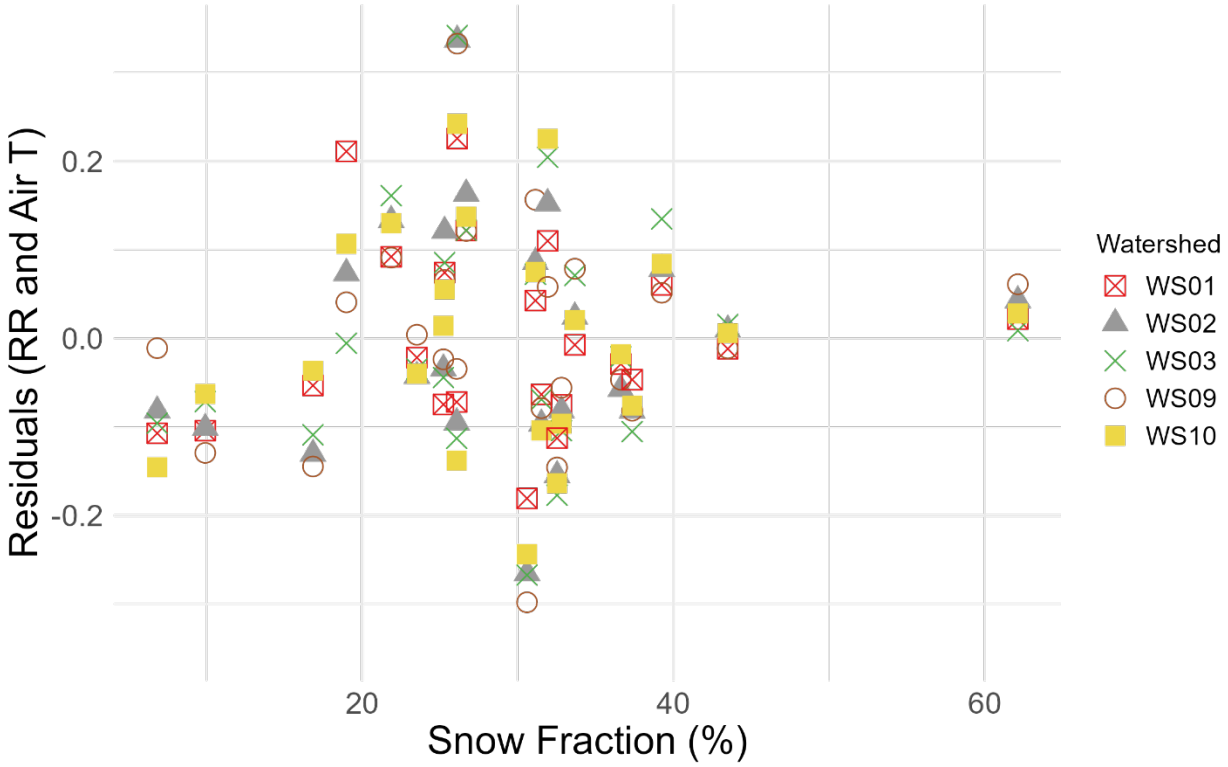

Figure 30. Residuals from linear regressions between winter runoff ratio and air temperature (from Figure 16) for watersheds in the transient snow zone, plotted against snow fraction. An absence of regression lines indicates no significant linear relationships ($p > 0.10$ for the regression). Corresponding Pearson correlation coefficients and p-values for each regression are presented in Table C.3 in Appendix C.

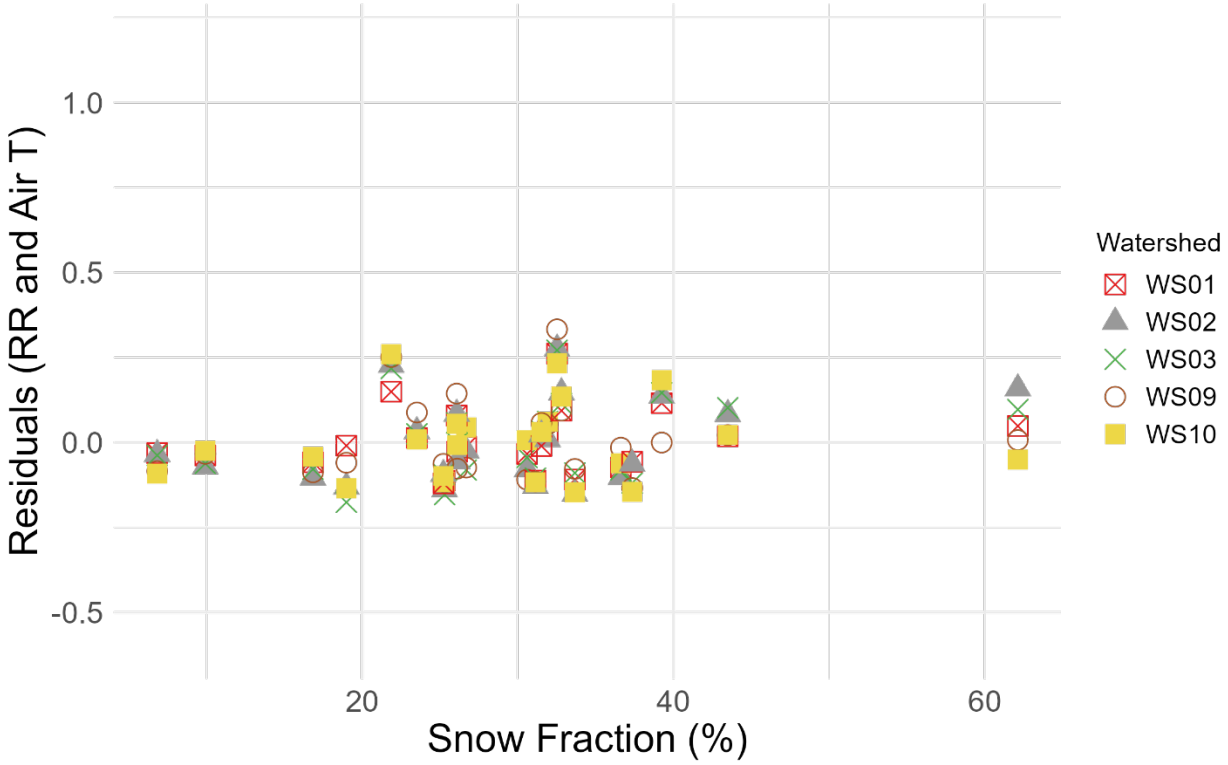

Figure 31. Residuals from linear regressions between spring runoff ratio and air temperature (from Figure 18) for watersheds in the transient snow zone, plotted against snow fraction. An absence of regression lines indicates no significant linear relationships ($p > 0.10$ for the regression). Corresponding Pearson correlation coefficients and p-values for each regression are presented in Table C.3 in Appendix C.

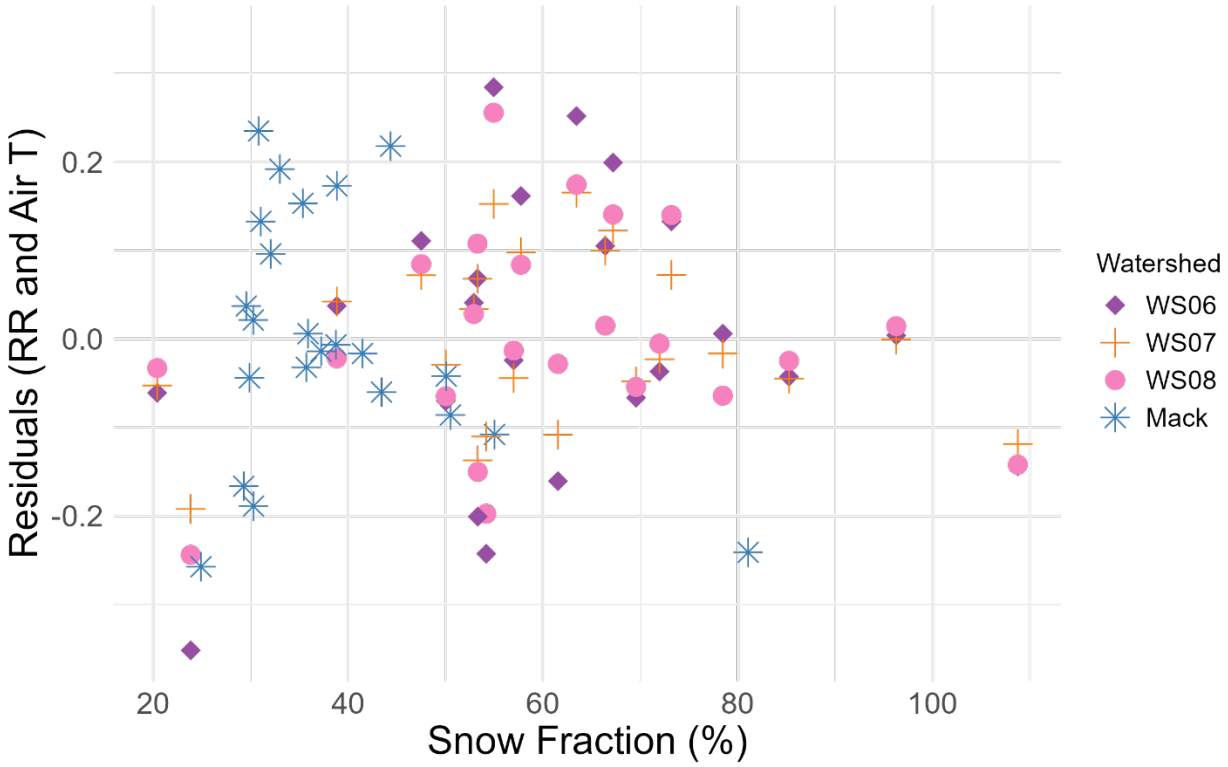

Figure 32. Residuals from linear regressions between winter runoff ratio and air temperature (from Figure 17) for watersheds in the seasonal snow zone, plotted against snow fraction. An absence of regression lines indicates no significant linear relationships ($p > 0.10$ for the regression). Corresponding Pearson correlation coefficients and p-values for each regression are presented in Table C.3 in Appendix C.

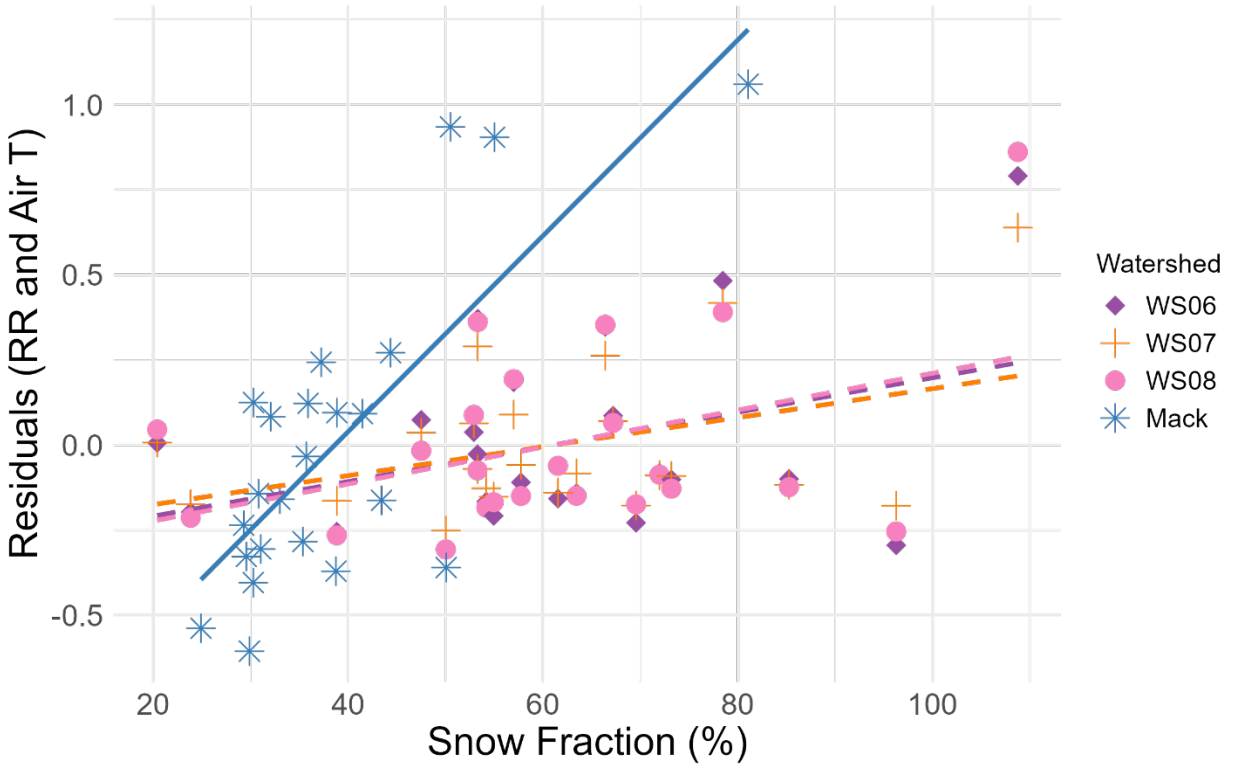

Figure 33. Residuals from linear regressions between spring runoff ratio and air temperature (from Figure 19) for watersheds in the seasonal snow zone, plotted against snow fraction. Solid lines indicate statistically significant regressions ($p < 0.05$ for the regression), dashed lines indicate marginally significant regressions ($p < 0.1$), and an absence of regression lines indicates no significant linear relationships ($p > 0.10$). Corresponding Pearson correlation coefficients and p-values for each regression are presented in Table C.3 in Appendix C.

Runoff ratio relationships to snow fraction varied by seasonal and snow zone (Figure 34 to 41). Runoff ratio was not related to snow fraction in the fall (Figures 34 and 35, Table C.4 in Appendix C). However, it was positively related to snow fraction at several transient snow zone watersheds (WS02, WS03, WS09, and WS10) in the winter ($r = 0.36$ to 0.48, $p \leq 0.1$) (Figure 36, Table C.4 in Appendix C). In contrast, runoff ratio was negatively related to snow fraction only in the winter at Mack Creek, the highest-elevation watershed in the seasonal snow zone ($r = -0.48$, $p = 0.021$), but was not related to snow fraction in any other seasonal snow zone watersheds (Figure 37, Table C.4 in Appendix C).

Runoff ratio in the spring was significantly positively related to snow fraction at WS02, WS03, WS06, WS07, and WS08 ($r = 0.42$ to 0.45) (Figures 38 and 39, Table C.4 in Appendix C) and very strongly related to snow fraction at Mack Creek ($r = 0.88$, $p < 0.001$) (Figure 39, Table C.4 in Appendix C). Runoff ratio in the summer was significantly positively related to snow fraction only at Mack Creek ($r = 0.54$, $p = 0.008$) (Figure 41, Table C.4 in Appendix C).

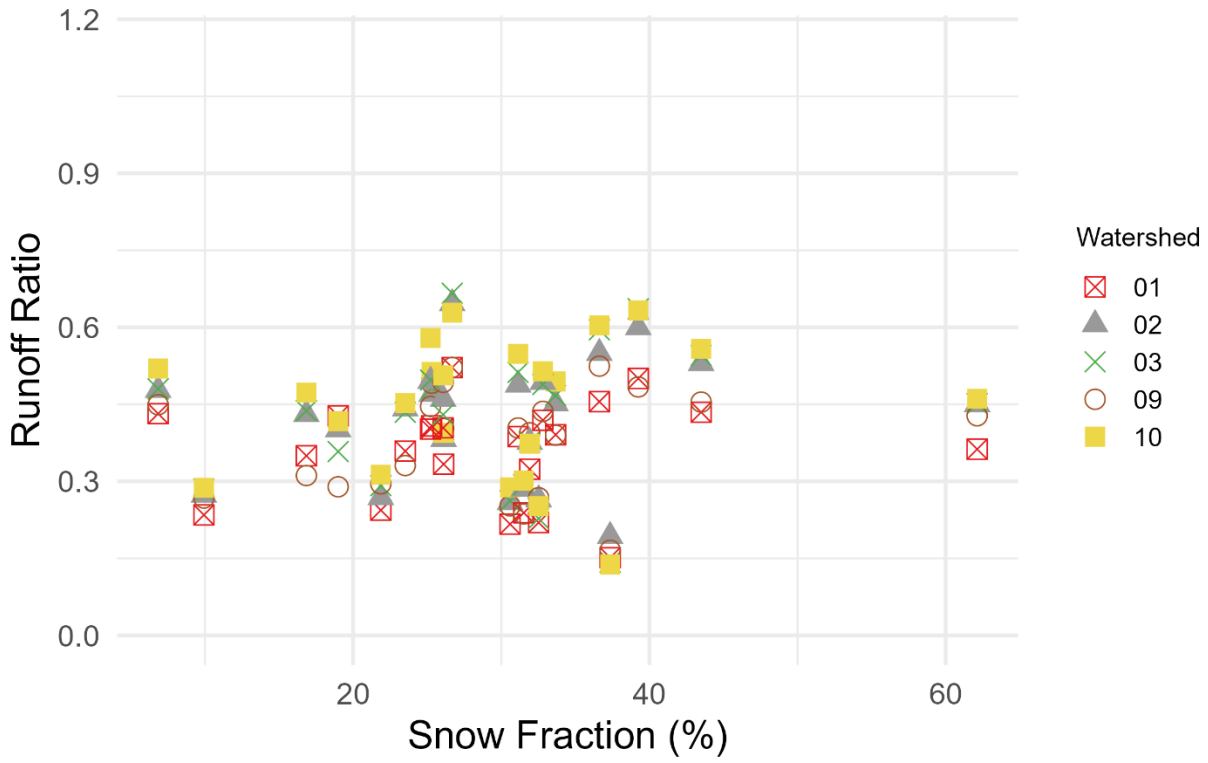

Figure 34. Linear regression relationships between runoff ratio and snow fraction in transient snow zone watersheds in the fall. An absence of regression lines indicates no significant linear relationships ($p > 0.10$). Corresponding Pearson correlation coefficients and p-values for each regression are presented in Table C.4 in Appendix C.

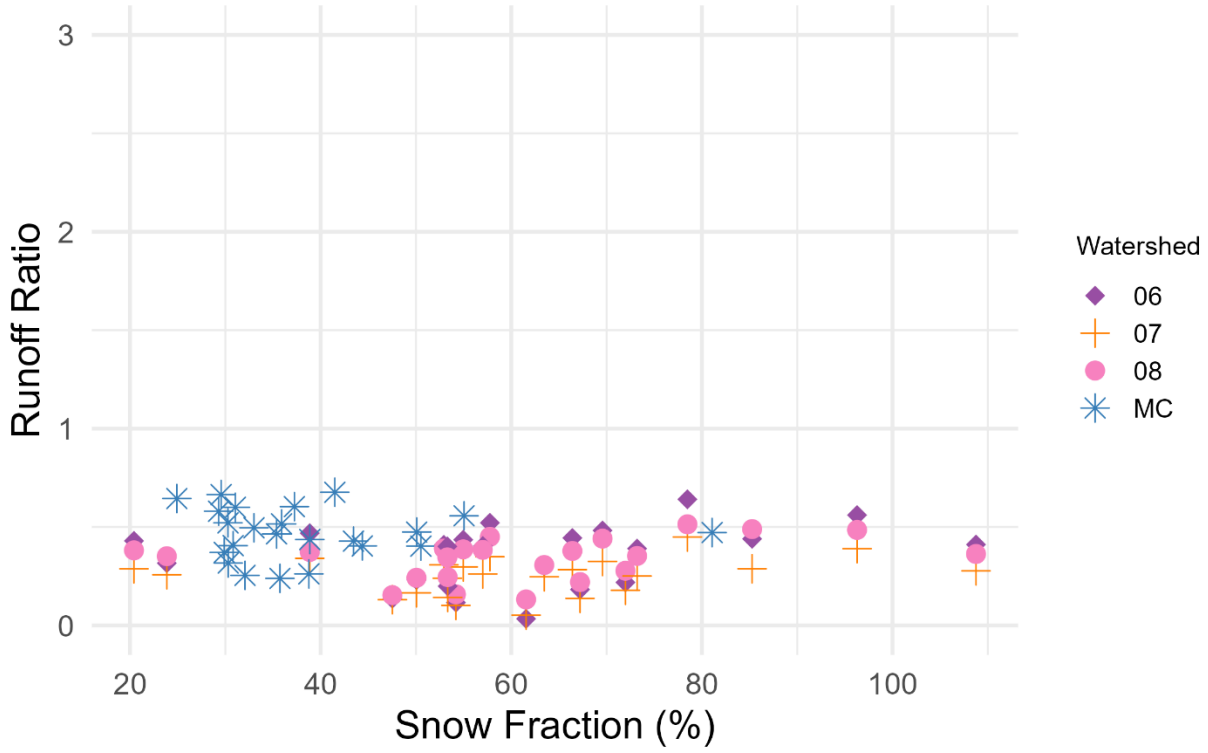

Figure 35. Linear regression relationships between runoff ratio and snow fraction in seasonal snow zone watersheds in the fall. An absence of regression lines indicates no significant linear relationships ($p > 0.10$). Corresponding Pearson correlation coefficients and p-values for each regression are presented in Table C.4 in Appendix C.

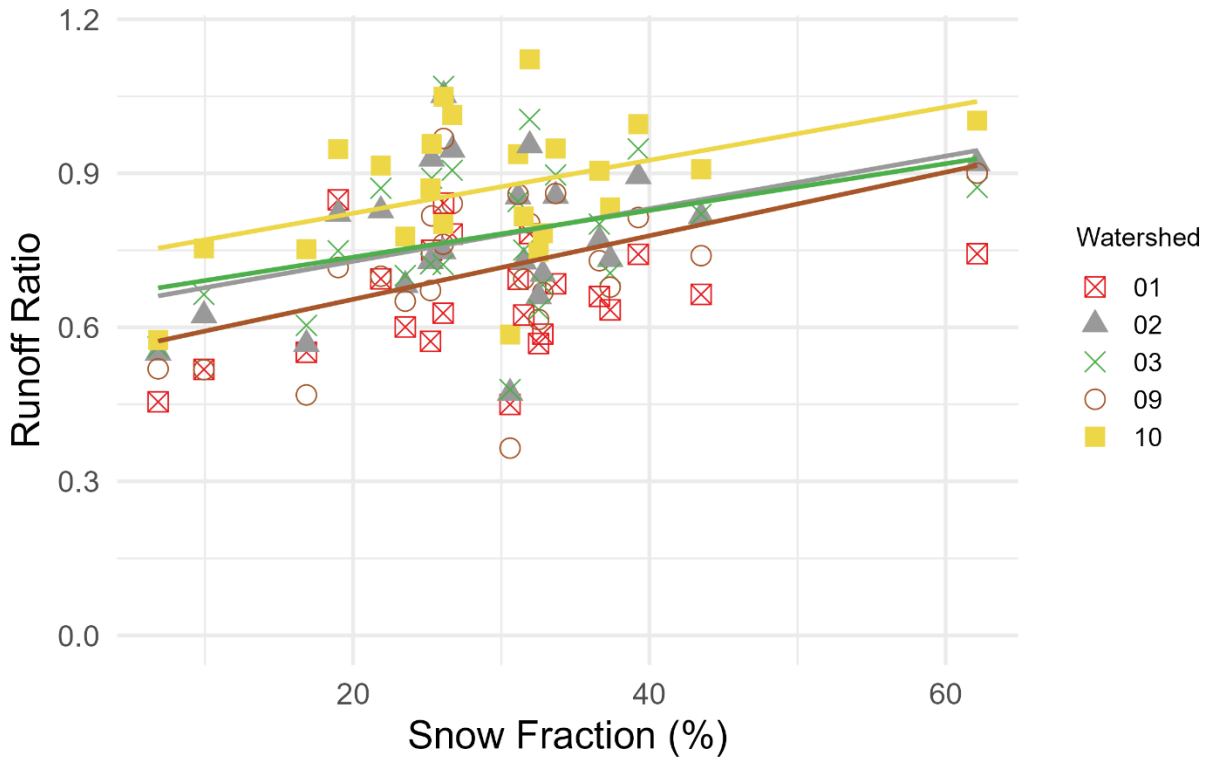

Figure 36. Linear regression relationships between runoff ratio and snow fraction in transient snow zone watersheds in the winter. Solid lines indicate statistically significant regressions ($p < 0.05$ for the regression). An absence of regression lines indicates no significant linear relationships ($p > 0.10$). Corresponding Pearson correlation coefficients and p-values for each regression are presented in Table C.4 in Appendix C.

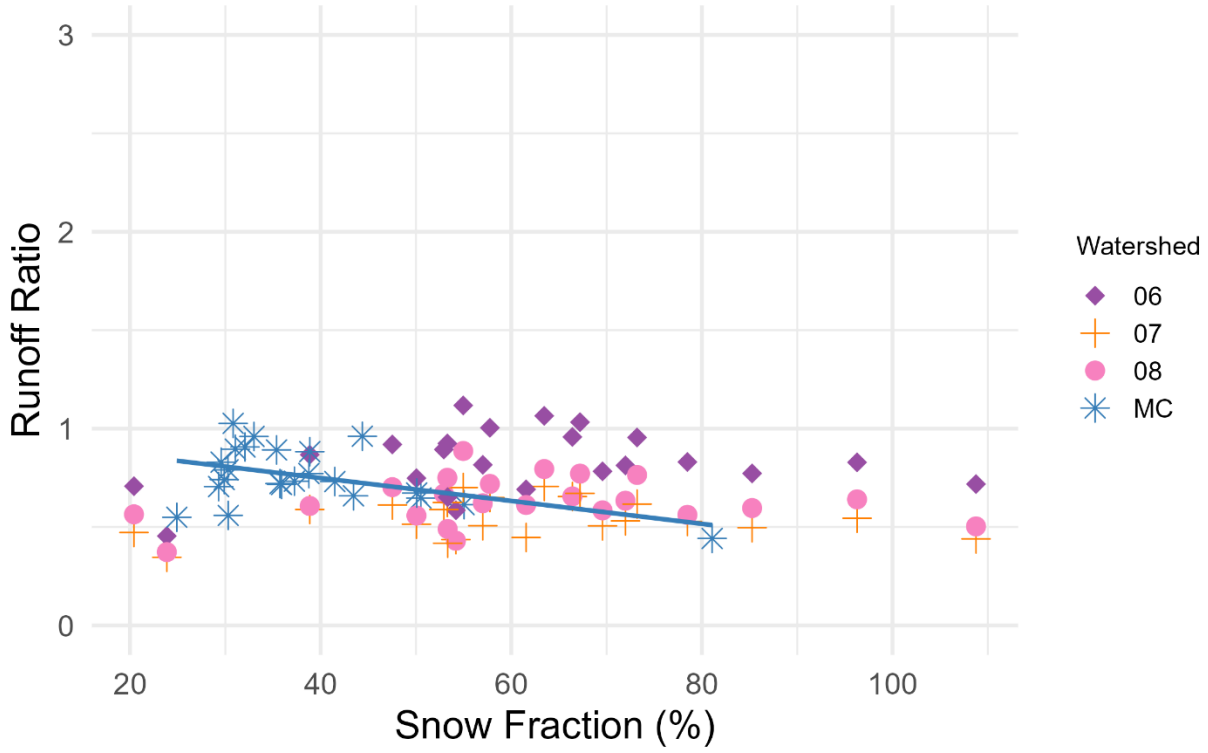

Figure 37. Linear regression relationships between runoff ratio and snow fraction in seasonal snow zone watersheds in the winter. Solid lines indicate statistically significant regressions ($p < 0.05$ for the regression). An absence of regression lines indicates no significant linear relationships ($p > 0.10$). Corresponding Pearson correlation coefficients and p-values for each regression are presented in Table C.4 in Appendix C.

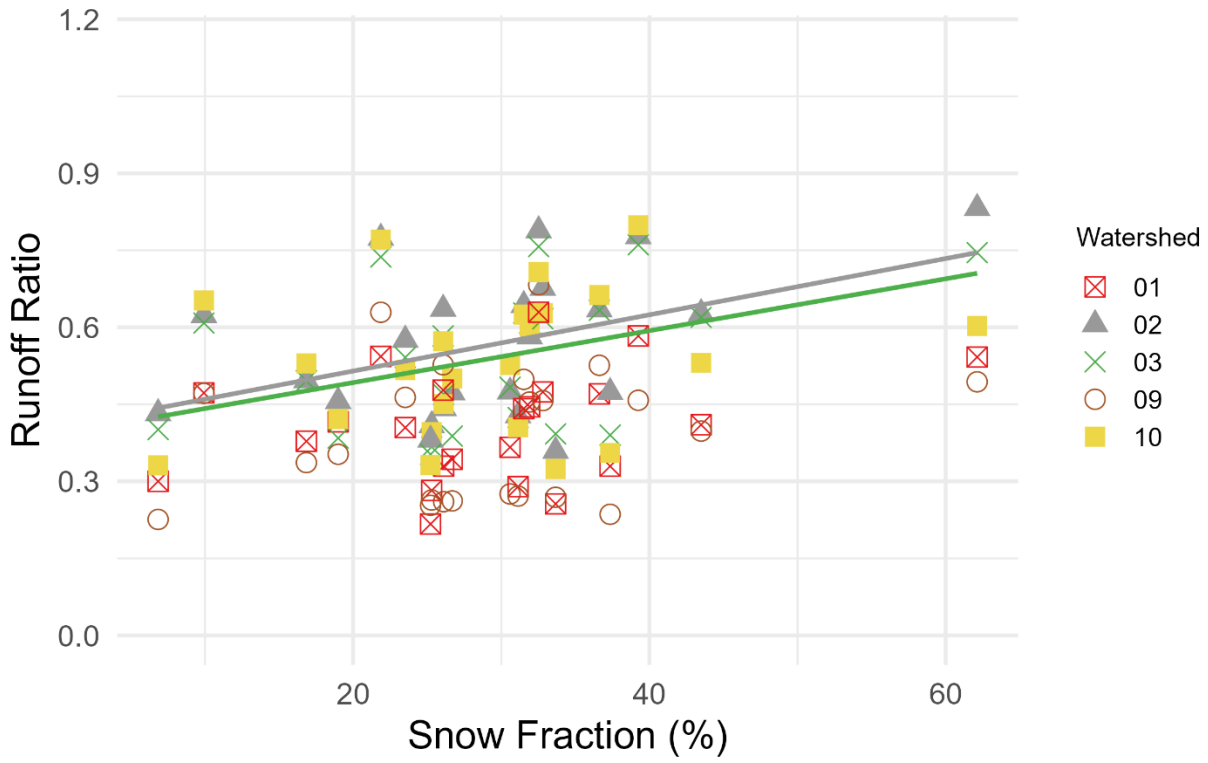

Figure 38. Linear regression relationships between runoff ratio and snow fraction in transient snow zone watersheds in the spring. Solid lines indicate statistically significant regressions ($p < 0.05$ for the regression). An absence of regression lines indicates no significant linear relationships ($p > 0.10$). Corresponding Pearson correlation coefficients and p-values for each regression are presented in Table C.4 in Appendix C.

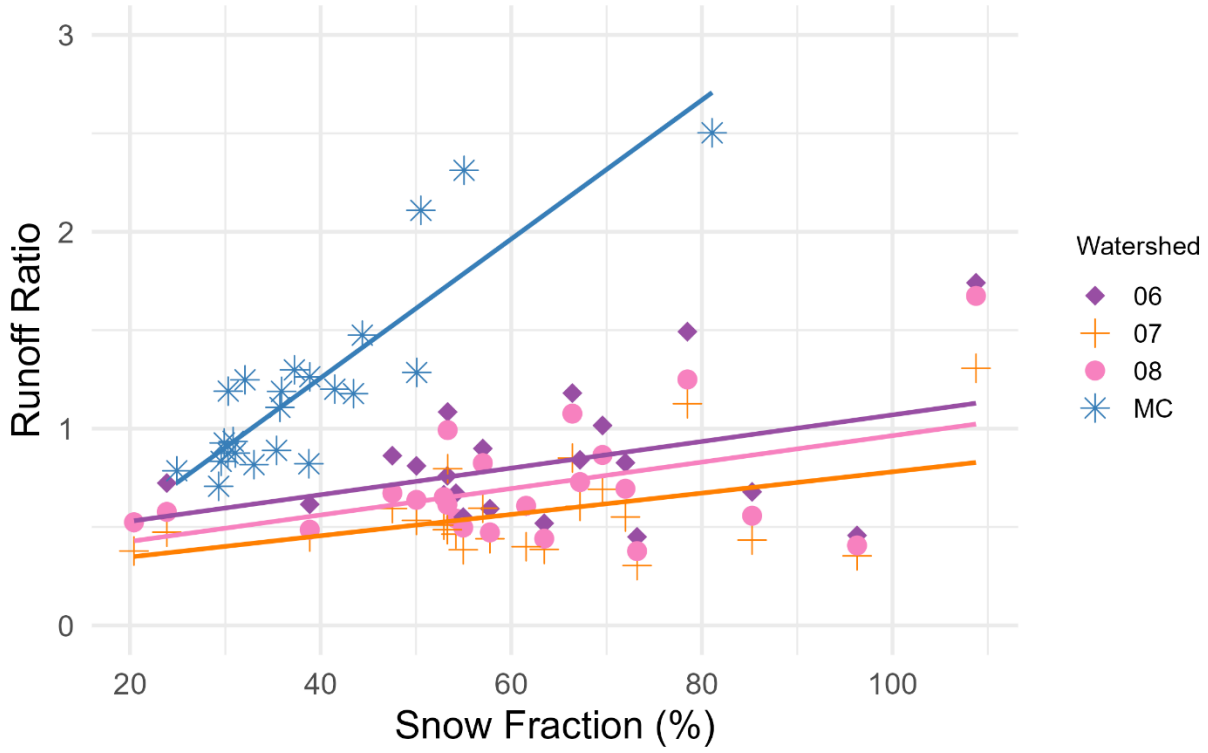

Figure 39. Linear regression relationships between runoff ratio and snow fraction in seasonal snow zone watersheds in the spring. Solid lines indicate statistically significant regressions ($p < 0.05$ for the regression). Corresponding Pearson correlation coefficients and p-values for each regression are presented in Table C.4 in Appendix C.

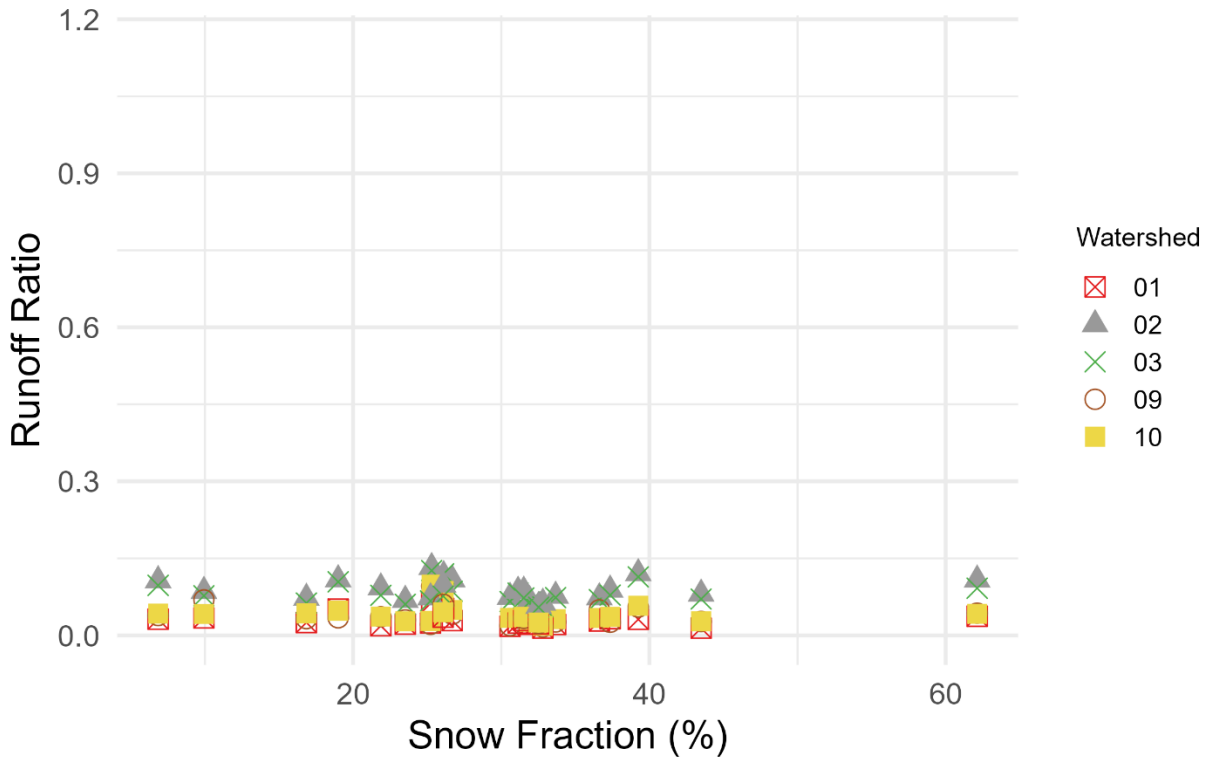

Figure 40. Linear regression relationships between runoff ratio and snow fraction in transient snow zone watersheds in the summer. An absence of regression lines indicates no significant linear relationships ($p > 0.10$). Corresponding Pearson correlation coefficients and p-values for each regression are presented Table C.4 in Appendix C.

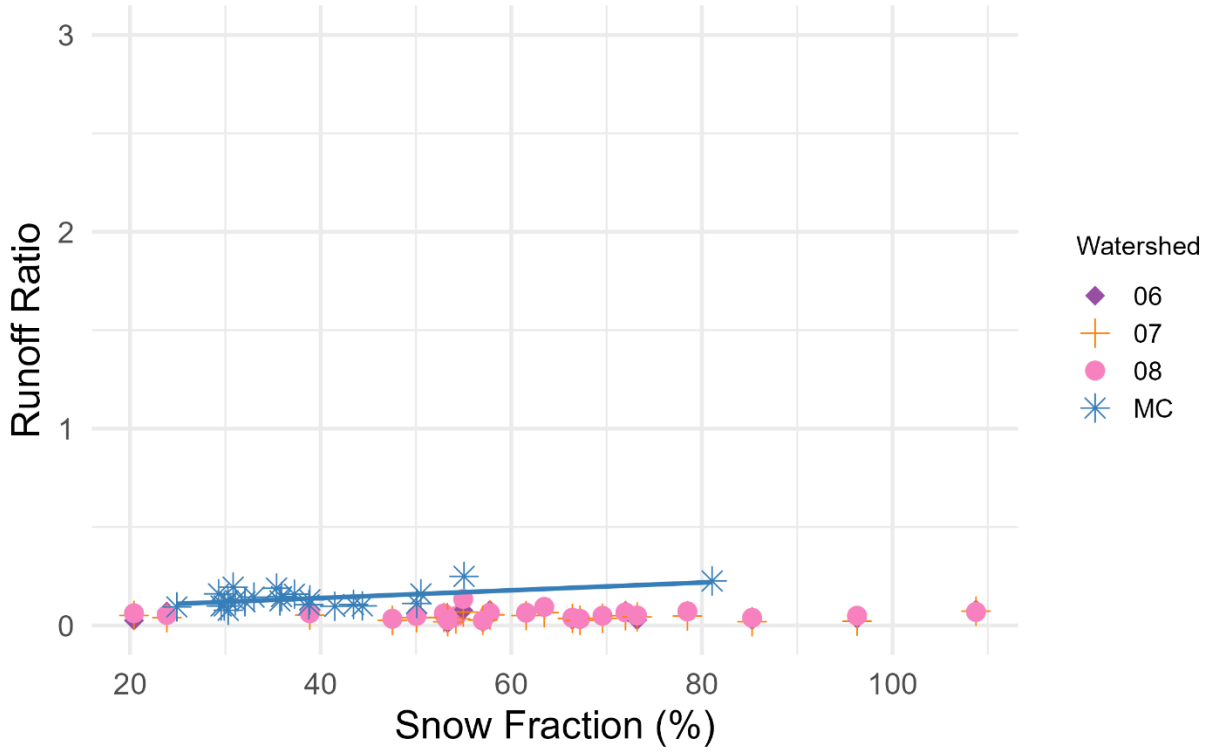

Figure 41. Linear regression relationships between runoff ratio and snow fraction in seasonal snow zone watersheds in the summer. Solid lines indicate statistically significant regressions ($p < 0.05$ for the regression). An absence of regression lines indicates no significant linear relationships ($p > 0.10$). Corresponding Pearson correlation coefficients and p-values for each regression are presented in Table C.4 in Appendix C.

4.4. Climate and Snow Effects on Summer Streamflow

In all study watersheds, multiple linear regression models revealed that spring precipitation and air temperature were the most consistently influential predictors of summer streamflow magnitude (blue solid and orange striped bars for July 1 streamflow and minimum summer flow, Figures 42 and 43). Consistent with results of bivariate correlations, July 1 streamflow was positively associated with spring precipitation in high-performing models for all watersheds except Mack Creek (Figure 42) and summer minimum flow was positively associated with spring precipitation in high-performing models for all watersheds except WS02, WS03, and Mack Creek (Figure 43). Nevertheless, effect sizes were consistently small; 1 mm increases in spring precipitation were associated with increases in July 1 streamflow ranging from 0.0006 mm (WS09, M9) to 0.0031 mm (WS06, M5, Table 4). Cross-validated R^2 values for these models tended to be higher for July 1 streamflow than for other response variables, indicating stronger predictive power for early summer flow than for minimum summer flow. Spring precipitation did not appear in any models that predicted summer low flow timing.

Spring air temperature (not included in bivariate correlation analysis) was a stronger predictor of summer streamflow magnitude than spring precipitation, and the relationship was consistently negative. Spring temperature was negatively related to July 1 streamflow in high-performing models for all watersheds except WS06, WS07, and WS08 (Figure 42) and with summer minimum flow in high-performing models for WS02, WS03, WS09, and Mack Creek (Figure 43). Effect sizes for spring temperature were higher than for spring precipitation. Increases of 1 °C in spring air temperature were associated with decreases in July 1 streamflow ranging from 0.0391 mm (WS01, M1) to 0.3705 mm (Mack Creek, M12), and reductions in summer low flow ranging from 0.0092 mm (WS09, M9) to 0.0264 mm (WS03, M6; Table 5). Winter air temperature did not appear in many models. It was a strong predictor in models for summer low flow timing in WS07(M4), and WS09 (M8), (Table 6), though the direction of the relationship was not consistent. In WS07, M4, a 1°C increase in winter air temperature was associated with a hastening of 5.38 days in summer low flow timing. Conversely, the same temperature increase in WS09, M8 was associated with a delay of summer low flow timing of 5.12 days. A similar inconsistency was observed for summer air temperature in WS02, WS03,

and WS08, in relation to the response variables of summer low flow and its timing (Figures 43 and 44). Winter and summer air temperature each explained at most 20% of the variance (R^2 contributions < 0.2), though this share was proportionally larger in models with lower total R^2.

Consistent with bivariate correlation analyses, snow variables played a more prominent role in explaining the timing than the magnitude of summer streamflow in multiple linear regression models (Figure 44, compared to Figures 42 and 43). The date of minimum flow in high-performing models was positively related to snow disappearance date (WS03, WS08 WS09, WS10, Mack Creek, lavender-colored bars) and/or snow fraction (WS02, WS06, WS08, pink bars), or negatively related to maximum SWE (WS03, WS09, WS10, and Mack Creek, dark purple striped bar) (Table 6, Figure 44). Effect sizes were relatively large for snow disappearance date and date of maximum SWE, but not for maximum SWE (Table 6). For example, a one-day delay in snow disappearance was associated with delays in low flow timing ranging from 0.243 days (WS09, M10) to 0.6787 days (Mack Creek, M12). A 1% increase in snow fraction was associated with delays in low flow timing ranging from 0.2811 (WS02, M1) to 0.3521 (WS08, M5). A 1 mm/day increase in snowmelt rate was associated with delays in low flow timing of up to 1.91 days (Mack Creek, M12) but hastening of flow in WS09 (−0.77 days, M10) (Table 6, Figure 44). These results suggest diverse controls on melt-driven streamflow recession. The appearance of several different snow variables in multiple regression models (Figures 42-44) is likely the result of the strong correlations among snow variables (Figure 12). Despite the strength of some individual snow variables in these models, cross-validated R^2 values for low flow timing were generally modest, indicating moderate predictive power (Table 6).

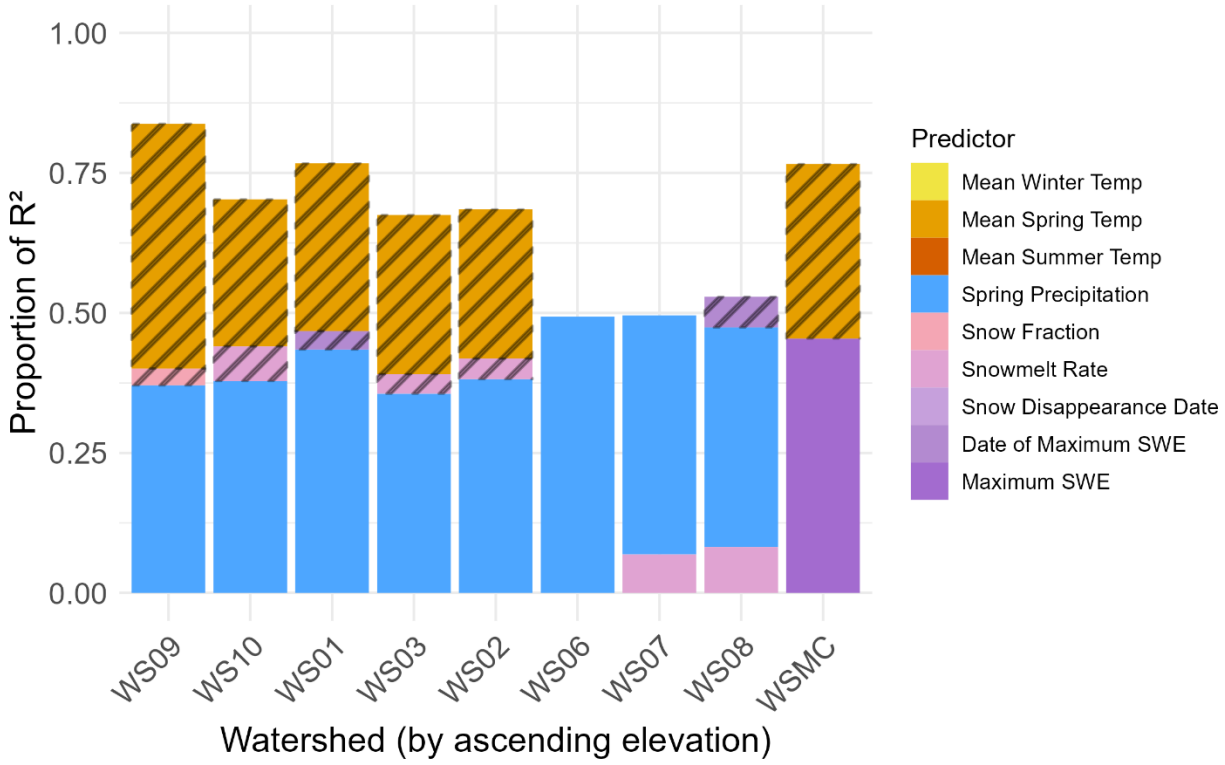

Figure 42. Relative contributions of precipitation, snow, and air temperature variables to the total explained variance (R^2) of multiple linear models with July 1 streamflow as the response variable. Relative contributions were calculated using the Lindeman, Merenda, and Gold (LMG) approach (Lindeman et al., 1980). Watersheds are arranged left to right by ascending mean elevation. Solid bar segments indicate explanatory variables with positive regression coefficients; striped segments represent negative coefficients.

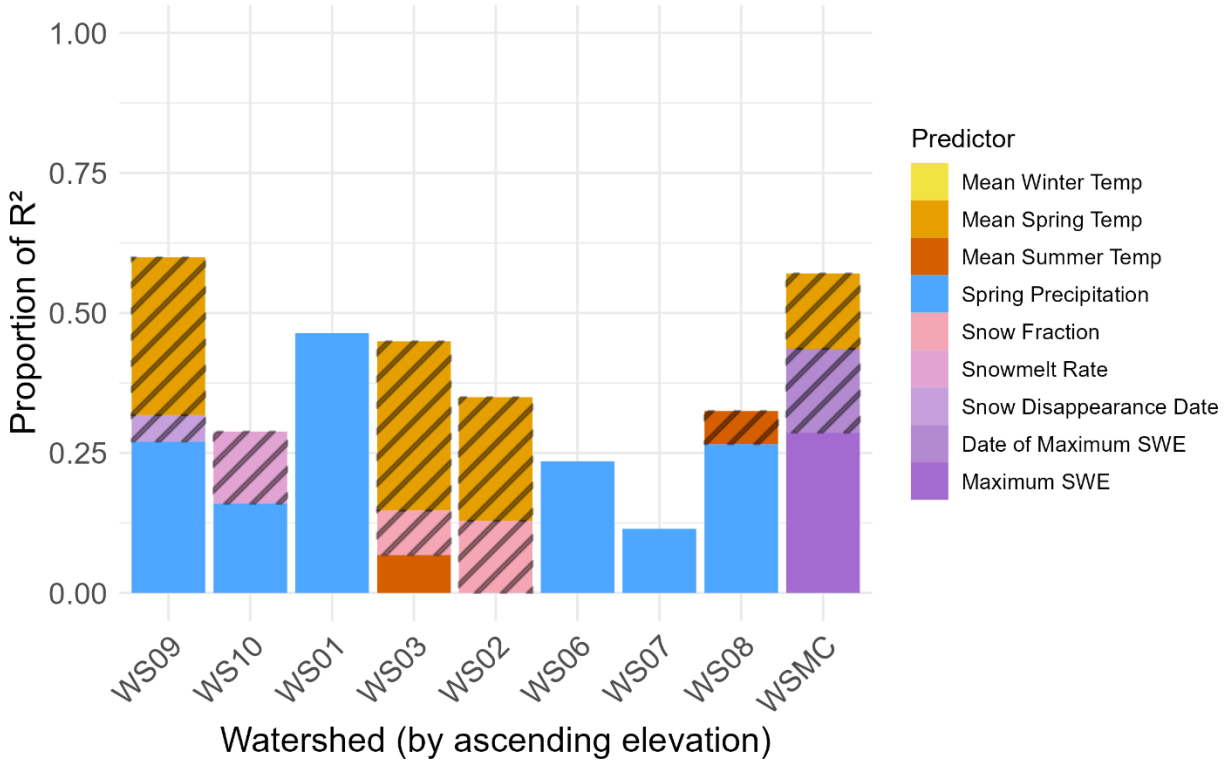

Figure 43. Relative contributions of precipitation, snow, and air temperature variables to the total explained variance (R^2) of multiple linear models with minimum summer flow as the response variable. Relative contributions were calculated using the Lindeman, Merenda, and Gold (LMG) approach (Lindeman et al., 1980). Watersheds are arranged left to right by ascending mean elevation. Solid bar segments indicate explanatory variables with positive regression coefficients; striped segments represent negative coefficients.

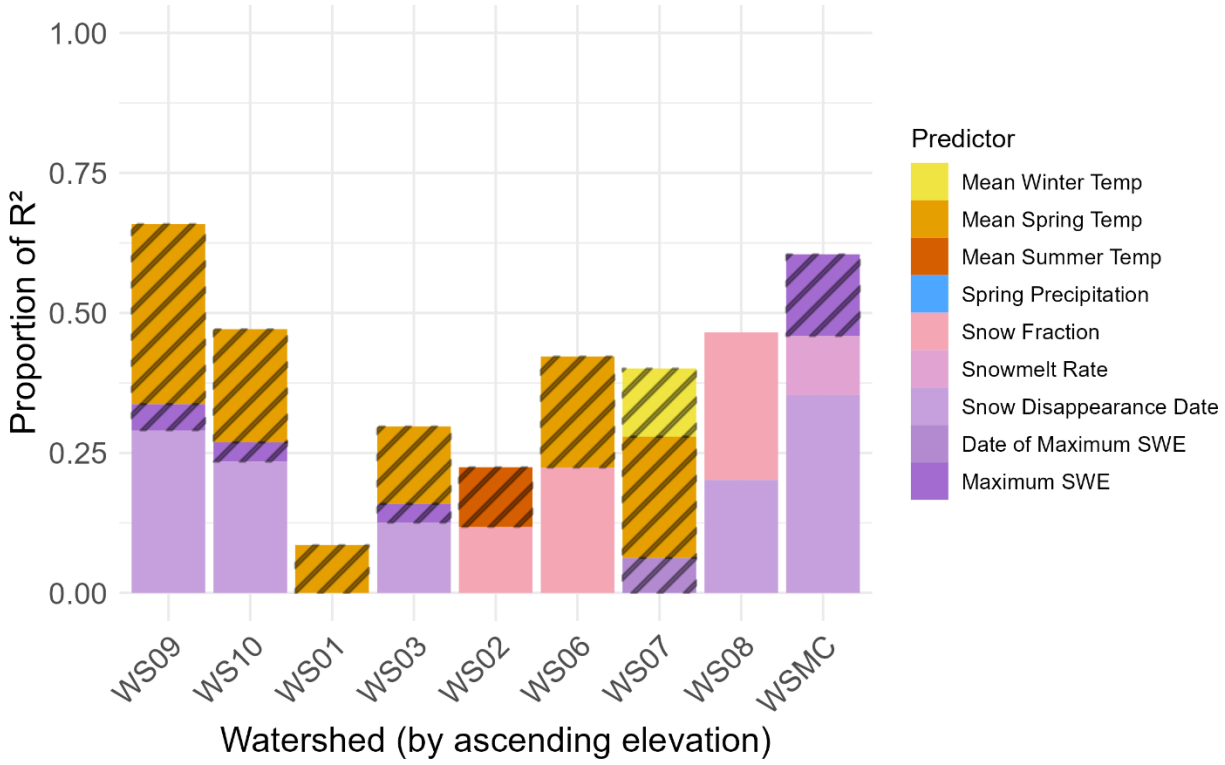

Figure 44. Relative contributions of precipitation, snow, and air temperature variables to the total explained variance (R^2) of multiple linear models with minimum summer flow date as the response variable. Relative contributions were calculated using the Lindeman, Merenda, and Gold (LMG) approach (Lindeman et al., 1980). Watersheds are arranged left to right by ascending mean elevation. Solid bar segments indicate explanatory variables with positive regression coefficients; striped segments represent negative coefficients.

Table 4: All-subsets regression results for July 1 unit streamflow as the response variable. For each watershed, high-performing models are shown; these are defined as models with overall cross-validated R^2 values greater than 0 and regression coefficients with *p*-values less than 0.1. Each model includes explanatory variables, their estimated coefficients, associated *p*-values, Lindeman, Merenda, and Gold (LMG) values (indicating the relative contribution of each explanatory variable to Pearson's R), and the cross-validated R^2 value. High performance models were identified based on AIC scores (Appendix Table C.5).

Watershed, Model	Explanatory Variable	Coefficient	p-value	LMG	CV-R^2
WS01, M1	Mean Spring Air T	-0.0391	0.0323	0.2723	0.6382
WS01, M1	Spring P	0.0009	0.0003	0.4589	0.6382
WS02, M2	Mean Spring Air T	-0.0631	0.0739	0.2408	0.5432
WS02, M2	Spring P	0.0014	0.0015	0.4124	0.5432
WS02, M3	Spring P	0.0019	0.0000	0.5915	0.5083
WS03, M4	Mean Spring Air T	-0.0629	0.0500	0.2586	0.5623
WS03, M4	Spring P	0.0012	0.0030	0.3838	0.5623
WS06, M5	Spring P	0.0031	0.0002	0.4935	0.3875
WS07, M6	Spring P	0.0015	0.0005	0.4418	0.3223
WS08, M7	SWE Maximum Date	-0.0060	0.0775	0.0547	0.3079
WS08, M7	Snowmelt Rate	0.0365	0.0297	0.0821	0.3079
WS08, M7	Spring P	0.0027	0.0005	0.3920	0.3079
WS08, M8	Spring P	0.0021	0.0014	0.3914	0.2120
WS09, M9	Snow Fraction	-0.0029	0.0923	0.0299	0.7160
WS09, M9	Mean Spring Air T	-0.0855	0.0001	0.4374	0.7160
WS09, M9	Spring P	0.0006	0.0055	0.3706	0.7160
WS09, M10	Mean Spring Air T	-0.0705	0.0003	0.4133	0.7003
WS09, M10	Spring P	0.0008	0.0005	0.3978	0.7003
WS10, M11	Snowmelt Rate	-0.0096	0.0703	0.0620	0.5773
WS10, M11	Mean Spring Air T	-0.0631	0.0218	0.2624	0.5773
WS10, M11	Spring P	0.0008	0.0075	0.3785	0.5773
Mack Creek, M12	Maximum SWE	0.0017	0.0000	0.4544	0.6750
Mack Creek, M12	Mean Spring Air T	-0.3705	0.0007	0.3114	0.6750
Mack Creek, M13	Snow Fraction	0.0468	0.0000	0.4794	0.6412
Mack Creek, M13	Mean Spring Air T	-0.3152	0.0045	0.2801	0.6412

Table 5: All-subsets regression results for minimum summer low flow as the response variable. For each watershed, high-performing models are shown; these are defined as models with overall cross-validated R^2 values greater than 0 and regression coefficients with *p*-values less than 0.1. Each model includes explanatory variables, their estimated coefficients, associated *p*-values, Lindeman, Merenda, and Gold (LMG) values (indicating the relative contribution of each explanatory variable to Pearson's R), and the cross-validated R^2 value. High performance models were identified based on AIC scores (Appendix Table C.5).

Watershed, Model	Explanatory Variable	Coefficient	p-value	LMG	CV-R^2
WS01, M1	Spring P	0.0001	0.0003	0.4640	0.3924
WS02, M2	Snow Fraction	-0.0020	0.0311	0.1286	0.0195
WS02, M2	Mean Spring Air T	-0.0221	0.0095	0.2208	0.0195
WS02, M3	Snowmelt Rate	-0.0041	0.0450	0.1097	0.0908
WS02, M3	Mean Spring Air T	-0.0220	0.0112	0.2184	0.0908
WS02, M4	Spring P	0.0002	0.0134	0.2576	0.1849
WS02, M5	Maximum SWE date	-0.0005	0.0853	0.0762	0.1528
WS02, M5	Mean Spring Air T	-0.0219	0.0144	0.2144	0.1528
WS03, M6	Snow Fraction	-0.0018	0.0571	0.0842	0.0977
WS03, M6	Mean Spring Air T	-0.0264	0.0037	0.2935	0.0977
WS06, M7	Spring P	0.0001	0.0191	0.2348	0.2219
WS08, M8	Spring P	0.0001	0.0133	0.2581	0.2540
WS09, M9	Mean Spring Air T	-0.0092	0.0384	0.2698	0.4189
WS09, M9	Spring P	0.0001	0.0329	0.2775	0.4189
WS09, M10	Snow Fraction	-0.0009	0.0474	0.0605	0.3479
WS09, M10	Mean Spring Air T	-0.0169	0.0001	0.4721	0.3479
WS10, M11	Snowmelt Rate	-0.0015	0.0913	0.1285	0.0933
WS10, M11	Spring P	0.0001	0.0588	0.1595	0.0933
WS10, M12	Spring P	0.0001	0.0463	0.1760	0.1337
Mack Creek, M13	Maximum SWE	0.0001	0.0008	0.2864	0.3235
Mack Creek, M13	Maximum SWE date	-0.0017	0.0018	0.1497	0.3235
Mack Creek, M13	Mean Spring Air T	-0.0158	0.0258	0.1343	0.3235
Mack Creek, M14	Maximum SWE	0.0001	0.0005	0.3234	0.2843
Mack Creek, M14	Maximum SWE date	-0.0014	0.0066	0.1157	0.2843
Mack Creek, M14	Spring P	0.0001	0.0519	0.1028	0.2843

Table 6. All-subsets regression results for minimum summer low flow date as the response variable. For each watershed, high-performing models are shown; these are defined as models with overall cross-validated R^2 values greater than 0 and regression coefficients with *p*-values less than 0.1. Each model includes explanatory variables, their estimated coefficients, associated *p*-values, Lindeman, Merenda, and Gold (LMG) values (indicating the relative contribution of each explanatory variable to Pearson's R), and the cross-validated R^2 value. High performance models were identified based on AIC scores (Appendix Table C.5).

Watershed, Model	Explanatory Variable	Coefficient	p-value	LMG	CV-R^2
WS02, M1	Snow Fraction	0.2811	0.0961	0.1263	0.0792
WS03, M2	Mean Spring Air T	-3.3358	0.0831	0.1362	0.0468
WS06, M3	Snow Fraction	0.2611	0.0210	0.2239	0.2720
WS06, M3	Mean Spring Air T	-4.0021	0.0307	0.1985	0.2720
WS07, M4	Maximum SWE Date	-0.2069	0.0422	0.0624	0.0738
WS07, M4	Mean Winter Air T	-5.3760	0.0264	0.1216	0.0738
WS07, M4	Mean Spring Air T	-5.8809	0.0080	0.2167	0.0738
WS08, M5	Snow Fraction	0.3521	0.0013	0.3954	0.2965
WS08, M6	Maximum SWE	0.0184	0.0021	0.3681	0.3138
WS09, M7	Maximum SWE	-0.0280	0.0420	0.0469	0.3947
WS09, M7	Snow Diss Date	0.2966	0.0005	0.2903	0.3947
WS09, M7	Mean Spring Air T	-6.5310	0.0004	0.3217	0.3947
WS09, M8	Snow Diss Date	0.3263	0.0010	0.2603	0.5367
WS09, M8	Mean Winter Air T	5.1199	0.0590	0.0713	0.5367
WS09, M8	Mean Spring Air T	-6.9977	0.0003	0.3167	0.5367
WS09, M9	Maximum SWE Date	-0.1378	0.0604	0.0642	0.4977
WS09, M9	Snow Diss Date	0.3150	0.0009	0.2658	0.4977
WS09, M9	Mean Spring Air T	-6.9098	0.0004	0.3176	0.4977
WS09, M10	Snow Diss Date	0.2434	0.0008	0.2864	0.4508
WS09, M10	Snowmelt Rate	-0.7720	0.0715	0.0287	0.4508
WS09, M10	Mean Spring Air T	-6.6107	0.0005	0.3271	0.4508
WS10, M11	Snow Diss Date	0.1573	0.0151	0.2255	0.2702
WS10, M11	Mean Spring Air T	-3.8246	0.0232	0.1963	0.2702
Mack Creek, M12	Maximum SWE	-0.0513	0.0009	0.1459	0.4487
Mack Creek, M12	Snow Diss Date	0.6787	0.0001	0.3535	0.4487
Mack Creek, M12	Snowmelt Rate	1.9114	0.0072	0.1053	0.4487

4.5. Cross-Correlation Analyses

Cross-correlation functions (CCFs) between daily snowpack loss (derived from daily SWE) and streamflow showed a consistent pattern: moderate positive correlations at lag 0 (r = 0.14 at WS06 to r = 0.30 at Mack Creek), followed by a steady decline toward zero at lags starting at approximately 130 days (Figure 45). Lower-elevation, transient-snow-zone watersheds (WS01, WS02, WS03, WS09, WS10) reached r = 0 between 123 and 128 lag days, whereas higher-elevation watersheds (WS06, WS07, WS08, Mack Creek) remained positively correlated until 149 to 155 lag days. Minimum cross-correlations (approximately r = −0.12) occurred near lag day 220 for all watersheds; beyond this point, the CCF gradually increased, returning toward positive values between lag days 312 and 330, with later lags at watersheds in the seasonal snow zone (Figure 45).

Snowpack loss values were nonzero primarily during the snow season (approximately December–May); consequently, CCF values outside this window reflect relationships between streamflow and extended sequences of zero snowpack loss. The difference in the lag at which CCFs reached zero between lower- and higher-elevation watersheds spanned ~30 lag days. This contrast is more evident in Figure 46, which aggregates individual watersheds by snow-zone: WS01, WS02, WS03, WS09, and WS10 comprise the transient-snow-zone group; WS06, WS07, and WS08 comprise the lower seasonal-snow-zone group; and Mack Creek represents the upper seasonal-snow zone. The composite results closely mirror the individual CCFs, and they emphasize Mack Creek's distinct behavior: lower positive correlations than the other seasonal-snow-zone watersheds for lags up to day 125, after which its trajectory aligns more closely with the seasonal-zone group.

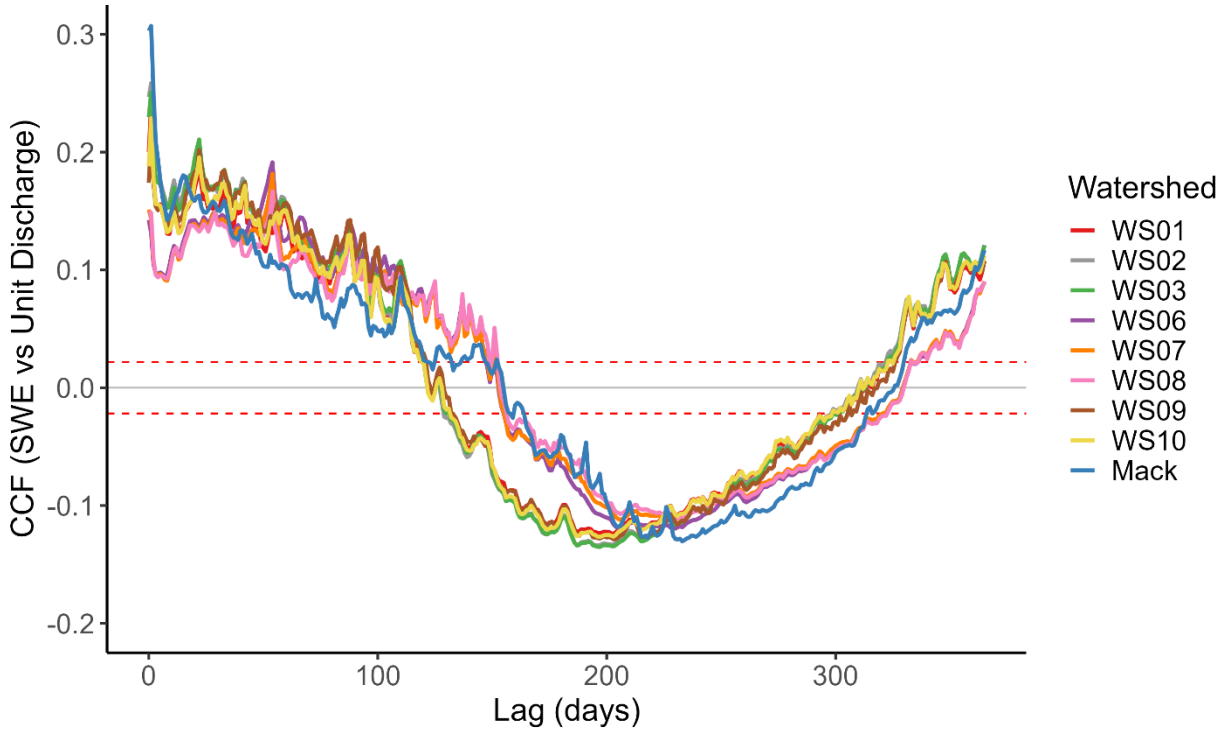

Figure 45. Cross-correlation functions (CCFs) between daily modeled snowmelt (mm) and unit streamflow (mm) for all study watersheds in the Andrews Forest (water years 1998 to 2020). Snowpack losses were derived from meteorological stations CENMET, VANMET, and UPLMET and paired with corresponding watersheds (as per section 3.2). Each colored line represents one watershed. The dashed red lines indicate the 95% confidence threshold for significance in the CCF.

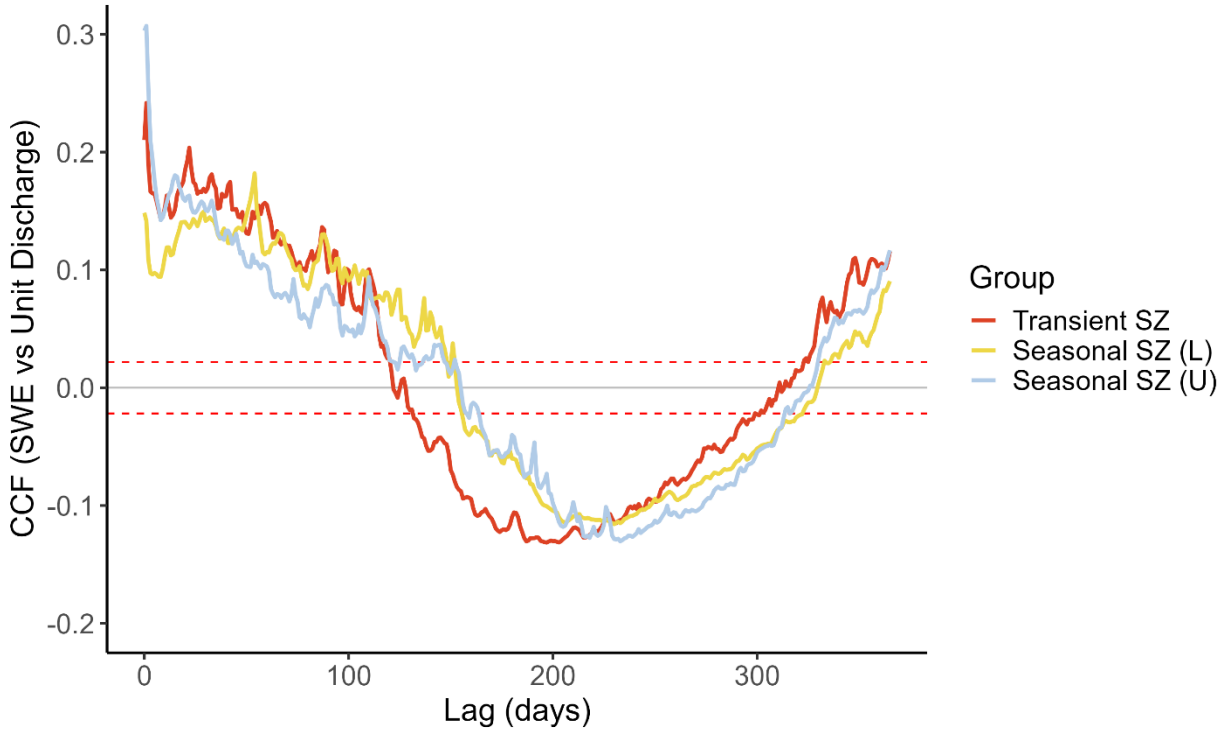

Figure 46. Cross-correlation functions (CCFs) between daily modeled snow loss (mm) and unit streamflow (mm) for all study watersheds in the Andrews Forest (water years 1998 to 2020), aggregated into three groups based on elevation and snow dynamics. WS01, WS02, WS03, WS09, and WS10 were placed in the transient snow zone group (Transient SZ); WS06, WS07, and WS08 were placed in the lower seasonal snow zone (Seasonal SZ (L); and Mack Creek as placed in the upper seasonal snow zone (Seasonal SZ (U). Snowmelt was derived from meteorological stations CENMET, VANMET, and UPLMET and paired with corresponding watersheds (as per section 3.2). The dashed red lines indicate the 95% confidence threshold for significance in the CCF.

5. Discussion

Over the 23-year study period, there were no significant temporal trends in temperature, precipitation, snow, or streamflow (Figure 4-7, Appendix Table B.2 and B.3). However, runoff ratio declined in some study watersheds (Figures 10 and 11, Appendix Table B.2).

Bivariate correlations indicated strong relationships among snow variables and among streamflow variables, and spring precipitation as the dominant control on early summer streamflow magnitude, particularly in low-elevation, transient snow zone watersheds (Figure 12, Figure 48).

Simple linear regressions by season indicated that warmer winter and spring temperatures were linked to lower runoff ratios (Figures, 16, 18, and 19, Figure 47, Table C.2 in Appendix C). Analyses of residuals from linear regressions indicated the controlling for air temperature, winter runoff ratios in the lower-elevation transient snow zone have declined over time (Figure 22). Analyses of residuals from linear regressions also indicated that controlling for air temperature, spring precipitation was negatively related to snow fraction (Figure 29) at Mack Creek. Snow fraction was positively associated with runoff ratios in spring at higher-elevation watersheds in the seasonal snow zone (Figure 33, Figure 47, Table C.3 in Appendix C).

Multiple regression models indicated that spring precipitation was positively associated with summer streamflow, whereas warmer spring temperature was associated with reduced July 1 streamflow and reduced summer minimum flow (Figures 42 and 43, Figure 48, Tables 4–5). Snow timing variables (snow disappearance date and melt rate), rather than snow magnitude variables, were important predictors of summer low flow timing, particularly in high-elevation, seasonal snow zone watersheds (Figure 44, Figure 48, Table 5). Consequently, rising temperatures are expected to reduce both early- and late-summer streamflow and to advance the timing of summer low flows (Figure 49). This may be attributed to snow losses and/or increased ET and soil moisture uptake.

Cross-correlation analysis showed that snowmelt contributions influenced streamflow on average ~30 days longer in watersheds in the seasonal snow zone than in the transient snow

zone (Figures 45 and 46). These findings highlight the dominant role of spring precipitation and temperature, and the added influence of snowpack on runoff timing and efficiency at higher elevations.

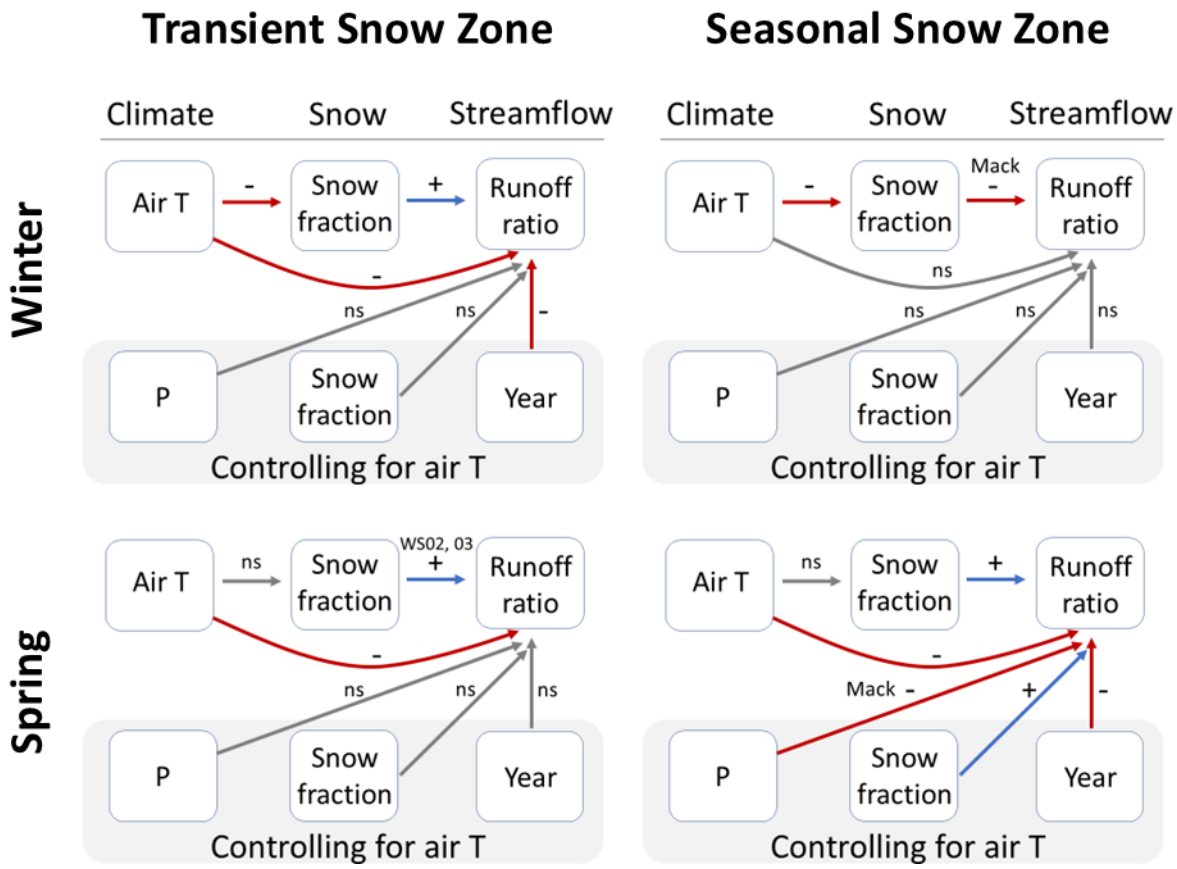

Figure 47. Summary of relationships between climate, snow, and streamflow variables for winter and spring, shown separately by snow zone. Arrows indicate the direction of the relationship and whether it is positive (blue with "+"), negative (red with "–"), or non-significant (gray, labeled "ns").

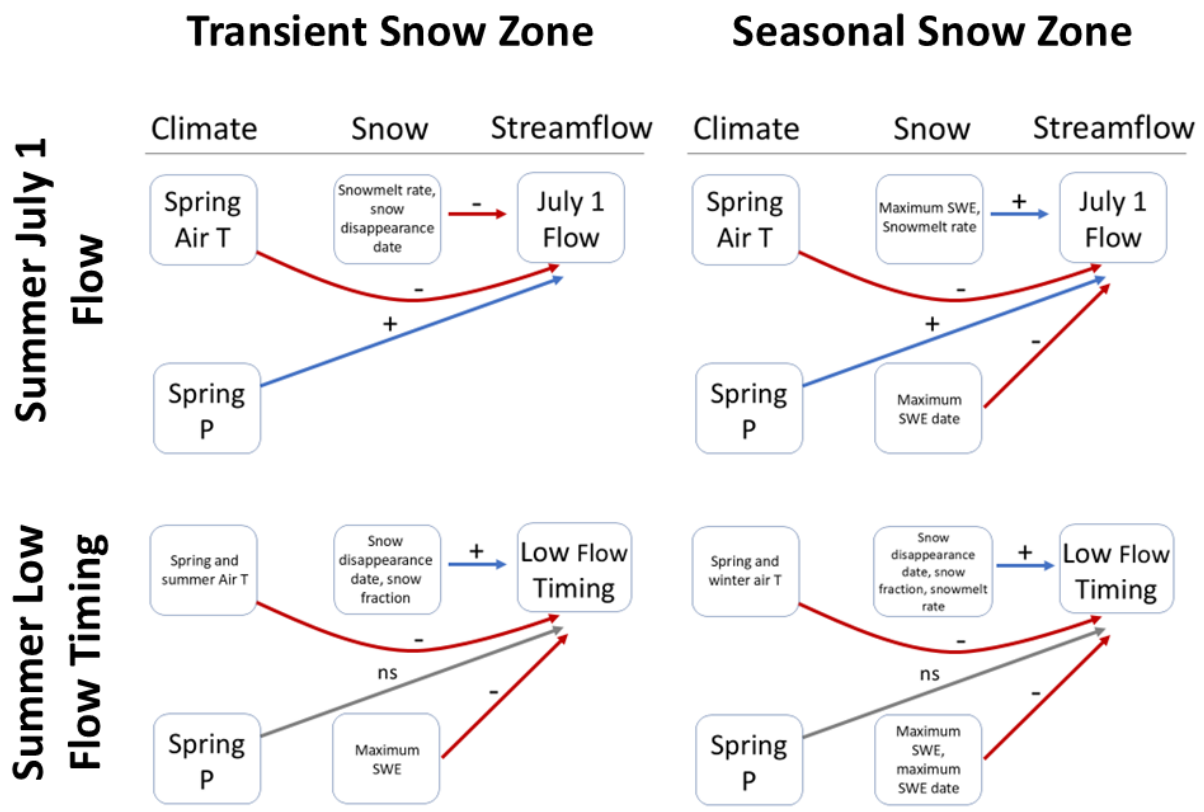

Figure 48. Summary of relationships between climate, snow, and streamflow variables for summer flow and low flow timing, shown separately by snow zone. Arrows indicate the direction of the relationship and whether it is positive (blue with "+"), negative (red with "–"), or non-significant (gray, labeled "ns").

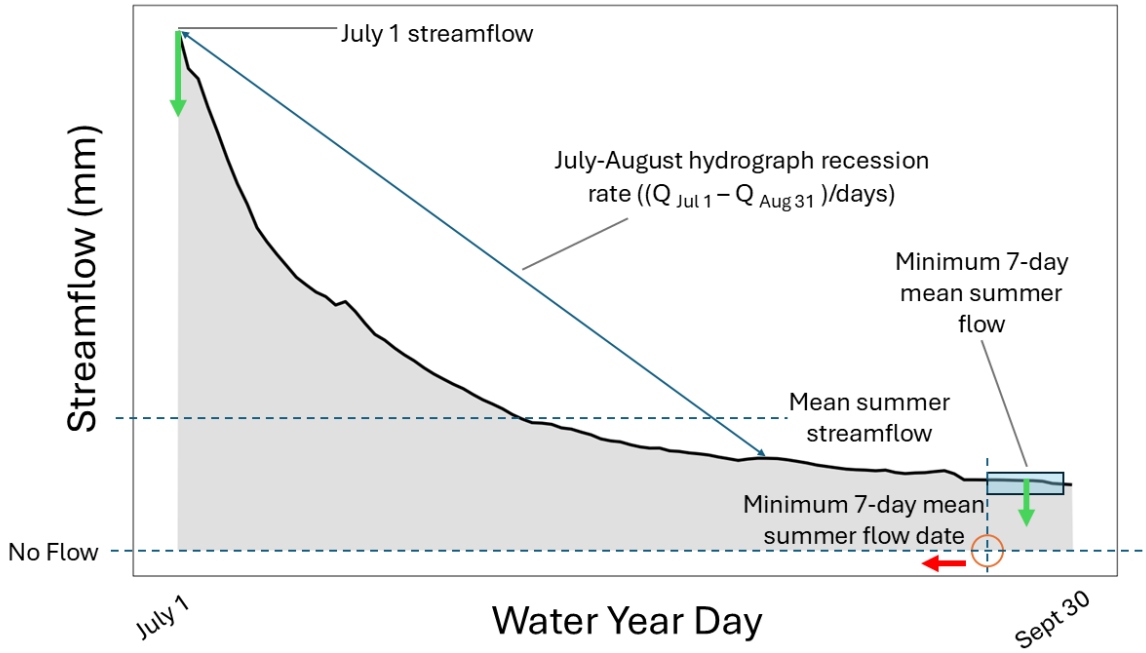

Figure 49. Theoretical differences in summer flow magnitude and timing metrics as a result of elevated air temperature.

5.1 Differences Between Transient and Seasonal Snow Zones

The strength and nature of snow–streamflow relationships differed substantially between the transient and seasonal snow zones (Figure 50). In low-elevation, transient snow zone watersheds, snow variables were weakly related to summer streamflow, with the primary influence observed in the timing of low flows rather than magnitude (Figures 42-44). In contrast, high-elevation, seasonal snow zone watersheds—particularly Mack Creek—exhibited stronger relationships between snow variables (e.g., melt rate, snow disappearance date) and both summer flow magnitude and timing (Figure 12, panel I). Although WS06, WS07, and WS08 are classified within the seasonal snow zone, their upper elevations (957–1048 m; Table 2) are close to the upper ranges of some transient snow zone watersheds (e.g., WS01, WS,02, WS03), and they displayed weaker snow–streamflow linkages than occurred at Mack Creek. Mack Creek is substantially higher in elevation (upper elevation at 1620 m) with deeper and more persistent snowpack, and it had consistently stronger snowmelt signals in streamflow response (Figures 12, 39, 41).

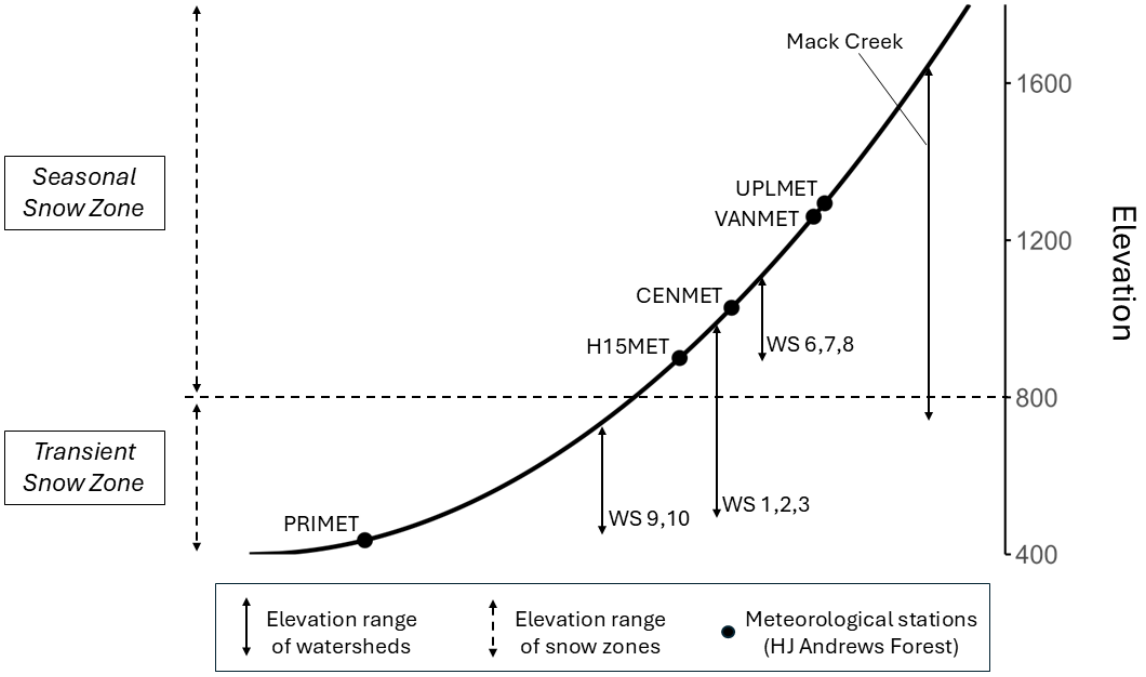

Figure 50. Study watershed and meteorological station elevations with snow zone delineation in the HJ Andrews Experimental Forest.

These results suggest that snow influence on streamflow increases with elevation, even within the seasonal snow zone, and that elevation may be a more important driver than zone classification alone. This is reflected in the period-of-record mean maximum SWE, which is 294 mm at CENMET (1028 m) compared to 999 mm at UPLMET (1284 m). Consistent with Jefferson et al. (2011), the fraction of watershed area in the seasonal snow zone appears to be the primary control on seasonal streamflow distribution. However, the results do not support their conclusion that watersheds with less than 50% seasonal snow-zone area are buffered from the effects of warming temperatures on seasonal hydrology; in this study, warmer winter and spring temperatures are associated with lower runoff ratios (Figures 16, 18, and 42).

Existing trends toward higher air temperatures (Jones et al., 2025) and lower snow fractions (Pierce et al., 2008) in the western US are associated with diminished snowpacks (Mote et al. 2005, Mote et al. 2018), that melt earlier (Muselman et al., 2017, Stewart et al., 2004) and at a slower rate (Musselman et al. 2017, Trujillo and Molotch, 2014). As a result, snowpacks in much of the western US may be expected to have SWE curves with lower SWE maxima, earlier melts, and higher melt rates. This SWE curve change can be understood as representative of conditions at lower elevation (Figure 51), with warmer winter air temperature and less precipitation falling as snow. As a result, snow accumulation and ablation in the lower seasonal snow zone may resemble that of the transient snow zone, and snow accumulation and ablation in the lower transient snow zone may begin to resemble that of the ephemeral snow zone.

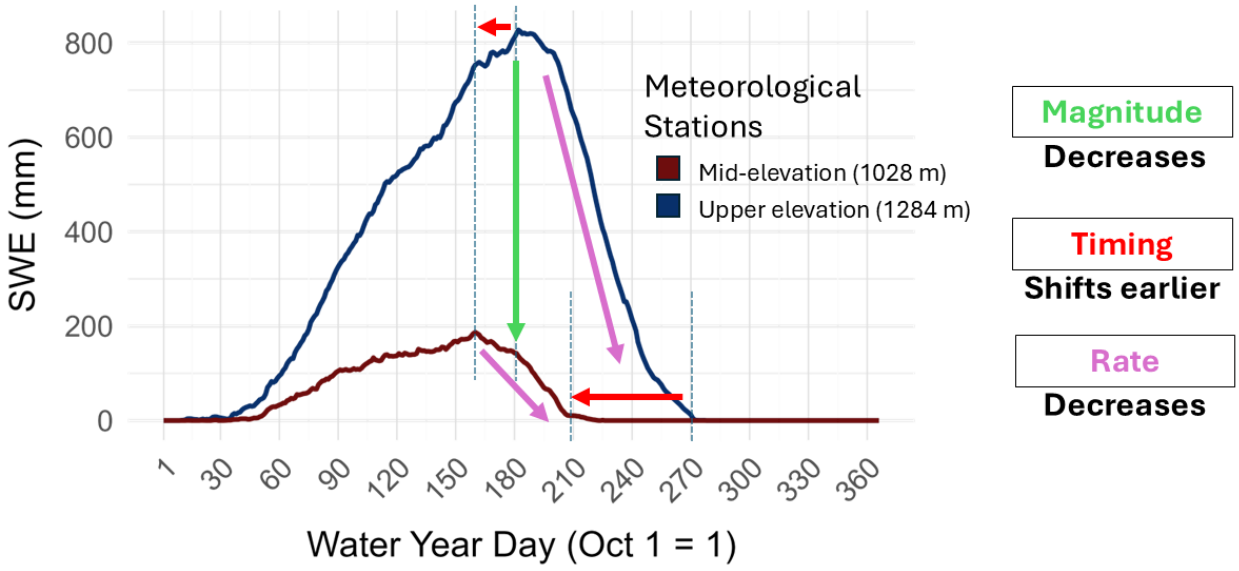

Figure 51. Theoretical differences in SWE curve shape based on elevation and air temperature increase within the seasonal snow zone. SWE magnitude, SWE accumulation and melt timing, and melt rate are shown.

5.2 Seasonal Controls and Shifting Runoff Ratio

Seasonal patterns shaped snow–climate–streamflow interactions in distinct ways. Warmer winter and spring temperatures were consistently associated with lower runoff ratios (Figures 16, 18, and 19), reflecting reduced snow accumulation, earlier melt, and potentially greater losses via ET. Trend analysis revealed declining winter runoff ratios in four watersheds—WS03, WS06, WS07, and WS10—which span both transient and seasonal snow zones but are all previously logged and now support relatively young, even-aged plantation forests (Figures 10 and 11, Appendix Table B.2). Unlogged watersheds showed no declines in winter runoff ratio. These stands grew from approximately 25 to 50 years old (WS06, WS07, WS10) and 35 to 60 years old (WS03) during the study period, suggesting that increasing water use by maturing trees may have contributed to reduced runoff ratios. Long-term watershed data from the Oregon Coast Range indicate that younger, dense Douglas fir plantations produce

more substantial summer low flow deficits than mature/old growth trees in less dense stands, and that gradual deficits may extend into the fall, spring, and winter (Segura et al., 2020).

After controlling for air temperature, residual analysis revealed a decline in winter runoff ratio over time in transient snow zone watersheds—WS01, WS02, WS03, and WS10—regardless of logging history (Figure 22, Table C.3 in Appendix C). In these watersheds, residuals shifted from positive to negative over the study period, indicating that winter runoff ratio declined independently of warming, possibly due to increasing winter ET in these relatively warm, low-elevation watersheds. Increasing winter ET during the study period may be attributed to elevated January air temperatures in the Andrews Forest (Jones et al., 2025). In spring, residuals of runoff ratio shifted from negative to positive with increasing snow fraction in the seasonal snow zone but not the transient snow zone (Figure 31 and Figure 33, Table C.3 in Appendix C), suggesting that after controlling for air temperature, snowmelt remains a key contributor to spring streamflow in the seasonal snow zone. Additionally, the direction of the relationship between snow fraction and winter runoff ratio varied by elevation. Snow fraction was positively related to runoff ratio in the transient snow zone, where a high snow fraction may contribute to snowmelt and hence directly to winter streamflow, and negatively related in Mack Creek, a higher-elevation watershed where a high snow fraction may indicate that snow is retained until snowmelt occurs in the spring (Figures 36 and 37). These differences may also account for the lower positive cross-correlations between snowmelt and streamflow at Mack Creek compared to other watersheds (Figures 45 and 46).

5.3 Mechanisms Regulating Snow Effects on Streamflow

Regression and correlation analyses provide further insight into the mechanisms regulating snow contributions to streamflow. The lack of correlation between the date of maximum SWE and melt rate or SWE magnitude in WS06, WS07, WS08 and Mack Creek (Figure 12 panel F to I) suggests that site-specific factors—such as aspect and canopy cover—influence snow dynamics. These watersheds and their corresponding meteorological station, VANMET, are located on southwest-facing slopes, which may partially explain their weaker snow–streamflow relationships. Conversely, in Mack Creek there were strong snow–streamflow relationships

consistent with deeper snowpack and delayed melt (Figure 12, panel I; Figures 36 and 37). Although spring temperature was associated with reductions in summer flow magnitude in all watersheds (Tables 4–6; Figures 42 to 44), and snow variables were significant predictors of the timing of low flows in all watersheds (Table 5; Figure 44), not all statistically significant explanatory variables may be meaningful in practice. For example, a 1 mm increase in spring precipitation was associated with only a 0.0006–0.0031 mm increase in July 1 streamflow (Table 4)—an effect that is statistically robust but likely negligible at the scale of watershed management. However, effect sizes were larger for air temperature, consistent with the influence of rising temperatures on vapor pressure deficit, evapotranspiration, and reduced runoff. Using mean monthly maximum and minimum temperature records from Jones et al. (2025) covering 45 years, the spring mid-range increased by about 2.1 °C. This magnitude of warming corresponds to an advance in summer low-flow timing of approximately 7.0 to 14.7 days within the last half century.

5.4 Relationships to Published Work

An apparent stationarity in snowpack over the period of record contrasts with broader regional assessments indicating widespread snowpack loss and warming over longer time scales (Li et al., 2017; Mote et al., 2018). However, natural decadal variability may obscure long-term trends at shorter temporal scales. Siler et al. (2019) found that the Pacific Decadal Oscillation (PDO) plays a dominant role in modulating snowpack in the Pacific Northwest, making it difficult to detect clear climate signals over shorter records. This likely accounts for the observed snowpack stability in the Andrews Forest across both transient and seasonal snow zones over the relatively short period of study (1998-2020).

Our findings regarding snowmelt contributions to summer streamflow generally reinforce those of Gordon et al. (2025), who showed that a shift from snow to rain was associated with reduced winter snow fractions, increased winter streamflow, and diminished summer flow. In such cases, a greater proportion of liquid water input passes through the system rapidly, reducing the potential for soil water storage in deeper soils that would sustain summer baseflow. However, in the Andrews Forest, transient snow zone watersheds displayed a different pattern—higher winter snow fractions were associated with higher runoff ratios in

both winter and spring, but not associated with summer flows. This suggests that in the lower-elevation transient snow zone, snowmelt may contribute to winter and early spring streamflow but is less influential during summer.

In a warming climate, small mountainous watersheds of the Western Cascades may experience a more asynchronous spring melt pulse, yet a more synchronized energy–water balance during the melt period. While this study identifies evaporative demand as a likely control, the role of subsurface storage in sustaining summer streamflow remains unclear and merits further investigation.

Generally, results align with previous work on snow–streamflow relationships in terms of timing and magnitude (Musselman et al., 2017; Stewart et al., 2004). Although snowpack clearly influences the timing of summer low flow, snowpack influence on summer streamflow magnitude appears limited. July 1 streamflow showed only weak correlations with snow variables, and the practical significance of these relationships was minimal. Not all snow metrics convey the same hydrologic signal, and snow is inherently dynamic. Therefore, future studies should carefully isolate the effects of snow volume, melt timing, and melt rate when evaluating snow–streamflow relationships.

5.5 Errors and Uncertainty

Snow, precipitation, and temperature data were obtained from four point-based meteorological stations and related to nine nearby study watersheds. This introduces a spatial mismatch, as precipitation amount and type can vary significantly with elevation and topography (Jefferson 2011). Since meteorological and stream gauging stations are not co-located but were still near enough for drawing meaningful comparisons, correlation-based analyses were used to account for spatial mismatches, rather than a mass balance.

Estimating snowpack mass balance and its contribution to streamflow is inherently challenging due to processes such as sublimation, evaporation, wind redistribution, and evapotranspiration (Cho et al. 2022; Tarboton and Luce 1996). In the cross-correlation analysis, SWE losses were interpreted primarily as melt (Figure 8). Given the dense, well-consolidated maritime snowpack typical of the Western Cascades, this assumption is reasonable, as non-melt

losses, like sublimation and evaporation, are more limited than in colder continental snowpacks, once snow has reached the ground (Dickerson-Lange et al., 2021; Roth and Nolin 2017).

Snow fraction estimates may also be biased low due to undercatch, where wind-driven snowfall fails to enter precipitation gauges. This can result in underestimation of up to 20% of snow-season precipitation (Metcalfe and Goodison, 1993). However, the use of double-fence intercomparison reference gauges at CENMET, VANMET, and UPLMET substantially reduces this source of error (Yang et al., 1998). While these limitations introduce some uncertainty, the spatial consistency of results across watersheds and seasons suggests that the patterns and relationships identified in this study remain robust.

Transient snow zones have more ephemeral snowpacks than those in the seasonal snow zone and are prone to midseason melt due to lower cold content. As a result, maximum SWE may sometimes prove inadequate in characterizing snow magnitude in transient snow zone snowpacks. Alternatively, snow water storage, calculated as the integrated area under the SWE curve, is a more robust approach to quantify the reservoir function of snowpacks, especially those without well-defined SWE maxima (Aragon and Hill, 2023). In this study, however, snow water storage was strongly and positively related to maximum SWE and the two can likely be used interchangeably ($r = 0.94$ to 0.98, $p < 0.000$).

6. Conclusion

This study integrates long-term snowpack records with multi-decadal climate and streamflow data to identify the dominant controls of summer low flow in steep, forested headwater areas of the Western Cascade Range of Oregon, USA. Correlation, regression, and cross-correlation analyses of climate and streamflow data for the period 1998 to 2020 in nine experimental watersheds (8.5 to 580 ha) over a range of elevation (410 to 1630 m), analyses revealed relationships that varied in space and time. Results indicated that physiography—particularly elevation and aspect— affect snow dynamics in space, producing differences in dynamics between transient and seasonal snow zones that in turn influence both the magnitude and timing of spring and summer streamflow (Jefferson, 2008; Jefferson, 2011). Results also indicated that temperature-driven evapotranspiration influences seasonal

snowpack dynamics, also influencing both the magnitude and timing of spring and summer streamflow (Newcomb et al. 2024). The analysis distinguishes between the influences of rainfall, snowfall, and seasonal air temperature, revealing that spring temperature is a consistent and strong negative predictor of summer flow magnitude, likely because increasing air temperature drives increases in ET, which are only partially compensated by weaker but persistent positive effects of spring precipitation on summer streamflow. Snowpack metrics were most strongly linked to the timing of summer low flows, especially in high-elevation watersheds.

This study examined watersheds across both transient and seasonal snow zones, whereas previous research has focused mainly on high-elevation, seasonal snow-dominated systems. Residual analyses further revealed declining winter runoff ratio in low-elevation, transient snow zone watersheds, including watersheds which contained forest plantations, potentially reflecting increased water use by maturing plantation forests. Collectively, these findings improve understanding of the seasonal and elevational mechanisms regulating snow–climate–streamflow interactions, and provide insights into the sensitivity of summer streamflow to changing snow and climate regimes.

While this study focused on seasonal correlations, incorporating direct measurements of potential and actual evapotranspiration (ET) would better clarify how air temperature influences not only snow fraction but runoff ratio. Empirically quantifying snowmelt contributions to streamflow remains challenging, even with high-resolution snow depth data. Future work could leverage isotope-based hydrograph separation, paired with process-based modeling and site-specific physiographic data, to more precisely evaluate the partitioning of snowmelt into ET and runoff. This would allow more mechanistic insight into how warming alters hydrologic partitioning and streamflow resilience in both the transient and seasonal snow zones.

These findings have practical implications for forest and watershed management, highlighting the need to consider stand age, elevation, and snow regime when planning for resilient summer streamflow under changing climate conditions.

7. References

Adam, J. C., Hamlet, A. F., & Lettenmaier, D. P. (2009). Implications of global climate change for snowmelt hydrology in the twenty-first century. *Hydrological Processes, 23*(7), 962–972. https://doi.org/10.1002/hyp.7201

Addor, N., Newman, A. J., Mizukami, N., & Clark, M. P. (2017). The CAMELS data set: Catchment attributes and meteorology for large-sample studies. *Hydrology and Earth System Sciences, 21*(10), 5293–5313. https://doi.org/10.5194/hess-21-5293-2017

Akaike, H., 1974. A new look at the statistical model identification. IEEE Trans. Autom. Control 19, 716–723. https://doi.org/10.1109/TAC.1974.1100705

Aragon, C. M., & Hill, D. F. (2023). Exploring snow storage and snowmelt timing metrics for hydrologic prediction. *Water Resources Research, 59*(4), e2022WR033777. https://doi.org/10.1029/2022WR033777

Austin, P. C., & Steyerberg, E. W. (2015). The number of subjects per variable required in linear regression analyses. *Journal of Clinical Epidemiology, 68*(6), 627–636. https://doi.org/10.1016/j.jclinepi.2014.12.014

Barnett, T. P., Adam, J. C., & Lettenmaier, D. P. (2005). Potential impacts of a warming climate on water availability in snow-dominated regions. *Nature, 438*(7066), 303–309. https://doi.org/10.1038/nature04141

Barnhart, T. B., Molotch, N. P., Livneh, B., Harpold, A. A., Knowles, J. F., & Schneider, D. (2016). Snowmelt rate dictates streamflow. *Geophysical Research Letters, 43*(15), 8006–8016. https://doi.org/10.1002/2016GL069690

Berris, S. N., & Harr, R. D. (1987). Comparative snow accumulation and melt during rainfall in forested and clear-cut plots in the western Cascades of Oregon. *Proceedings of the 55th Western Snow Conference*, 27–38.

Berghuijs, W., Woods, R. & Hrachowitz, M. A precipitation shift from snow towards rain leads to a decrease in streamflow. *Nature Clim Change* 4, 583–586 (2014). https://doi.org/10.1038/nclimate2246

Boisramé, G., Harpold, A., & Tague, C. (2024). Relationships between snowpack, low flows and stream temperature in mountain watersheds of the US west coast. *Hydrological Processes, 38*(5), e15157. https://doi.org/10.1002/hyp.15157

Bosson, E., Sabel, U., Gustafsson, L.-G., Sassner, M., & Destouni, G. (2012). Influences of shifts in climate, landscape, and permafrost on terrestrial hydrology. *Journal of Geophysical Research: Atmospheres, 117*(D5), D05120. https://doi.org/10.1029/2011JD016429

Campbell, John L., Charles T. Driscoll, Julia A. Jones, Emery R. Boose, Hilary A. Dugan, Peter M. Groffman, C. Rhett Jackson, Jeremy B. Jones, Glenn P. Juday, Noah R. Lottig, Brooke E. Penaluna, Roger W. Ruess, Katharine Suding, Jonathan R. Thompson, and Jess K. Zimmerman (2022). *Forest and freshwater ecosystem responses to climate change and variability at US LTER sites.* BioScience, 72(9), 851–870. https://doi.org/10.1093/biosci/biab124

Christner, J., & Harr, R. D. (1982). Peak streamflows from the transient snow zone, Western Cascades, Oregon. *Proceedings of the 50th Western Snow Conference*, 27–38.

Eunsang Cho, Carrie M. Vuyovich, Sujay V. Kumar, Melissa L. Wrzesien, Rhae Sung Kim, and Jennifer M. Jacobs (2022). Precipitation biases and snow physics limitations drive uncertainty in modeled SWE across the

western United States. *Hydrology and Earth System Sciences, 26*, 5721–5742. https://doi.org/10.5194/hess-26-5721-2022

Daly, C. and W.A. McKee. 2019. Meteorological data from benchmark stations at the Andrews Experimental Forest, 1957 to present ver 36. Environmental Data Initiative. https://doi.org/10.6073/pasta/c021a2ebf1f91adf0ba3b5e53189c84f

Dickerson-Lange, S. E., Vano, J. A., Gersonde, R., & Lundquist, J. D. (2021). Ranking forest effects on snow storage: A decision tool for forest management. *Water Resources Research, 57*(10), e2020WR027926. https://doi.org/10.1029/2020WR027926

Godsey, S. E., Kirchner, J. W., & Tague, C. L. (2014). Effects of changes in winter snowpacks on summer low flows: Case studies in the Sierra Nevada, California, USA. *Hydrological Processes, 28* (22), 5048–5064. https://doi.org/10.1002/hyp.9943

Goodman, Arianna C.; Segura, Catalina; Jones, Julia A.; Swanson, Frederick J. 2022. Seventy years of watershed response to floods and changing forestry practices in western Oregon, USA. Earth Surface Processes and Landforms. 1-16. doi:https://doi.org/10.1002/esp.5537

Grömping, U. (2006). *Relative Importance for Linear Regression in R: The Package relaimpo.* Journal of Statistical Software, **17**(1), 1–27. https://doi.org/10.18637/jss.v017.i01

Gordon, B. L., Brooks, P. D., Krogh, S. A., Boisramé, G. F. S., Carroll, R. W. H., McNamara, J. P., & Harpold, A. A. (2022). Why does snowmelt-driven streamflow response to warming vary? A data-driven review and predictive framework. *Environmental Research Letters, 17*(5), 053004. https://doi.org/10.1088/1748-9326/ac64b4

Hudson, A. R., Peters, D. P. C., Blair, J. M., Childers, D. L., Doran, P. T., Geil, K., Gooseff, M., Gross, K. L., Haddad, N. M., Pastore, M. A., Rudgers, J. A., Sala, O., Seabloom, E. W., & Shaver, G. (2022). Cross-site comparisons of dryland ecosystem response to climate change in the US Long-Term Ecological Research Network. *BioScience, 72*(9), 889–907. https://doi.org/10.1093/biosci/biab134

Huntington, T. G., Hodgkins, G. A., Keim, B. D., & Dudley, R. W. (2004). Changes in the proportion of precipitation occurring as snow in New England (1949–2000). *Journal of Climate, 17*(13), 2626–2636.

Jefferson, A., Nolin, A., Lewis, S., & Tague, C. (2008). *Hydrogeologic controls on streamflow sensitivity to climate variation*. Hydrological Processes. https://doi.org/10.1002/hyp.7041

Jefferson, A. J. (2011). Seasonal versus transient snow and the elevation dependence of climate sensitivity in maritime mountainous regions. *Geophysical Research Letters, 38*, L16402. https://doi.org/10.1029/2011GL048346

Johnson, S., Wondzell, S., Rothacher, J., 2019. Andrews Forest Data Web Site [WWW Document]. Stream Disch. Gaged Watersheds HJ Andrews Exp. For. 1949 Present. https://doi.org/10.6073/pasta/ba33b8509dfd018f39f39f40d9f6dd7b

Jones, J. A., & Perkins, R. M. (2010). Extreme flood sensitivity to snow and forest harvest, western Cascades, Oregon, United States. *Water Resources Research, 46*(12), W12512. https://doi.org/10.1029/2009WR008632

Jones, J. A., & Driscoll, C. T. (2022). Long-term ecological research on ecosystem responses to climate change. *BioScience, 72*(9), 814–826. https://doi.org/10.1093/biosci/biac021

Jones, J. A., Daly, C., Schulze, M., & Still, C. J. (2025). Microclimate refugia are transient in stable old forests, Pacific Northwest, USA. *AGU Advances, 6*, e2024AV001492. https://doi.org/10.1029/2024AV001492

Knowles, N., Dettinger, M. D., & Cayan, D. R. (2006). Trends in snowfall versus rainfall in the western United States. *Journal of Climate, 19*(18), 4545–4559. https://doi.org/10.1175/JCLI3850.1

Li, D., Wrzesien, M. L., Durand, M., Adam, J., & Lettenmaier, D. P. (2017). How much runoff originates as snow in the western United States, and how will that change in the future? *Geophysical Research Letters, 44*(12), 6163–6172. https://doi.org/10.1002/2017GL073551

Leach, J. A., Webster, K. L., Hudson, D. T., Buttle, J., & Nehemy, M. (2024). Zero-flow dynamics for headwater streams in a humid forested landscape. *Hydrological Processes, 38*(12), e70025. https://doi.org/10.1002/hyp.70025

Li, D., Wrzesien, M. L., Durand, M., Adam, J., & Lettenmaier, D. P. (2017). How much runoff originates as snow in the western United States, and how will that change in the future? *Geophysical Research Letters, 44*(12), 6163–6172. https://doi.org/10.1002/2017GL073551

Lindeman, R. H., Merenda, P. F., & Gold, R. Z. (1980). *Introduction to Bivariate and Multivariate Analysis.* Glenview, IL: Scott, Foresman.

Maindonald, J. H., & Braun, W. J. (2010). *Data Analysis and Graphics Using R: An Example-Based Approach* (3rd ed.). Cambridge University Press.

Mankin, J. S., Viviroli, D., Singh, D., Hoekstra, A. Y., & Diffenbaugh, N. S. (2015). The potential for snow to supply human water demand in the present and future. *Environmental Research Letters, 10*(11), 114016. https://doi.org/10.1088/1748-9326/10/11/114016

McCabe, G. J. (2018). *Warming is driving decreases in snow fractions while runoff remains stable*. *Journal of Hydrometeorology, 19*(5). https://doi.org/10.1175/JHM-D-17-0227.1

Metcalfe, J. R., & Goodison, B. E. (1993, January). Correction of Canadian winter precipitation data. In *Proc. Eighth Symp. on Meteorological Observations and Instrumentation* (pp. 338-343). Anaheim, CA: Amer. Meteor. Soc.

Miller, A. (2002). *Subset selection in regression* (2nd ed.). Chapman & Hall/CRC. https://doi.org/10.1201/9781420035933

Mote, P. W., Hamlet, A. F., Clark, M. P., & Lettenmaier, D. P. (2005). Declining mountain snowpack in western North America. *Bulletin of the American Meteorological Society, 86*(1), 39–49. https://doi.org/10.1175/BAMS-86-1-39

Mote, P. W., Li, S., Lettenmaier, D. P., Xiao, M., & Engel, R. (2018). Dramatic declines in snowpack in the western US. *npj Climate and Atmospheric Science, 1*, 2. https://doi.org/10.1038/s41612-018-0012-1

Musselman, K. N., Clark, M. P., Liu, C., Ikeda, K., & Rasmussen, R. (2017). Slower snowmelt in a warmer world. *Nature Climate Change, 7*(3), 214–219. https://doi.org/10.1038/nclimate3225

Musselman, K. N., Addor, N., Vano, J. A., & Molotch, N. P. (2021). Winter melt trends portend widespread declines in snow water resources. *Nature Climate Change, 11*, 418–424. https://doi.org/10.1038/s41558-021-01014-9

Newcomb, S. K., Van Kirk, R. W., Godsey, S. E., & Kraft, M. (2024). Alignment between water inputs and vegetation green-up reduces next year's runoff efficiency. *Hydrological Processes, 38*(6), e15211. https://doi.org/10.1002/hyp.15211

Newman, A. J., Clark, M. P., Sampson, K., Wood, A., Hay, L. E., Bock, A., Viger, R. J., & Blodgett, D. (2015). Development of a large-sample watershed-scale hydrometeorological dataset for the contiguous USA: Dataset characteristics and assessment of regional variability in hydrologic model performance. *Hydrology and Earth System Sciences, 19*, 209–223. https://doi.org/10.5194/hess-19-209-2015

Nolin, A. W., & Daly, C. (2006). Mapping "At Risk" Snow in the Pacific Northwest. *Journal of Hydrometeorology, 7*(5), 1164–1171. https://doi.org/10.1175/JHM543.1

Office for Coastal Management Partners, 2025: USFS 2020 Lidar: Wallowa-Whitman National Forest from 2010-06-15 to 2010-08-15. NOAA National Centers for Environmental Information, https://www.fisheries.noaa.gov/inport/item/69262

Ortega Melendez, J. (2024). *Drivers of relative streamflow contributions in mountainous headwater streams* [Master's thesis, Oregon State University]. ScholarsArchive@OSU.

Pierce, D. W., Barnett, T. P., Hidalgo, H. G., Das, T., Bonfils, C., Santer, B. D., Bala, G., & Dettinger, M. D. (2008). Attribution of declining western U.S. snowpack to human effects. *Journal of Climate, 21*(23), 6425–6444. https://doi.org/10.1175/2008JCLI2405.1

Pohlert, T. (2023). *trend: Non-Parametric Trend Tests and Change-Point Detection* (R package version 1.1.6). https://CRAN.R-project.org/package=trend.

Roth, T. R., & Nolin, A. W. (2017). Forest impacts on snow accumulation and ablation across an elevation gradient in a temperate montane environment. *Hydrology and Earth System Sciences, 21*(11), 5427–5442. https://doi.org/10.5194/hess-21-5427-2017

Safeeq, M., Shukla, S., Arismendi, I., Grant, G. E., Lewis, S. L., & Nolin, A. W. (2013). Influence of winter season climate variability on snow–precipitation ratio in the western United States. *International Journal of Climatology, 33*(15), 3733–3743. https://doi.org/10.1002/joc.3595

Segura, C., Bladon, K. D., Hatten, J. A., Jones, J. A., Hale, V. C., & Ice, G. G. (2020). Long-term effects of forest harvesting on summer low flow deficits in the Coast Range of Oregon. *Journal of Hydrology, 585*, 124749. https://doi.org/10.1016/j.jhydrol.2020.124749

Segura, C. (2021). Snow drought reduces water transit times in headwater streams. *Hydrological Processes, 35*(12), e14437. https://doi.org/10.1002/hyp.14437

Siler, N., Proistosescu, C. & Po-Chedley, S. Natural Variability Has Slowed the Decline in Western U.S. Snowpack Since the 1980s. *Geophysical Research Letters* 46, 346–355 (2019). https://doi.org/10.1029/2018GL081080

Sen, P. K. (1968). Estimates of the regression coefficient based on Kendall's tau. *Journal of the American Statistical Association, 63*(324), 1379–1389.

Stewart, I. T., Cayan, D. R., & Dettinger, M. D. (2004). Changes in snowmelt runoff timing in western North America under a "business as usual" climate change scenario. *Climatic Change, 62*(1–3), 217–232. https://doi.org/10.1023/B:CLIM.0000013702.22656.e8

Swanson, F. J., & James, M. E. (1975). *Geology and geomorphology of the H. J. Andrews Experimental Forest, western Cascades, Oregon*. USDA Forest Service, Pacific Northwest Forest and Range Experiment Station.

Swanson, F. J., & Jones, J. A. (2002). *Geomorphology and hydrology of the H. J. Andrews Experimental Forest, Oregon*.

Tague, C., Grant, G., Farrell, M., Choate, J., & Jefferson, A. (2008). Deep groundwater mediates streamflow response to climate warming in the Oregon Cascades. *Climatic Change, 86*(1–2), 189–210. https://doi.org/10.1007/s10584-007-9294-8

Tarboton, D. G., & Luce, C. H. (1996, December). *Utah Energy Balance Snow Accumulation and Melt Model (UEB): Computer Model Technical Description and Users Guide* (Technical Report). Utah Water Research Laboratory, Utah State University; USDA Forest Service Intermountain Research Station. Retrieved from https://hydrology.usu.edu/dtarb/snow/snowrep.pdf

Trujillo, E., & Molotch, N. P. (2014). Snowpack regimes of the western United States. *Water Resources Research, 50*(7), 5611–5623. https://doi.org/10.1002/2013WR014753

Wei, T., & Simko, V. (2021). *corrplot: Visualization of a correlation matrix* (R package version 0.92). R package.

Yang, D., Goodison, B. E., Metcalfe, J. R., Golubev, V. S., Bates, R., Pangburn, T., & Hanson, C. L. (1998). Accuracy of NWS 8" standard nonrecording precipitation gauge: Results and application of WMO intercomparison. *Journal of Atmospheric and Oceanic Technology, 15*(1), 54–68. https://doi.org/10.1175/1520-0426(1998)015<0054:AONSNP>2.0.CO;2

8. Appendix

Appendix A: Data Interpolation

Missing climate data were filled using several methods. Gaps in SWE at CENMET, VANMET, and UPLMET were filled by linear interpolation for short gaps shorter than 5 days. Overall, SWE interpolations were used for 22 days at CENMET, 50 days at VANMET, and 23 days at UPLMET. At VANMET, three longer gaps of 9, 11, and 12 days, totaling 32 days, were also interpolated. Longer SWE gaps at CENMET were estimated based on linear relationships between SWE data at CENMET, VANMET, and UPLMET, while longer VANMET gaps were filled based on relationships between SWE at VANMET and CENMET. Following interpolation, remaining missing values totaled 125 days (CENMET), 257 days (UPLMET), and 74 days (VANMET). Periods were retained as missing where interpolations produced unreasonable estimates, typically during extended gaps or when nearby stations were also missing data. Throughout the period of interpolation (01-06-1987 to 09-30-2023), there remained 223 missing days at CENMET, 611 missing days at VANMET, and 426 missing days at UPLMET.

Gaps in precipitation and air temperature at CENMET, UPLMET, H15MET, PRIMET, and VANMET were filled using the average of values predicted from linear relationships with nearby stations. Missing data at CENMET, UPLMET, H15MET, and PRIMET were estimated from relationships among these stations, and temperature gap-filling also included CS2MET. At VANMET, precipitation gaps were filled from relationships with CENMET, UPLMET, H15MET, and PRIMET, and temperature gaps also used VARMET.

Table A. 1: Linearly interpolated climate variables and their source stations (in order of ascending station elevation). For each variable, the table reports the meteorological station from which values were derived, the interpolation period, and the count of days initially missing in the raw record (prior to interpolation).

Variable	Meteorological Station	Corresponding Interpolation Stations	Interpolation Period	Days Missing Initially
SWE				
	CENMET	VANMET, UPLMET	1997-01-01 to 2023-09-30	281
	VANMET	CENMET, VARMET	1997-01-01 to 2023-09-30	630
	UPLMET	VANMET	1997-01-01 to 2023-09-30	785
Precipitation				
	PRIMET	C2SMET, H15MET, CENMET, UPLMET	1979-10-01 to 2023-09-30	9
	CENMET	PRIMET, H15MET, UPLMET	1979-10-01 to 2023-09-30	5825
	H15MET	PRIMET, CENMET, UPLMET	1979-10-01 to 2023-09-30	269
	UPLMET	PRIMET, H15MET, CENMET	1979-10-01 to 2023-09-30	7325
Air Temperature				
	CENMET	C2SMET, PRIMET, H15MET, CENMET	1979-10-01 to 2023-09-30	6064
	VANMET	H15MET, CENMET, VARMET, UPLMET	1979-10-01 to 2023-09-30	3104
	UPLMET	C2SMET, PRIMET, CENMET	1979-10-01 to 2023-09-30	7420

Appendix B: Interannual Trends in Climate, Snow, and Streamflow

Table B. 1: Summary of long-term trends in annual air temperature, maximum snow water equivalent (SWE), precipitation, and snow fraction at four meteorological stations in the Andrews Forest (CENMET, H15MET, VANMET, UPLMET) over the study period, water years 1998–2020. Results are shown for both linear regression (slope, R-value, p-value) and non-parametric Mann–Kendall trend analyses (Sen's slope, Kendall's tau, MK p-value).

Variable	Meteorological Station	Slope	R-value	p-value	Sen's Slope	Kendall's Tau	Mann-Kendall p-value
Air Temperature							
	CENMET	-0.011	-0.107	0.627	-0.018	-0.130	0.398
	VANMET	-0.008	-0.081	0.713	-0.013	-0.115	0.460
	UPLMET	0.020	0.189	0.387	0.014	0.123	0.428
Maximum SWE							
	CENMET	2.394	0.086	0.697	2.199	0.051	0.751
	VANMET	-2.842	-0.052	0.814	-2.036	-0.012	0.958
	UPLMET	-5.536	-0.066	0.766	-5.000	-0.043	0.792
Precipitation							
	CENMET	1.357	0.025	0.909	-1.333	-0.004	1.000
	H15MET	-1.461	-0.028	0.898	-3.356	-0.020	0.916
	UPLMET	7.601	0.132	0.548	1.912	0.028	0.874
Snow Fraction							
	CENMET	-0.090	-0.054	0.807	0.081	0.020	0.916
	VANMET	0.176	0.078	0.736	0.385	0.086	0.608
	UPLMET	-0.322	-0.175	0.436	-0.318	-0.065	0.693

Table B. 2: Summary of long-term trends in annual runoff ratio and unit streamflow across nine gauged study watersheds in the Andrews Forest (over the study period, water years 1998–2020. Results are shown for both linear regression (slope, R-value, p-value) and non-parametric Mann–Kendall trend analyses (Sen's slope, Kendall's tau, MK p-value).

Variable	Watershed	Slope	R-value	p-value	Sen's Slope	Kendall's Tau	Mann-Kendall p-value
Runoff Ratio							
	WS01	-0.003	-0.292	0.176	-0.004	-0.281	0.064
	WS02	-0.002	-0.197	0.367	-0.004	-0.241	0.113
	WS03	-0.003	-0.269	0.214	-0.005	-0.281	0.064
	WS06	-0.004	-0.322	0.133	-0.006	-0.281	0.064
	WS07	-0.004	-0.465	0.025	-0.005	-0.375	0.013
	WS08	<0.001	-0.035	0.872	-0.001	-0.107	0.492
	WS09	0.001	0.043	0.846	-0.001	-0.043	0.792
	WS10	-0.003	-0.258	0.234	-0.004	-0.289	0.057
	Mack Creek	-0.002	-0.207	0.344	-0.002	-0.123	0.428
Unit Streamflow							
	WS01	-9.296	-0.247	0.256	-14.672	-0.249	0.102
	WS02	-9.040	-0.192	0.380	-14.013	-0.178	0.245
	WS03	-11.381	-0.230	0.290	-17.566	-0.202	0.187
	WS06	-11.837	-0.220	0.313	-15.332	-0.162	0.291
	WS07	-10.360	-0.290	0.180	-12.494	-0.241	0.113
	WS08	-2.918	-0.072	0.744	-7.033	-0.107	0.492
	WS09	-2.688	-0.059	0.789	-9.585	-0.162	0.291
	WS10	-10.625	-0.214	0.326	-16.207	-0.162	0.291
	Mack Creek	-3.452	-0.066	0.766	-8.688	-0.067	0.673

Table B. 3: Summary of long-term seasonal trends in air temperature and precipitation at four meteorological stations in the Andrews Forest (CENMET, H15MET, VANMET, and UPLMET) over the study period, water years 1998–2020. Results are presented for each season (fall, winter, spring, and summer) using both linear regression (slope, R-value, p-value) and non-parametric Mann–Kendall trend analyses (Sen's slope, Kendall's tau, and MK p-value).

Variable	Meteorological Station	Season	Slope	R-value	p-value	Sen's Slope	Kendall's Tau	Mann-Kendall p-value
Seasonal Air Temperature								
	CENMET	Fall	-0.043	-0.332	0.122	-0.054	-0.209	0.170
	CENMET	Winter	-0.026	-0.154	0.483	-0.030	-0.130	0.398
	CENMET	Spring	0.033	0.172	0.432	0.033	0.154	0.316
	CENMET	Summer	-0.007	-0.062	0.779	0.005	0.012	0.958
	VANMET	Fall	-0.039	-0.293	0.175	-0.029	-0.130	0.398
	VANMET	Winter	-0.023	-0.119	0.588	-0.035	-0.138	0.369
	VANMET	Spring	0.044	0.243	0.264	0.048	0.202	0.187
	VANMET	Summer	-0.013	-0.092	0.675	0.003	0.016	0.937
	UPLMET	Fall	-0.009	-0.064	0.772	-0.003	-0.012	0.958
	UPLMET	Winter	0.022	0.119	0.587	0.016	0.067	0.673
	UPLMET	Spring	0.052	0.269	0.215	0.047	0.273	0.073
	UPLMET	Summer	0.018	0.143	0.514	0.027	0.138	0.369
Seasonal Precipitation								
	CENMET	Fall	-3.431	-0.086	0.695	-3.612	-0.067	0.673
	CENMET	Winter	0.162	0.005	0.983	-2.808	-0.083	0.597
	CENMET	Spring	2.793	0.172	0.432	3.568	0.154	0.316
	H15MET	Fall	-1.583	-0.041	0.851	0.636	0.004	1.000
	H15MET	Winter	-2.280	-0.067	0.761	-5.470	-0.099	0.526
	H15MET	Spring	1.130	0.069	0.755	2.553	0.107	0.492
	UPLMET	Fall	0.552	0.013	0.952	-1.171	-0.028	0.874
	UPLMET	Winter	-0.591	-0.014	0.949	-2.986	-0.028	0.874
	UPLMET	Spring	3.666	0.190	0.385	4.900	0.138	0.369

Appendix C: Climate and Snow Effects on Seasonal Streamflow

Table C.1: Pearson correlation coefficients and p-values from linear regressions in correlation matrices, for all study watersheds. Only precipitation, snow, and streamflow variables with p-values below 0.1 were included. Shorthand names are shown

Watershed	Variable 1	Variable 2	R-value	p-value
1	Total Annual Precipitation	Maximum SWE	0.483	0.020
1	Total Annual Precipitation	Snow Disappearance Date	0.372	0.081
1	Total Annual Precipitation	Date of Maximum SWE	0.370	0.083
1	Total Spring Precipitation	Summer Hydrograph Recession Rate	0.817	<0.001
1	Total Spring Precipitation	July 1 Streamflow	0.812	<0.001
1	Total Spring Precipitation	Summer Low Flow	0.681	<0.001
1	Total Spring Precipitation	Mean Summer Streamflow	0.625	0.001
1	Snow Fraction	Maximum SWE	0.829	<0.001
1	Snow Fraction	Melt Rate	0.783	<0.001
1	Snow Fraction	Date of Maximum SWE	0.695	<0.001
1	Snow Fraction	Snow Disappearance Date	0.683	<0.001
1	Snow Disappearance Date	Date of Maximum SWE	0.694	<0.001
1	Snow Disappearance Date	Maximum SWE	0.612	0.002
1	Snow Disappearance Date	Melt Rate	0.359	0.093
1	Date of Maximum SWE	Melt Rate	0.732	<0.001
1	Date of Maximum SWE	Maximum SWE	0.599	0.003
1	Maximum SWE	Melt Rate	0.788	<0.001
1	July 1 Streamflow	Summer Hydrograph Recession Rate	0.970	<0.001
1	July 1 Streamflow	Summer Low Flow	0.686	<0.001
1	July 1 Streamflow	Mean Summer Streamflow	0.615	0.002
1	Mean Summer Streamflow	Summer Low Flow	0.808	<0.001
1	Mean Summer Streamflow	Summer Hydrograph Recession Rate	0.526	0.010
1	Summer Low Flow	Summer Hydrograph Recession Rate	0.594	0.003
2	Total Annual Precipitation	Maximum SWE	0.483	0.020
2	Total Annual Precipitation	Snow Disappearance Date	0.372	0.081
2	Total Annual Precipitation	Date of Maximum SWE	0.370	0.083
2	Total Spring Precipitation	Summer Hydrograph Recession Rate	0.811	<0.001
2	Total Spring Precipitation	July 1 Streamflow	0.769	<0.001
2	Total Spring Precipitation	Mean Summer Streamflow	0.701	<0.001
2	Total Spring Precipitation	Summer Low Flow	0.507	0.013
2	Snow Fraction	Maximum SWE	0.829	<0.001
2	Snow Fraction	Melt Rate	0.783	<0.001
2	Snow Fraction	Date of Maximum SWE	0.695	<0.001
2	Snow Fraction	Snow Disappearance Date	0.683	<0.001
2	Snow Fraction	Summer Low Flow Date	0.355	0.096
2	Snow Disappearance Date	Date of Maximum SWE	0.694	<0.001
2	Snow Disappearance Date	Maximum SWE	0.612	0.002

2	Snow Disappearance Date	Melt Rate	0.359	0.093
2	Date of Maximum SWE	Melt Rate	0.732	<0.001
2	Date of Maximum SWE	Maximum SWE	0.599	0.003
2	Maximum SWE	Melt Rate	0.788	<0.001
2	July 1 Streamflow	Summer Hydrograph Recession Rate	0.955	<0.001
2	July 1 Streamflow	Mean Summer Streamflow	0.813	<0.001
2	July 1 Streamflow	Summer Low Flow	0.751	<0.001
2	Mean Summer Streamflow	Summer Low Flow	0.801	<0.001
2	Mean Summer Streamflow	Summer Hydrograph Recession Rate	0.746	<0.001
2	Summer Low Flow	Summer Hydrograph Recession Rate	0.628	0.001
3	Total Annual Precipitation	Maximum SWE	0.483	0.020
3	Total Annual Precipitation	Snow Disappearance Date	0.372	0.081
3	Total Annual Precipitation	Date of Maximum SWE	0.370	0.083
3	Total Spring Precipitation	Summer Hydrograph Recession Rate	0.807	<0.001
3	Total Spring Precipitation	July 1 Streamflow	0.751	<0.001
3	Total Spring Precipitation	Mean Summer Streamflow	0.659	0.001
3	Total Spring Precipitation	Summer Low Flow	0.527	0.010
3	Snow Fraction	Maximum SWE	0.829	<0.001
3	Snow Fraction	Melt Rate	0.783	<0.001
3	Snow Fraction	Date of Maximum SWE	0.695	<0.001
3	Snow Fraction	Snow Disappearance Date	0.683	<0.001
3	Snow Disappearance Date	Date of Maximum SWE	0.694	<0.001
3	Snow Disappearance Date	Maximum SWE	0.612	0.002
3	Snow Disappearance Date	Melt Rate	0.359	0.093
3	Date of Maximum SWE	Melt Rate	0.732	<0.001
3	Date of Maximum SWE	Maximum SWE	0.599	0.003
3	Maximum SWE	Melt Rate	0.788	<0.001
3	July 1 Streamflow	Summer Hydrograph Recession Rate	0.968	<0.001
3	July 1 Streamflow	Mean Summer Streamflow	0.778	<0.001
3	July 1 Streamflow	Summer Low Flow	0.773	<0.001
3	Mean Summer Streamflow	Summer Low Flow	0.781	<0.001
3	Mean Summer Streamflow	Summer Hydrograph Recession Rate	0.712	<0.001
3	Summer Low Flow	Summer Hydrograph Recession Rate	0.671	<0.001
6	Total Annual Precipitation	Maximum SWE	0.741	<0.001
6	Total Annual Precipitation	Snow Disappearance Date	0.715	<0.001
6	Total Annual Precipitation	Melt Rate	0.513	0.012
6	Total Annual Precipitation	Snow Fraction	0.468	0.024
6	Total Spring Precipitation	Summer Hydrograph Recession Rate	0.716	<0.001
6	Total Spring Precipitation	July 1 Streamflow	0.703	<0.001
6	Total Spring Precipitation	Mean Summer Streamflow	0.661	0.001
6	Total Spring Precipitation	Summer Low Flow	0.485	0.019
6	Snow Fraction	Maximum SWE	0.698	<0.001
6	Snow Fraction	Melt Rate	0.606	0.002
6	Snow Fraction	Snow Disappearance Date	0.574	0.004

6	Snow Fraction	Summer Low Flow Date	0.516	0.012
6	Snow Disappearance Date	Maximum SWE	0.829	<0.001
6	Snow Disappearance Date	Melt Rate	0.664	0.001
6	Snow Disappearance Date	Summer Low Flow Date	0.472	0.023
6	Maximum SWE	Melt Rate	0.842	<0.001
6	Maximum SWE	Summer Low Flow Date	0.399	0.059
6	July 1 Streamflow	Summer Hydrograph Recession Rate	0.996	<0.001
6	July 1 Streamflow	Mean Summer Streamflow	0.946	<0.001
6	July 1 Streamflow	Summer Low Flow	0.767	<0.001
6	Mean Summer Streamflow	Summer Hydrograph Recession Rate	0.926	<0.001
6	Mean Summer Streamflow	Summer Low Flow	0.840	<0.001
6	Summer Low Flow	Summer Hydrograph Recession Rate	0.719	<0.001
7	Total Annual Precipitation	Maximum SWE	0.741	<0.001
7	Total Annual Precipitation	Snow Disappearance Date	0.715	<0.001
7	Total Annual Precipitation	Melt Rate	0.513	0.012
7	Total Annual Precipitation	Snow Fraction	0.468	0.024
7	Total Spring Precipitation	Summer Hydrograph Recession Rate	0.693	<0.001
7	Total Spring Precipitation	July 1 Streamflow	0.665	0.001
7	Total Spring Precipitation	Mean Summer Streamflow	0.593	0.003
7	Snow Fraction	Maximum SWE	0.698	<0.001
7	Snow Fraction	Melt Rate	0.606	0.002
7	Snow Fraction	Snow Disappearance Date	0.574	0.004
7	Snow Disappearance Date	Maximum SWE	0.829	<0.001
7	Snow Disappearance Date	Melt Rate	0.664	0.001
7	Snow Disappearance Date	Mean Summer Streamflow	0.365	0.087
7	Maximum SWE	Melt Rate	0.842	<0.001
7	July 1 Streamflow	Summer Hydrograph Recession Rate	0.993	<0.001
7	July 1 Streamflow	Mean Summer Streamflow	0.857	<0.001
7	July 1 Streamflow	Summer Low Flow	0.625	0.001
7	Mean Summer Streamflow	Summer Hydrograph Recession Rate	0.823	<0.001
7	Mean Summer Streamflow	Summer Low Flow	0.773	<0.001
7	Summer Low Flow	Summer Hydrograph Recession Rate	0.543	0.007
8	Total Annual Precipitation	Maximum SWE	0.741	<0.001
8	Total Annual Precipitation	Snow Disappearance Date	0.715	<0.001
8	Total Annual Precipitation	Melt Rate	0.513	0.012
8	Total Annual Precipitation	Snow Fraction	0.468	0.024
8	Total Annual Precipitation	Summer Low Flow Date	0.396	0.062
8	Total Spring Precipitation	July 1 Streamflow	0.626	0.001
8	Total Spring Precipitation	Summer Hydrograph Recession Rate	0.617	0.002
8	Total Spring Precipitation	Mean Summer Streamflow	0.540	0.008
8	Total Spring Precipitation	Summer Low Flow	0.508	0.013
8	Snow Fraction	Maximum SWE	0.698	<0.001
8	Snow Fraction	Summer Low Flow Date	0.629	0.001
8	Snow Fraction	Melt Rate	0.606	0.002

8	Snow Fraction	Snow Disappearance Date	0.574	0.004
8	Snow Disappearance Date	Maximum SWE	0.829	<0.001
8	Snow Disappearance Date	Melt Rate	0.664	0.001
8	Snow Disappearance Date	Summer Low Flow Date	0.578	0.004
8	Maximum SWE	Melt Rate	0.842	<0.001
8	Maximum SWE	Summer Low Flow Date	0.607	0.002
8	Melt Rate	Summer Low Flow Date	0.472	0.023
8	July 1 Streamflow	Summer Hydrograph Recession Rate	0.988	<0.001
8	July 1 Streamflow	Mean Summer Streamflow	0.675	<0.001
8	July 1 Streamflow	Summer Low Flow	0.545	0.007
8	Mean Summer Streamflow	Summer Low Flow	0.718	<0.001
8	Mean Summer Streamflow	Summer Hydrograph Recession Rate	0.627	0.001
8	Summer Low Flow	Summer Hydrograph Recession Rate	0.448	0.032
9	Total Annual Precipitation	Maximum SWE	0.483	0.020
9	Total Annual Precipitation	Snow Disappearance Date	0.372	0.081
9	Total Annual Precipitation	Date of Maximum SWE	0.370	0.083
9	Total Spring Precipitation	Summer Hydrograph Recession Rate	0.812	<0.001
9	Total Spring Precipitation	July 1 Streamflow	0.795	<0.001
9	Total Spring Precipitation	Mean Summer Streamflow	0.678	<0.001
9	Total Spring Precipitation	Summer Low Flow	0.660	0.001
9	Snow Fraction	Maximum SWE	0.829	<0.001
9	Snow Fraction	Melt Rate	0.783	<0.001
9	Snow Fraction	Date of Maximum SWE	0.695	<0.001
9	Snow Fraction	Snow Disappearance Date	0.683	<0.001
9	Snow Disappearance Date	Date of Maximum SWE	0.694	<0.001
9	Snow Disappearance Date	Maximum SWE	0.612	0.002
9	Snow Disappearance Date	Summer Low Flow Date	0.542	0.008
9	Snow Disappearance Date	Melt Rate	0.359	0.093
9	Date of Maximum SWE	Melt Rate	0.732	<0.001
9	Date of Maximum SWE	Maximum SWE	0.599	0.003
9	Maximum SWE	Melt Rate	0.788	<0.001
9	July 1 Streamflow	Summer Hydrograph Recession Rate	0.921	<0.001
9	July 1 Streamflow	Summer Low Flow	0.834	<0.001
9	July 1 Streamflow	Mean Summer Streamflow	0.688	<0.001
9	July 1 Streamflow	Summer Low Flow Date	0.482	0.020
9	Mean Summer Streamflow	Summer Low Flow	0.777	<0.001
9	Mean Summer Streamflow	Summer Hydrograph Recession Rate	0.605	0.002
9	Summer Low Flow	Summer Hydrograph Recession Rate	0.713	<0.001
9	Summer Low Flow Date	Summer Hydrograph Recession Rate	0.370	0.082
10	Total Annual Precipitation	Maximum SWE	0.483	0.020
10	Total Annual Precipitation	Snow Disappearance Date	0.372	0.081
10	Total Annual Precipitation	Date of Maximum SWE	0.370	0.083
10	Total Spring Precipitation	Summer Hydrograph Recession Rate	0.803	<0.001
10	Total Spring Precipitation	July 1 Streamflow	0.769	<0.001

10	Total Spring Precipitation	Mean Summer Streamflow	0.520	0.011
10	Total Spring Precipitation	Summer Low Flow	0.420	0.046
10	Snow Fraction	Maximum SWE	0.829	<0.001
10	Snow Fraction	Melt Rate	0.783	<0.001
10	Snow Fraction	Date of Maximum SWE	0.695	<0.001
10	Snow Fraction	Snow Disappearance Date	0.683	<0.001
10	Snow Fraction	Summer Low Flow Date	0.367	0.085
10	Snow Fraction	Summer Low Flow	-0.354	0.098
10	Snow Disappearance Date	Date of Maximum SWE	0.694	<0.001
10	Snow Disappearance Date	Maximum SWE	0.612	0.002
10	Snow Disappearance Date	Summer Low Flow Date	0.497	0.016
10	Snow Disappearance Date	Melt Rate	0.359	0.093
10	Date of Maximum SWE	Melt Rate	0.732	<0.001
10	Date of Maximum SWE	Maximum SWE	0.599	0.003
10	Date of Maximum SWE	Summer Low Flow Date	0.361	0.090
10	Maximum SWE	Melt Rate	0.788	<0.001
10	Melt Rate	Summer Low Flow	-0.381	0.073
10	July 1 Streamflow	Summer Hydrograph Recession Rate	0.973	<0.001
10	July 1 Streamflow	Summer Low Flow	0.652	0.001
10	July 1 Streamflow	Mean Summer Streamflow	0.579	0.004
10	Mean Summer Streamflow	Summer Low Flow	0.732	<0.001
10	Mean Summer Streamflow	Summer Hydrograph Recession Rate	0.513	0.012
10	Summer Low Flow	Summer Hydrograph Recession Rate	0.536	0.008
Mack Creek	Total Annual Precipitation	Maximum SWE	0.695	<0.001
Mack Creek	Total Annual Precipitation	July 1 Streamflow	0.557	0.006
Mack Creek	Total Annual Precipitation	Snow Fraction	0.546	0.007
Mack Creek	Total Annual Precipitation	Summer Hydrograph Recession Rate	0.542	0.008
Mack Creek	Total Annual Precipitation	Mean Summer Streamflow	0.538	0.008
Mack Creek	Total Annual Precipitation	Melt Rate	0.506	0.014
Mack Creek	Total Annual Precipitation	Summer Low Flow	0.423	0.044
Mack Creek	Total Spring Precipitation	Date of Maximum SWE	0.379	0.075
Mack Creek	Total Spring Precipitation	Snow Disappearance Date	0.370	0.082
Mack Creek	Snow Fraction	Maximum SWE	0.917	<0.001
Mack Creek	Snow Fraction	Melt Rate	0.895	<0.001
Mack Creek	Snow Fraction	Summer Hydrograph Recession Rate	0.802	<0.001
Mack Creek	Snow Fraction	July 1 Streamflow	0.798	<0.001
Mack Creek	Snow Fraction	Mean Summer Streamflow	0.501	0.015
Mack Creek	Snow Disappearance Date	Date of Maximum SWE	0.647	0.001
Mack Creek	Snow Disappearance Date	Summer Low Flow Date	0.393	0.063
Mack Creek	Snow Disappearance Date	July 1 Streamflow	-0.352	0.099
Mack Creek	Date of Maximum SWE	Summer Low Flow Date	0.438	0.037
Mack Creek	Maximum SWE	Melt Rate	0.897	<0.001
Mack Creek	Maximum SWE	Summer Hydrograph Recession Rate	0.764	<0.001
Mack Creek	Maximum SWE	July 1 Streamflow	0.762	<0.001

Mack Creek	Maximum SWE	Mean Summer Streamflow	0.616	0.002
Mack Creek	Maximum SWE	Summer Low Flow	0.465	0.025
Mack Creek	Melt Rate	Summer Hydrograph Recession Rate	0.697	<0.001
Mack Creek	Melt Rate	July 1 Streamflow	0.670	<0.001
Mack Creek	Melt Rate	Mean Summer Streamflow	0.390	0.066
Mack Creek	July 1 Streamflow	Summer Hydrograph Recession Rate	0.994	<0.001
Mack Creek	July 1 Streamflow	Mean Summer Streamflow	0.754	<0.001
Mack Creek	July 1 Streamflow	Summer Low Flow	0.542	0.008
Mack Creek	Mean Summer Streamflow	Summer Low Flow	0.786	<0.001
Mack Creek	Mean Summer Streamflow	Summer Hydrograph Recession Rate	0.716	<0.001
Mack Creek	Summer Low Flow	Summer Hydrograph Recession Rate	0.487	0.018
Mack Creek	Summer Low Flow	Summer Low Flow Date	-0.388	0.067

Table C.2: Pearson correlation coefficients and p-values from linear regressions between air temperature and runoff ratio for all study watersheds across all seasons.

Watershed	Season	R-value	p-value
1	Fall	<0.001	0.995
2	Fall	-0.030	0.874
3	Fall	-0.050	0.828
6	Fall	-0.110	0.609
7	Fall	-0.060	0.789
8	Fall	-0.110	0.622
9	Fall	-0.130	0.545
10	Fall	-0.070	0.755
Mack Creek	Fall	-0.080	0.721
1	Winter	-0.340	0.108
2	Winter	-0.400	0.056
3	Winter	-0.340	0.112
6	Winter	-0.140	0.536
7	Winter	-0.080	0.719
8	Winter	-0.090	0.677
9	Winter	-0.510	0.014
10	Winter	-0.440	0.035
Mack Creek	Winter	0.280	0.189
1	Spring	-0.500	0.014
2	Spring	-0.490	0.018
3	Spring	-0.510	0.013
6	Spring	-0.520	0.011
7	Spring	-0.470	0.024
8	Spring	-0.430	0.042
9	Spring	-0.440	0.034
10	Spring	-0.550	0.006
Mack Creek	Spring	-0.360	0.095
1	Summer	0.030	0.903
2	Summer	0.070	0.750
3	Summer	-0.010	0.962
6	Summer	0.070	0.752
7	Summer	0.020	0.914
8	Summer	-0.100	0.651
9	Summer	-0.120	0.572
10	Summer	-0.080	0.725
Mack Creek	Summer	-0.200	0.365

Table C.3: Pearson correlation coefficients and p-values from linear regressions between the residuals of the runoff ratio–air temperature relationship and water year, precipitation, and snow fraction for all study watersheds.

Watershed	Season	Variable	R-value	p-value
1	Winter	Water Year	-0.530	0.009
2	Winter	Water Year	-0.410	0.050
3	Winter	Water Year	-0.430	0.040
6	Winter	Water Year	-0.150	0.499
7	Winter	Water Year	-0.240	0.266
8	Winter	Water Year	0.090	0.676
9	Winter	Water Year	-0.290	0.185
10	Winter	Water Year	-0.490	0.017
Mack Creek	Winter	Water Year	0.030	0.882
1	Winter	Precipitation	0.190	0.394
2	Winter	Precipitation	0.160	0.461
3	Winter	Precipitation	0.210	0.330
6	Winter	Precipitation	0.200	0.366
7	Winter	Precipitation	0.180	0.424
8	Winter	Precipitation	0.160	0.460
9	Winter	Precipitation	0.250	0.245
10	Winter	Precipitation	0.160	0.476
Mack Creek	Winter	Precipitation	0.070	0.756
1	Winter	Snow Fraction	0.060	0.800
2	Winter	Snow Fraction	0.090	0.685
3	Winter	Snow Fraction	0.090	0.676
6	Winter	Snow Fraction	0.140	0.536
7	Winter	Snow Fraction	0.060	0.799
8	Winter	Snow Fraction	0.090	0.691
9	Winter	Snow Fraction	0.090	0.674
10	Winter	Snow Fraction	0.090	0.697
Mack Creek	Winter	Snow Fraction	-0.290	0.174
1	Spring	Water Year	0.070	0.742
2	Spring	Water Year	0.150	0.486
3	Spring	Water Year	0.090	0.673
6	Spring	Water Year	-0.020	0.912
7	Spring	Water Year	-0.100	0.643
8	Spring	Water Year	0.040	0.851
9	Spring	Water Year	0.260	0.223
10	Spring	Water Year	-0.050	0.813
Mack Creek	Spring	Water Year	-0.200	0.362
1	Spring	Precipitation	-0.050	0.812
2	Spring	Precipitation	-0.160	0.454
3	Spring	Precipitation	-0.130	0.565

6	Spring	Precipitation	-0.300	0.164
7	Spring	Precipitation	-0.330	0.129
8	Spring	Precipitation	-0.300	0.170
9	Spring	Precipitation	0.120	0.573
10	Spring	Precipitation	-0.020	0.912
Mack Creek	Spring	Precipitation	-0.380	0.072
1	Spring	Snow Fraction	0.190	0.390
2	Spring	Snow Fraction	0.350	0.102
3	Spring	Snow Fraction	0.320	0.134
6	Spring	Snow Fraction	0.370	0.080
7	Spring	Snow Fraction	0.400	0.062
8	Spring	Snow Fraction	0.400	0.060
9	Spring	Snow Fraction	0.100	0.661
10	Spring	Snow Fraction	0.090	0.693
Mack Creek	Spring	Snow Fraction	0.770	<0.001

Table C.4: Pearson correlation coefficients and p-values from linear regressions between snow fraction and runoff ratio for all study watersheds during fall, winter, and spring.

Watershed	Season	R-value	p-value
1	Fall	0.050	0.822
2	Fall	0.150	0.502
3	Fall	0.150	0.505
6	Fall	0.250	0.248
7	Fall	0.220	0.317
8	Fall	0.290	0.179
9	Fall	0.170	0.445
10	Fall	0.090	0.689
Mack Creek	Fall	-0.050	0.834
1	Winter	0.330	0.128
2	Winter	0.400	0.056
3	Winter	0.360	0.094
6	Winter	0.200	0.367
7	Winter	0.090	0.674
8	Winter	0.130	0.556
9	Winter	0.480	0.020
10	Winter	0.430	0.041
Mack Creek	Winter	-0.480	0.021
1	Spring	0.300	0.162
2	Spring	0.440	0.035
3	Spring	0.420	0.047
6	Spring	0.420	0.044
7	Spring	0.440	0.034
8	Spring	0.450	0.033
9	Spring	0.210	0.338
10	Spring	0.230	0.302
Mack Creek	Spring	0.880	<0.001
1	Summer	-0.150	0.482
2	Summer	-0.030	0.886
3	Summer	-0.050	0.810
6	Summer	0.070	0.735
7	Summer	0.020	0.924
8	Summer	0.020	0.943
9	Summer	-0.180	0.420
10	Summer	-0.150	0.484
Mack Creek	Summer	0.540	0.008

Table C.5: Top models from all-subsets linear regressions (≤ 3 explanatory variables per model) for each *watershed × dependent-variable* pair. Rows list the selected predictors and summary statistics: Akaike Information Criterion (AIC), cross-validated R^2 (CV- R^2), root-mean-square error (RMSE), and model F-statistic. For each watershed–dependent variable combination, the best-performing (lowest) AIC model is reported along with any competing models with ΔAIC ≤ 2 relative to that best model.

Watershed	Response Variable	Explanatory Variable(s)	AIC	CV-R2	RMSE	F-statistic
1	July 1 streamflow	Maximum SWE date, Mean spring air T, Spring P	-45.576	0.667	0.072	20.881
1	July 1 streamflow	Mean spring air T, Spring P	-44.262	0.638	0.078	27.203
1	July 1 streamflow	Snowmelt rate, Mean spring air T, Spring P	-43.681	0.617	0.075	18.729
1	Summer low flow	Spring P	-129.002	0.392	0.013	18.176
1	Summer low flow	Mean spring air T, Spring P	-128.015	0.389	0.013	9.495
1	Summer low flow	Maximum SWE date, Spring P	-127.304	0.383	0.013	8.902
1	Summer low flow	Snowmelt rate, Spring P	-127.233	0.365	0.013	8.844
1	Summer low flow	Maximum SWE date, Mean spring air T, Spring P	-127.218	0.412	0.012	6.677
1	Summer low flow	Snow fraction, Spring P	-127.165	0.274	0.013	8.788
1	Summer low flow	Snowmelt rate, Mean spring air T, Spring P	-127.117	0.320	0.012	6.619
1	Summer low flow	Snow fraction, Mean spring air T, Spring P	-127.096	0.260	0.012	6.608
1	Summer low flow	Snow diss date, Spring P	-127.086	0.306	0.013	8.723
1	Summer low flow	Mean winter air T, Spring P	-127.026	0.316	0.013	8.674
1	Summer low flow	Mean summer air T, Spring P	-127.008	0.274	0.013	8.660
1	Summer low flow	Maximum SWE, Spring P	-127.004	0.301	0.013	8.657
1	Summer low flow date	Mean spring air T	181.547	-0.035	10.993	1.961
1	Summer low flow date	Snow diss date	181.600	0.021	11.006	1.908
1	Summer low flow date	Snow diss date, Mean spring air T	181.779	0.023	10.579	1.807
1	Summer low flow date	Snow fraction	181.857	-0.028	11.068	1.653
1	Summer low flow date	Mean winter air T	182.006	0.010	11.104	1.507
1	Summer low flow date	Maximum SWE date, Snow diss date, Mean spring air T	182.381	-0.205	10.262	1.613
1	Summer low flow date	Snow fraction, Mean spring air T	182.549	-0.045	10.757	1.419
1	Summer low flow date	Mean spring air T, Spring P	182.614	-0.080	10.773	1.386
1	Summer low flow date	Mean winter air T, Mean spring air T	182.784	0.001	10.813	1.302
1	Summer low flow date	Snowmelt rate, Snow fraction	182.894	-0.089	10.838	1.249
1	Summer low flow date	Snow diss date, Mean spring air T, Spring P	183.042	0.030	10.411	1.388

1	Summer low flow date	Maximum SWE	183.127	-0.074	11.378	0.437
1	Summer low flow date	Snowmelt rate, Snow fraction, Mean spring air T	183.207	-0.088	10.448	1.333
1	Summer low flow date	Maximum SWE date, Snow diss date	183.246	-0.184	10.922	1.078
1	Summer low flow date	Maximum SWE date	183.293	-0.091	11.419	0.282
1	Summer low flow date	Maximum SWE, Snow fraction	183.329	-0.148	10.941	1.038
1	Summer low flow date	Snow diss date, Snow fraction	183.347	-0.198	10.946	1.029
1	Summer low flow date	Maximum SWE, Mean spring air T	183.401	-0.088	10.959	1.003
1	Summer low flow date	Snowmelt rate	183.411	-0.159	11.448	0.173
1	Summer low flow date	Snow diss date, Mean winter air T	183.467	-0.038	10.974	0.972
1	Summer low flow date	Maximum SWE, Snow diss date, Mean spring air T	183.487	-0.103	10.512	1.240
1	Summer low flow date	Maximum SWE date, Mean spring air T	183.533	-0.227	10.990	0.940
1	Summer low flow date	Mean spring air T, Mean summer air T	183.537	-0.093	10.991	0.938
1	Summer low flow date	Snowmelt rate, Mean spring air T	183.545	-0.189	10.993	0.934
2	July 1 streamflow	Snowmelt rate, Mean spring air T, Spring P	-13.313	0.519	0.146	13.767
2	July 1 streamflow	Maximum SWE date, Mean spring air T, Spring P	-13.234	0.558	0.146	13.698
2	July 1 streamflow	Mean spring air T, Spring P	-13.106	0.543	0.153	18.834
2	July 1 streamflow	Mean spring air T, Mean summer air T, Spring P	-11.899	0.531	0.150	12.569
2	July 1 streamflow	Snow fraction, Mean spring air T, Spring P	-11.727	0.470	0.151	12.427
2	July 1 streamflow	Mean winter air T, Mean spring air T, Spring P	-11.714	0.515	0.151	12.417
2	July 1 streamflow	Maximum SWE, Mean spring air T, Spring P	-11.590	0.460	0.151	12.316
2	July 1 streamflow	Snow diss date, Mean spring air T, Spring P	-11.387	0.469	0.152	12.152
2	July 1 streamflow	Spring P	-11.342	0.508	0.166	30.410
2	Summer low flow	Snow fraction, Mean spring air T	-73.066	0.019	0.042	5.370
2	Summer low flow	Snowmelt rate, Mean spring air T	-72.323	0.091	0.042	4.882
2	Summer low flow	Maximum SWE, Snow fraction, Mean spring air T	-72.145	0.079	0.041	3.869
2	Summer low flow	Spring P	-72.029	0.185	0.044	7.285
2	Summer low flow	Snow fraction, Mean spring air T, Mean summer air T	-72.016	0.002	0.041	3.812
2	Summer low flow	Snow fraction, Mean spring air T, Spring P	-71.950	0.010	0.041	3.783
2	Summer low flow	Snow fraction, Mean winter air T, Mean spring air T	-71.830	-0.074	0.041	3.730
2	Summer low flow	Snowmelt rate, Mean spring air T, Spring P	-71.706	0.164	0.041	3.676
2	Summer low flow	Snowmelt rate, Snow fraction, Mean spring air T	-71.513	-0.045	0.041	3.592
2	Summer low flow	Snow diss date, Spring P	-71.436	0.096	0.043	4.318

2	Summer low flow	Maximum SWE date, Snow fraction, Mean spring air T	-71.315	-0.075	0.041	3.507
2	Summer low flow	Snowmelt rate, Spring P	-71.291	0.105	0.043	4.228
2	Summer low flow	Mean summer air T, Spring P	-71.241	0.142	0.043	4.198
2	Summer low flow	Snow fraction, Spring P	-71.241	-0.060	0.043	4.198
2	Summer low flow	Snow diss date, Snow fraction, Mean spring air T	-71.088	-0.064	0.042	3.410
2	Summer low flow	Maximum SWE date, Mean spring air T	-71.077	0.153	0.043	4.097
2	Summer low flow date	Snow fraction, Mean summer air T	167.445	-0.023	7.747	2.896
2	Summer low flow date	Maximum SWE, Snow fraction, Mean summer air T	167.663	-0.018	7.452	2.492
2	Summer low flow date	Mean spring air T, Mean summer air T, Spring P	167.750	-0.207	7.466	2.458
2	Summer low flow date	Mean spring air T, Mean summer air T	167.815	-0.091	7.809	2.690
2	Summer low flow date	Snow fraction, Mean spring air T, Mean summer air T	167.824	-0.101	7.478	2.430
2	Summer low flow date	Snow fraction	168.189	0.079	8.223	3.035
2	Summer low flow date	Snowmelt rate, Mean summer air T	168.319	-0.146	7.895	2.415
2	Summer low flow date	Mean summer air T	168.480	-0.132	8.275	2.734
2	Summer low flow date	Snow fraction, Mean spring air T	168.533	0.027	7.932	2.300
2	Summer low flow date	Snow diss date, Mean spring air T, Mean summer air T	168.550	-0.309	7.597	2.158
2	Summer low flow date	Mean spring air T	168.556	0.010	8.289	2.655
2	Summer low flow date	Snowmelt rate, Mean spring air T, Mean summer air T	168.581	-0.255	7.602	2.147
2	Summer low flow date	Snowmelt rate	168.660	0.053	8.307	2.548
2	Summer low flow date	Mean spring air T, Spring P	168.931	-0.126	8.001	2.089
2	Summer low flow date	Snow diss date, Mean summer air T	168.964	-0.107	8.007	2.072
2	Summer low flow date	Snowmelt rate, Mean spring air T	168.968	-0.010	8.007	2.069
2	Summer low flow date	Maximum SWE date, Mean summer air T	169.003	-0.181	8.013	2.051
2	Summer low flow date	Mean winter air T, Mean summer air T	169.166	-0.114	8.042	1.966
2	Summer low flow date	Maximum SWE date, Mean spring air T, Mean summer air T	169.238	-0.518	7.712	1.908
2	Summer low flow date	Snow fraction, Mean winter air T, Mean summer air T	169.306	-0.141	7.723	1.883
2	Summer low flow date	Maximum SWE, Snow fraction	169.329	0.066	8.070	1.882
2	Summer low flow date	Mean winter air T, Mean spring air T, Mean summer air T	169.329	-0.243	7.727	1.875
2	Summer low flow date	Snowmelt rate, Snow fraction, Mean summer air T	169.405	-0.149	7.740	1.848
2	Summer low flow date	Snow fraction, Mean summer air T, Spring P	169.414	-0.127	7.741	1.845
2	Summer low flow date	Snow diss date, Snow fraction, Mean summer air T	169.440	-0.078	7.746	1.836
2	Summer low flow date	Maximum SWE date, Snow fraction, Mean summer air T	169.445	-0.139	7.747	1.834

3	July 1 streamflow	Snowmelt rate, Mean spring air T, Spring P	-18.110	0.555	0.131	13.153
3	July 1 streamflow	Mean spring air T, Spring P	-17.910	0.562	0.138	17.961
3	July 1 streamflow	Maximum SWE date, Mean spring air T, Spring P	-17.702	0.569	0.133	12.810
3	July 1 streamflow	Snow fraction, Mean spring air T, Spring P	-16.637	0.530	0.136	11.944
3	July 1 streamflow	Maximum SWE, Mean spring air T, Spring P	-16.614	0.539	0.136	11.925
3	July 1 streamflow	Mean winter air T, Mean spring air T, Spring P	-16.448	0.541	0.136	11.794
3	July 1 streamflow	Snow diss date, Mean spring air T, Spring P	-16.384	0.526	0.136	11.744
3	July 1 streamflow	Mean spring air T, Mean summer air T, Spring P	-16.244	0.542	0.137	11.634
3	Summer low flow	Snow fraction, Mean spring air T, Mean summer air T	-71.961	0.041	0.041	5.168
3	Summer low flow	Snow fraction, Mean spring air T	-71.145	0.098	0.043	6.068
3	Summer low flow	Mean spring air T, Mean summer air T, Spring P	-70.997	0.167	0.042	4.696
3	Summer low flow	Mean summer air T, Spring P	-70.622	0.092	0.044	5.707
3	Summer low flow	Snow diss date, Mean spring air T, Mean summer air T	-70.001	-0.031	0.043	4.229
3	Summer low flow	Snow fraction, Mean spring air T, Spring P	-69.971	0.082	0.043	4.215
3	Summer low flow date	Maximum SWE, Snow diss date, Mean spring air T	178.807	0.026	9.495	2.680
3	Summer low flow date	Snow diss date, Mean spring air T	179.239	0.079	10.011	2.803
3	Summer low flow date	Mean spring air T	179.554	0.047	10.527	3.312
3	Summer low flow date	Maximum SWE date, Snow diss date, Mean spring air T	180.366	0.081	9.822	2.089
3	Summer low flow date	Snow diss date	180.376	-0.043	10.717	2.459
3	Summer low flow date	Snow diss date, Mean spring air T, Mean summer air T	180.485	-0.110	9.848	2.045
3	Summer low flow date	Maximum SWE, Snow fraction, Mean spring air T	180.603	0.118	9.873	2.003
3	Summer low flow date	Maximum SWE, Mean winter air T, Mean spring air T	180.669	-0.057	9.887	1.979
6	July 1 streamflow	Spring P	22.370	0.388	0.345	20.462
6	July 1 streamflow	Maximum SWE date, Snowmelt rate, Spring P	23.628	0.357	0.325	7.754
6	July 1 streamflow	Snowmelt rate, Spring P	24.016	0.345	0.343	10.050
6	July 1 streamflow	Mean summer air T, Spring P	24.234	0.347	0.344	9.861
6	July 1 streamflow	Maximum SWE date, Spring P	24.236	0.335	0.344	9.859
6	July 1 streamflow	Mean spring air T, Spring P	24.271	0.301	0.345	9.829
6	July 1 streamflow	Mean winter air T, Spring P	24.299	0.322	0.345	9.805
6	July 1 streamflow	Maximum SWE, Spring P	24.308	0.363	0.345	9.797
6	July 1 streamflow	Snow diss date, Spring P	24.331	0.352	0.345	9.777
6	July 1 streamflow	Snow fraction, Spring P	24.335	0.339	0.345	9.774

6	Summer low flow	Spring P	-97.991	0.222	0.025	6.443
6	Summer low flow	Mean winter air T, Spring P	-97.860	0.091	0.024	4.174
6	Summer low flow	Snowmelt rate, Mean winter air T, Spring P	-97.110	-0.019	0.024	3.145
6	Summer low flow	Snow diss date, Spring P	-96.778	0.170	0.025	3.523
6	Summer low flow	Snow fraction, Spring P	-96.523	0.178	0.025	3.374
6	Summer low flow	Maximum SWE, Mean winter air T, Spring P	-96.516	0.064	0.024	2.904
6	Summer low flow	Maximum SWE date, Mean winter air T, Spring P	-96.459	0.023	0.024	2.880
6	Summer low flow	Maximum SWE, Spring P	-96.156	0.182	0.025	3.162
6	Summer low flow	Maximum SWE date, Spring P	-96.142	0.208	0.025	3.154
6	Summer low flow	Snowmelt rate, Spring P	-96.066	0.185	0.025	3.110
6	Summer low flow	Mean summer air T, Spring P	-96.019	0.198	0.025	3.084
6	Summer low flow	Mean spring air T, Spring P	-96.006	0.158	0.025	3.077
6	Summer low flow date	Snow fraction, Mean spring air T	174.353	0.272	9.002	7.312
6	Summer low flow date	Maximum SWE date, Snow fraction, Mean spring air T	175.271	0.214	8.793	5.159
6	Summer low flow date	Snowmelt rate, Snow fraction, Mean spring air T	176.061	0.222	8.945	4.771
6	Summer low flow date	Snow fraction, Mean winter air T, Mean spring air T	176.065	0.253	8.946	4.769
6	Summer low flow date	Snow diss date, Snow fraction, Mean spring air T	176.135	0.017	8.959	4.736
6	Summer low flow date	Snow fraction, Mean spring air T, Mean summer air T	176.296	0.058	8.991	4.658
6	Summer low flow date	Maximum SWE, Snow fraction, Mean spring air T	176.299	0.230	8.991	4.657
6	Summer low flow date	Snow fraction, Mean spring air T, Spring P	176.335	0.125	8.998	4.640
7	July 1 streamflow	Snowmelt rate, Spring P	-5.788	0.325	0.179	9.831
7	July 1 streamflow	Maximum SWE date, Snowmelt rate, Spring P	-5.700	0.340	0.172	7.315
7	July 1 streamflow	Spring P	-5.449	0.322	0.189	16.619
7	July 1 streamflow	Maximum SWE, Spring P	-5.223	0.326	0.182	9.350
7	July 1 streamflow	Snowmelt rate, Mean winter air T, Spring P	-4.670	0.236	0.176	6.717
7	July 1 streamflow	Mean spring air T, Spring P	-4.665	0.297	0.184	8.886
7	July 1 streamflow	Snow diss date, Spring P	-4.400	0.291	0.185	8.670
7	July 1 streamflow	Snowmelt rate, Mean spring air T, Spring P	-4.389	0.244	0.177	6.559
7	July 1 streamflow	Snowmelt rate, Mean summer air T, Spring P	-4.205	0.284	0.178	6.456
7	July 1 streamflow	Mean summer air T, Spring P	-4.119	0.301	0.186	8.443
7	July 1 streamflow	Snowmelt rate, Snow fraction, Spring P	-3.973	0.264	0.179	6.328
7	July 1 streamflow	Maximum SWE, Mean summer air T, Spring P	-3.905	0.297	0.179	6.290

7	July 1 streamflow	Maximum SWE, Snowmelt rate, Spring P	-3.798	0.307	0.179	6.232
7	July 1 streamflow	Snow fraction, Spring P	-3.792	0.216	0.187	8.183
7	July 1 streamflow	Snow diss date, Snowmelt rate, Spring P	-3.791	0.284	0.179	6.228
7	Summer low flow	Spring P	-91.349	-0.060	0.029	2.714
7	Summer low flow	Snowmelt rate, Spring P	-91.093	-0.295	0.028	2.182
7	Summer low flow	Snowmelt rate, Mean spring air T, Spring P	-90.817	-0.515	0.027	1.982
7	Summer low flow	Snowmelt rate	-90.468	-0.108	0.030	1.823
7	Summer low flow	Maximum SWE, Spring P	-90.405	-0.361	0.028	1.823
7	Summer low flow	Maximum SWE date, Snowmelt rate, Spring P	-90.204	-0.514	0.027	1.764
7	Summer low flow	Maximum SWE, Mean spring air T, Spring P	-90.171	-0.582	0.027	1.752
7	Summer low flow	Mean spring air T, Spring P	-90.118	-0.138	0.029	1.676
7	Summer low flow	Maximum SWE date	-89.765	-0.159	0.030	1.136
7	Summer low flow	Maximum SWE	-89.762	-0.142	0.030	1.133
7	Summer low flow	Mean winter air T, Spring P	-89.681	-0.416	0.029	1.457
7	Summer low flow	Snow diss date, Snowmelt rate, Spring P	-89.631	-0.455	0.028	1.565
7	Summer low flow	Snow diss date, Mean spring air T, Spring P	-89.598	-0.341	0.028	1.553
7	Summer low flow	Maximum SWE date, Spring P	-89.594	-0.417	0.029	1.414
7	Summer low flow	Mean winter air T	-89.593	-0.135	0.030	0.971
7	Summer low flow	Mean summer air T, Spring P	-89.591	-0.085	0.029	1.412
7	Summer low flow	Snowmelt rate, Snow fraction, Spring P	-89.583	-0.401	0.028	1.548
7	Summer low flow	Snow diss date, Spring P	-89.473	-0.329	0.029	1.354
7	Summer low flow	Snowmelt rate, Mean winter air T, Spring P	-89.439	-0.438	0.028	1.499
7	Summer low flow	Snow fraction, Spring P	-89.415	-0.334	0.029	1.325
7	Summer low flow	Maximum SWE, Snow diss date, Spring P	-89.387	-0.725	0.028	1.481
7	Summer low flow date	Maximum SWE date, Mean winter air T, Mean spring air T	173.253	0.074	8.415	4.235
7	Summer low flow date	Snowmelt rate, Mean winter air T, Mean spring air T	174.652	-0.117	8.675	3.611
8	July 1 streamflow	Maximum SWE date, Snowmelt rate, Spring P	11.880	0.308	0.252	7.106
8	July 1 streamflow	Snowmelt rate, Spring P	13.750	0.200	0.274	7.934
8	July 1 streamflow	Spring P	13.764	0.212	0.286	13.504
8	Summer low flow	Mean summer air T, Spring P	-103.321	0.248	0.022	4.811
8	Summer low flow	Spring P	-103.154	0.254	0.023	7.306
8	Summer low flow	Mean winter air T, Mean summer air T, Spring P	-102.852	0.168	0.021	3.693

8	Summer low flow	Mean winter air T, Spring P	-102.571	0.200	0.022	4.335
8	Summer low flow	Mean spring air T, Mean summer air T, Spring P	-102.283	0.266	0.021	3.447
8	Summer low flow	Mean spring air T, Spring P	-101.673	0.239	0.022	3.787
8	Summer low flow	Maximum SWE, Mean winter air T, Spring P	-101.599	0.184	0.021	3.161
8	Summer low flow	Mean spring air T, Mean summer air T	-101.504	0.176	0.022	3.686
8	Summer low flow	Snow fraction, Mean summer air T, Spring P	-101.418	0.200	0.021	3.086
8	Summer low flow	Maximum SWE date, Spring P	-101.384	0.246	0.022	3.615
8	Summer low flow	Maximum SWE date, Mean summer air T, Spring P	-101.371	0.239	0.021	3.067
8	Summer low flow	Snowmelt rate, Mean summer air T, Spring P	-101.362	0.199	0.021	3.063
8	Summer low flow	Maximum SWE, Mean summer air T, Spring P	-101.336	0.193	0.022	3.053
8	Summer low flow	Mean winter air T, Mean spring air T, Spring P	-101.321	0.250	0.022	3.047
8	Summer low flow	Snow diss date, Mean summer air T, Spring P	-101.321	0.222	0.022	3.047
8	Summer low flow date	Snow diss date, Snow fraction	169.359	0.297	8.076	8.706
8	Summer low flow date	Snow fraction, Mean summer air T	169.763	0.300	8.147	8.380
8	Summer low flow date	Snow fraction, Mean winter air T, Mean summer air T	169.920	0.322	7.827	6.278
8	Summer low flow date	Snow diss date, Snow fraction, Mean summer air T	169.952	0.262	7.832	6.261
8	Summer low flow date	Maximum SWE, Snow fraction	169.995	0.347	8.188	8.195
8	Summer low flow date	Maximum SWE, Snow fraction, Mean summer air T	169.996	0.301	7.840	6.237
8	Summer low flow date	Snow fraction, Mean winter air T	170.158	0.362	8.217	8.067
8	Summer low flow date	Snow fraction	170.188	0.297	8.588	13.735
8	Summer low flow date	Snow diss date, Snow fraction, Mean winter air T	170.667	0.340	7.955	5.875
8	Summer low flow date	Snow fraction, Mean spring air T	170.722	0.222	8.319	7.629
8	Summer low flow date	Snow fraction, Mean spring air T, Mean summer air T	170.753	0.171	7.970	5.830
8	Summer low flow date	Maximum SWE date, Snow diss date, Snow fraction	170.857	0.208	7.988	5.775
8	Summer low flow date	Maximum SWE, Snow fraction, Mean spring air T	171.121	0.208	8.034	5.637
8	Summer low flow date	Snow fraction, Mean winter air T, Mean spring air T	171.194	0.236	8.047	5.599
8	Summer low flow date	Maximum SWE, Snow diss date, Snow fraction	171.200	0.146	8.048	5.596
8	Summer low flow date	Maximum SWE	171.206	0.314	8.780	12.231
8	Summer low flow date	Snow diss date, Snow fraction, Spring P	171.302	0.087	8.066	5.543
8	Summer low flow date	Snow diss date, Snow fraction, Mean spring air T	171.345	0.055	8.073	5.521
8	Summer low flow date	Snow diss date, Snowmelt rate, Snow fraction	171.348	0.259	8.074	5.519
9	July 1 streamflow	Snow fraction, Mean spring air T, Spring P	-47.937	0.716	0.069	32.738

9	July 1 streamflow	Snowmelt rate, Mean spring air T, Spring P	-46.486	0.719	0.071	30.350
9	July 1 streamflow	Mean spring air T, Spring P	-46.416	0.700	0.074	42.937
9	July 1 streamflow	Maximum SWE date, Mean spring air T, Spring P	-46.413	0.699	0.071	30.235
9	July 1 streamflow	Snow diss date, Mean spring air T, Spring P	-46.274	0.599	0.071	30.013
9	July 1 streamflow	Maximum SWE, Mean spring air T, Spring P	-45.995	0.667	0.072	29.575
9	Summer low flow	Snow diss date, Mean spring air T, Spring P	-109.792	0.394	0.018	9.479
9	Summer low flow	Maximum SWE date, Mean spring air T, Spring P	-109.469	0.487	0.018	9.258
9	Summer low flow	Mean spring air T, Spring P	-108.977	0.419	0.019	12.090
9	Summer low flow	Snow fraction, Mean spring air T, Spring P	-108.882	0.396	0.018	8.865
9	Summer low flow	Snow fraction, Mean spring air T	-108.243	0.348	0.019	11.396
9	Summer low flow	Mean winter air T, Mean spring air T, Spring P	-108.151	0.408	0.019	8.389
9	Summer low flow	Mean spring air T, Mean summer air T, Spring P	-108.008	0.405	0.019	8.298
9	Summer low flow	Snow fraction, Mean spring air T, Mean summer air T	-107.796	0.330	0.019	8.164
9	Summer low flow date	Maximum SWE, Snow diss date, Mean spring air T	170.923	0.395	8.000	12.238
9	Summer low flow date	Snow diss date, Mean winter air T, Mean spring air T	171.634	0.537	8.124	11.673
9	Summer low flow date	Maximum SWE date, Snow diss date, Mean spring air T	171.681	0.498	8.132	11.636
9	Summer low flow date	Snow diss date, Snowmelt rate, Mean spring air T	172.027	0.451	8.194	11.367
10	July 1 streamflow	Snowmelt rate, Mean spring air T, Spring P	-30.110	0.577	0.101	14.982
10	July 1 streamflow	Maximum SWE, Mean spring air T, Spring P	-28.834	0.584	0.104	13.831
10	July 1 streamflow	Snow fraction, Mean spring air T, Spring P	-28.692	0.565	0.104	13.708
10	July 1 streamflow	Mean winter air T, Mean spring air T, Spring P	-28.344	0.564	0.105	13.407
10	Summer low flow	Snowmelt rate, Spring P	-107.941	0.093	0.019	4.045
10	Summer low flow	Maximum SWE date, Spring P	-107.652	0.066	0.020	3.870
10	Summer low flow	Mean winter air T, Spring P	-107.068	0.069	0.020	3.522
10	Summer low flow	Snow fraction, Spring P	-106.886	-0.038	0.020	3.416
10	Summer low flow	Snowmelt rate, Mean spring air T	-106.702	0.064	0.020	3.309
10	Summer low flow	Spring P	-106.580	0.134	0.021	4.485
10	Summer low flow	Maximum SWE, Snowmelt rate, Spring P	-106.430	0.028	0.019	2.753
10	Summer low flow	Maximum SWE date, Snowmelt rate, Spring P	-106.343	0.063	0.019	2.719
10	Summer low flow	Snowmelt rate, Mean spring air T, Spring P	-106.283	0.096	0.019	2.696
10	Summer low flow	Snowmelt rate, Mean summer air T, Spring P	-106.085	-0.008	0.019	2.618
10	Summer low flow	Snowmelt rate, Mean winter air T, Spring P	-106.070	0.055	0.019	2.612

10	Summer low flow	Snow diss date, Snowmelt rate, Spring P	-105.995	-0.069	0.019	2.583
10	Summer low flow	Snowmelt rate, Snow fraction, Spring P	-105.971	-0.033	0.019	2.574
10	Summer low flow date	Maximum SWE, Snow diss date, Mean spring air T	172.594	0.244	8.296	5.638
10	Summer low flow date	Snow diss date, Mean spring air T	172.639	0.270	8.673	7.294
10	Summer low flow date	Snow diss date, Mean winter air T, Mean spring air T	173.852	0.264	8.526	5.001
10	Summer low flow date	Maximum SWE date, Snow diss date, Mean spring air T	173.957	0.158	8.545	4.949
10	Summer low flow date	Snow diss date, Snow fraction, Mean spring air T	174.351	0.239	8.619	4.757
10	Summer low flow date	Snow diss date, Mean spring air T, Mean summer air T	174.545	0.125	8.655	4.664
10	Summer low flow date	Snow diss date, Snowmelt rate, Mean spring air T	174.560	0.130	8.658	4.657
Mack Creek	July 1 streamflow	Maximum SWE, Mean spring air T	40.772	0.675	0.493	32.698
Mack Creek	July 1 streamflow	Maximum SWE date, Snow fraction, Mean spring air T	40.843	0.645	0.473	23.075
Mack Creek	July 1 streamflow	Snow fraction, Mean spring air T	41.378	0.641	0.500	31.587
Mack Creek	July 1 streamflow	Maximum SWE, Snow fraction, Mean spring air T	41.501	0.682	0.480	22.245
Mack Creek	July 1 streamflow	Maximum SWE, Maximum SWE date, Mean spring air T	42.130	0.640	0.487	21.474
Mack Creek	July 1 streamflow	Maximum SWE, Mean winter air T, Mean spring air T	42.142	0.606	0.487	21.460
Mack Creek	July 1 streamflow	Maximum SWE, Mean spring air T, Spring P	42.528	0.680	0.491	20.998
Mack Creek	July 1 streamflow	Maximum SWE, Snow diss date, Mean spring air T	42.573	0.548	0.491	20.944
Mack Creek	July 1 streamflow	Maximum SWE, Mean spring air T, Mean summer air T	42.731	0.657	0.493	20.757
Mack Creek	July 1 streamflow	Maximum SWE, Snowmelt rate, Mean spring air T	42.753	0.616	0.493	20.731
Mack Creek	Summer low flow	Maximum SWE, Maximum SWE date, Mean spring air T	-82.142	0.324	0.033	8.409
Mack Creek	Summer low flow	Maximum SWE, Maximum SWE date, Spring P	-80.661	0.284	0.034	7.490
Mack Creek	Summer low flow date	Maximum SWE, Snow diss date, Snowmelt rate	168.292	0.449	7.555	9.686